CP violation and the CKM matrix

Andreas Höcker
CERN, CH–1211 Geneva 23, Switzerland

Zoltan Ligeti
Lawrence Berkeley National Laboratory, University of California, Berkeley, CA 94720
Center for Theoretical Physics, Massachusetts Institute of Technology, Cambridge, MA 02139

Abstract
Our knowledge of quark-flavor physics and *CP* violation increased tremendously over the past five years. It is confirmed that the Standard Model correctly describes the dominant parts of the observed *CP*-violating and flavor-changing phenomena. Not only does *CP* violation provide some of the most precise constraints on the flavor sector, but several measurements performed at the *B*-factories achieved much better precision than had been expected. We review the present status of the Cabibbo-Kobayashi-Maskawa matrix and *CP* violation, recollect the relevant experimental and theoretical inputs, display the results from the global CKM fit, and discuss their implications for the Standard Model and some of its extensions.

CERN-PH-EP/2006-007, LBNL-59882, MIT-CTP 3729

CONTENTS

1 Introduction

1.1 Quark Mixing and *CP* Violation in the Standard Model

In the Standard Model (SM), quark masses and their mixing and *CP* violation have a common origin. Local gauge invariance forbids bare mass terms for fermions, just as it forbids gauge boson masses. Masses are generated after spontaneous electroweak symmetry breaking, owing to the Yukawa couplings of the fermions to the Higgs condensate. Therefore *CP* violation and flavor-changing interactions also probe the electroweak scale, complementary to other studies at the energy frontier. Because the nature of the Higgs condensate is not known, it is interesting to study as many different aspects of it as possible.

Historically, flavor physics and *CP* violation were excellent probes of new physics: the absence of the decay $K_L^0 \to \mu^+\mu^-$ predicted the charm quark; *CP* violation in $K^0\overline{K}^0$ mixing predicted the third generation; the $K^0\overline{K}^0$ mass difference predicted the charm mass; the mass difference of the heavy and light mass eigenstates of the $B^0\overline{B}^0$ mesons predicted the heavy top mass. These measurements put strong constraints on extensions of the SM, and imply that if there is new physics at the TeV scale, it must have a very special flavor and *CP* structure to satisfy these

constraints.

The SM contains three sources of *CP* violation (if the quark masses are nonzero and nondegenerate). One of them occurs in the Cabibbo-Kobayashi-Maskawa (CKM) matrix [1, 2] that describes the mixing of the quark generations, and the corresponding *CP*-violating parameter is of order unity. This source of *CP* violation is discussed in detail in this review. With the SM amended to include neutrino masses, *CP* violation is also possible in the mixing of leptons. We have no experimental information on the size of this effect yet. The third source of *CP* violation occurs in flavor-conserving strong-interaction processes. However, the experimental upper bound on the neutron electric dipole moment implies that this $(\theta_{\rm QCD}/16\pi^2)F_{\mu\nu}\widetilde{F}^{\mu\nu}$ term in the SM Lagrangian is at best tiny, $\theta_{\rm QCD} \lesssim 10^{-10}$ (for a review, see [3]). This is usually referred to as the *strong CP problem*. Thus we know that neither *CP* violation in the lepton sector nor that corresponding to $\theta_{\rm QCD}$ can play any role in quark-flavor physics experiments.

Interestingly, there already exists strong evidence for *CP* violation beyond the SM. Assuming that the evolution of the universe began in a matter-antimatter symmetric state or that inflation washed out any previously existing asymmetry, the three sources of *CP* violation in the SM mentioned above cannot explain the observed baryon-to-entropy ratio, $n_B/s \approx 9 \times 10^{-11}$. The SM contains all three Sakharov conditions [4] — baryon number violation, *C* and *CP* violation, and deviation from thermal equilibrium — required to generate such an asymmetry. However, the asymmetry generated by the SM is many orders of magnitudes too small [5]. This implies that there must be *CP* violation beyond the SM, but it does not have to be in the quark sector, nor in flavor-changing processes.[1] Nevertheless, because most new physics scenarios predict or naturally have observable effects in quark-flavor physics experiments, it is interesting to thoroughly test this sector of the SM.

1.2 The CKM Matrix

The Yukawa interaction of the quarks is given by

$$\mathcal{L}_Y = -Y^d_{ij}\,\overline{Q^I_{Li}}\,\phi\,d^I_{Rj} - Y^u_{ij}\,\overline{Q^I_{Li}}\,\varepsilon\,\phi^*\,u^I_{Rj} + \text{h.c.}, \tag{1}$$

where $Y^{u,d}$ are 3×3 complex matrices, ϕ is the Higgs field, i and j are generation labels, and ε is the 2×2 antisymmetric tensor. The Q^I_L are left-handed quark doublets, and d^I_R and u^I_R are right-handed down- and up-type quark singlets, respectively, in the weak-eigenstate basis. When ϕ acquires a vacuum expectation value, $\langle\phi\rangle = (0, v/\sqrt{2})$, Eq. (1) yields Dirac mass terms for quarks with 3×3 mass matrices

$$M^u = \frac{vY^u}{\sqrt{2}}\,, \qquad M^d = \frac{vY^d}{\sqrt{2}}\,. \tag{2}$$

[1] The baryon asymmetry may be explained by leptogenesis [6]. The discovery of neutrino masses makes the seesaw mechanism and the existence of very massive right-handed neutrinos likely. These may decay out of equilibrium through *CP*-violating interaction, generating nonzero lepton number, which can subsequently be converted by part into a baryon asymmetry by $(B+L)$-violating but $(B-L)$-conserving sphaleron processes present in the SM.

To move from the basis of the flavor eigenstates to the basis of the mass eigenstates, one performs the transformation

$$U_L^{u(d)} M^{u(d)} U_R^{u(d)\dagger} = \mathrm{diag}\Big(m_{u(d)}, m_{c(s)}, m_{t(b)}\Big)\,, \tag{3}$$

where $U_L^{u,d}$ and $U_R^{u,d}$ are unitary matrices and the masses m_q are real. The quark mass matrices are diagonalized by different transformations for the left-handed up- and down-quarks, which are part of the same $\mathrm{SU}(2)_L$ doublet,

$$Q_L^I = \begin{pmatrix} u_{Li}^I \\ d_{Li}^I \end{pmatrix} = (U_L^{u\dagger})_{ij} \begin{pmatrix} u_{Lj} \\ (U_L^u U_L^{d\dagger})_{jk}\, d_{Lk} \end{pmatrix}. \tag{4}$$

By convention, we pulled out $(U_L^{u\dagger})_{ij}$, so that the "misalignment" between the two transformations operates on the down-type quark mass eigenstates. Thus the charged-current weak interaction is modified by the product of the diagonalizing matrices of the up- and down-type quark mass matrices, the so-called CKM matrix [1, 2],

$$V = U_L^u U_L^{d\dagger} = \begin{pmatrix} V_{ud} & V_{us} & V_{ub} \\ V_{cd} & V_{cs} & V_{cb} \\ V_{td} & V_{ts} & V_{tb} \end{pmatrix}. \tag{5}$$

However, the neutral-current part of the Lagrangian in the mass eigenstate basis remains unchanged, i.e., there are no flavor-changing neutral currents (FCNC) at tree level.

Being the product of unitary matrices, V itself is unitary, $VV^\dagger = \mathrm{I}$. This requirement and the freedom to arbitrarily choose the global phases of the quark fields reduce the initial nine unknown complex elements of V to three real numbers and one phase, where the latter accounts for CP violation. Because these four numbers effectively govern the rates of all tree- and loop-level electroweak transitions that involve the charged current, it is a compelling exercise to overconstrain V. If inconsistencies among different measurements occurred, it would reveal the existence of physics beyond the SM.

The charged-current couplings among left-handed quark fields are proportional to the elements of V. The right-handed quarks have no W-boson interaction in the SM, and the Z, photon and gluon couplings are flavor-diagonal. For left-handed leptons, flavor-mixing can be introduced in a manner similar to that of quarks.

The first CKM element, the Cabibbo quark-mixing angle θ_C, was introduced in 1963 [1] to explain the small weak-interaction decay rates for particles carrying strangeness. When CP violation was discovered in 1964 by the observation of the CP-odd decay $K_L^0 \to \pi^+\pi^-$ [7], researchers had not yet perceived the intimate relation between the dynamical rules of quark-flavor mixing and the phenomenon of CP violation. Hence the terrain was open for speculations. In 1970, Glashow, Iliopoulos & Maiani (GIM) [8] used the unitary quark-mixing ansatz to postulate the existence of a fourth quark with quantum number charm to explain the observed suppression of strangeness-changing neutral currents (e.g., $K_L^0 \to \mu^+\mu^-$). This mechanism yields the absence of tree-level FCNCs in the SM. In 1973 the concept of quark-flavor mixing and CP violation were unified when Kobayashi & Maskawa showed that for at least three generations of quarks, there would be enough physical degrees of freedom left in the quark-flavor mixing matrix to allow for a nonzero phase [2]. This example demonstrates how, throughout the history of

particle physics, discoveries and developments in flavor physics have led to spectacular progress. The subsequent discovery of bottom and top quarks, and even a third lepton generation, as well as the observation of direct *CP* violation in the kaon system backed the KM idea. The *B*-factories provided the proof that the KM mechanism is the dominant source of *CP* violation at the electroweak scale with the measurement of $\sin 2\beta$ in agreement with the KM expectation [9].

Beyond the description of *CP* violation, the three-generation CKM matrix provides a consistent framework for understanding a huge variety of observations. This includes understanding the very different neutral-meson mixing frequencies governed by FCNC box diagrams (the GIM mechanism is not effective for top quark loops and hence large mixing amplitudes are possible), to the precise predictions of rare decays of K and B mesons. Using the measurements of the $K^0\overline{K}^0$ and $B^0\overline{B}^0$ mixing frequencies, the KM ansatz could be used to predict the scales of charm and top-quark masses, respectively. Consequently, the hierarchical structure of the CKM matrix guides experimentalists in their quest for observables that can precisely determine its elements: *a*) The quarks occurring in the box diagrams govern the mixing frequency, and hence determine whether or not the neutral meson mixing can be observed experimentally; *b*) the lifetimes of the lightest mesons with a given flavor depend on the CKM elements in the dominant weak decays; to measure time-dependent *CP* asymmetries, the lifetime and the mixing frequency should be comparable; *c*) the CKM mixing hierarchy between the generations determines the relative size of the observable *CP*-violating effects, and which mixing and decay amplitudes contribute to the process. The conjunction of these considerations have led to the understanding that asymmetric-energy *B*-factories would allow theoretically clean measurements of *CP*-violating observables in the B_d sector. As a result of the successful operation of the *B*-factories, for the first time, significantly overconstraining the CKM matrix with many dynamically different processes, and hence testing the KM theory, was possible. This—and not the measurement of the CKM phase's *value* per se—has been and is the primary motivation for investing important resources into the physics of quark flavors. The overwhelming success of the KM theory hides however the problem that the *origin* of the observed flavor structure (mass hierarchy, mixing and *CP* violation) is not understood within the SM.

1.3 Unitarity Constraints

We have seen in the previous section that quark-flavor (or weak interaction) eigenstates and mass eigenstates are not equivalent. Hence the quark flavors mix through their couplings to the charged weak current. The CKM matrix, which describes the three-generation quark-flavor mixing in the SM, would be greatly simplified if, for instance, two of the up- or down-type quarks had equal masses and were therefore indistinguishable (see Sec. 1.3.2). Because there is no empirical evidence for such degeneracy, the full variable space for the CKM elements must be considered. Fortunately, the number of free parameters can be greatly reduced by very general considerations. Unitarity and the freedom to arbitrarily choose the global phase of a quark field, reduce the original $2n_g^2$ unknowns (where $n_g = 3$ is the number of generations) to $(n_g-1)^2$ unknowns. Among these $n_g(n_g-1)/2$ are rotation angles and $(n_g-1)(n_g-2)/2$ phases describe *CP* violation. Three generations allow for only a single *CP*-violating phase. (In the lepton

sector and if neutrinos are Majorana fermions, there are $n_g - 1$ additional CP-violating phases, which are however not observable in oscillation experiments.)

Among the infinite number of possibilities to parameterize the CKM matrix in terms of four independent parameters, we recall the two most popular ones for the purpose of this review.

1.3.1 CKM Parameterizations

Chau and Keung [10] proposed the "standard parameterization" of V. It is obtained by the product of three (complex) rotation matrices, where the rotations are characterized by the Euler angles θ_{12}, θ_{13} and θ_{23}, which are the mixing angles between the generations, and one overall phase δ,

$$V = \begin{pmatrix} c_{12}c_{13} & s_{12}c_{13} & s_{13}e^{-i\delta} \\ -s_{12}c_{23} - c_{12}s_{23}s_{13}e^{i\delta} & c_{12}c_{23} - s_{12}s_{23}s_{13}e^{i\delta} & s_{23}c_{13} \\ s_{12}s_{23} - c_{12}c_{23}s_{13}e^{i\delta} & -c_{12}s_{23} - s_{12}c_{23}s_{13}e^{i\delta} & c_{23}c_{13} \end{pmatrix}, \tag{6}$$

where $c_{ij} = \cos\theta_{ij}$ and $s_{ij} = \sin\theta_{ij}$ for $i < j = 1, 2, 3$. This parameterization satisfies exactly the unitarity relation.[2]

Following the observation of a hierarchy between the mixing angles, $s_{13} \ll s_{23} \ll s_{12} \ll 1$, Wolfenstein [11] proposed an expansion of the CKM matrix in terms of the four parameters λ, A, ρ and η ($\lambda \simeq |V_{us}| \approx 0.23$ being the expansion parameter), which is widely used in the contemporary literature. We use the definitions to *all orders* [12]

$$\begin{aligned} s_{12} &\equiv \lambda\,, \\ s_{23} &\equiv A\lambda^2\,, \\ s_{13}e^{-i\delta} &\equiv A\lambda^3(\rho - i\eta)\,. \end{aligned} \tag{7}$$

Inserting the above definitions into Eq. (6) gives exact expressions for all CKM elements. Although expanding Eq. (6) in λ is illustrative,

$$V = \begin{pmatrix} 1 - \frac{1}{2}\lambda^2 - \frac{1}{8}\lambda^4 & \lambda & A\lambda^3(\rho - i\eta) \\ -\lambda & 1 - \frac{1}{2}\lambda^2 - \frac{1}{8}\lambda^4(1 + 4A^2) & A\lambda^2 \\ A\lambda^3(1 - \rho - i\eta) & -A\lambda^2 + \frac{1}{2}A\lambda^4\,(1 - 2(\rho + i\eta)) & 1 - \frac{1}{2}A^2\lambda^4 \end{pmatrix} + \mathcal{O}(\lambda^5)\,, \tag{8}$$

it is not necessary, nor is it necessary to truncate the expansion at any order in λ. In Ref. [13] and in this review no such approximation is made.

1.3.2 The Jarlskog Invariant

A phase-convention-independent measure of CP violation in the SM is given by

$$\begin{aligned} \mathrm{Im}\det\left([M^u M^{u\dagger}, M^d M^{d\dagger}]\right) &= 2\,J\,(m_t^2 - m_c^2)(m_t^2 - m_u^2)(m_c^2 - m_u^2) \\ &\quad \times (m_b^2 - m_s^2)(m_b^2 - m_d^2)(m_s^2 - m_d^2)\,. \end{aligned} \tag{9}$$

[2] This phase δ describes CP violation. It should not be confused with the CP-conserving hadronic phases that are introduced later.

The Jarlskog invariant [14], J, contains the dependence on the CKM elements,

$$\mathrm{Im}\left(V_{ij}V_{kl}V_{il}^*V_{kj}^*\right) = J\sum_{m,n=1}^{3}\varepsilon_{ikm}\,\varepsilon_{jln}\,, \tag{10}$$

where V_{ij} are the CKM matrix elements and ε_{ikm} is the total antisymmetric tensor. Hence owing to the unitarity of V, the nonvanishing imaginary parts of all quadri-products of CKM elements are equal up to their sign. One representation of Eq. (10) reads, for instance, $J = \mathrm{Im}(V_{ud}V_{cs}V_{us}^*V_{cd}^*)$. A nonvanishing KM phase and hence CP violation requires $J \neq 0$. The Jarlskog parameter expressed in the standard parameterization (6) reads

$$J = c_{12}c_{23}c_{13}^2 s_{12}s_{23}s_{13}\sin\delta\,, \tag{11}$$

and, using the Wolfenstein parameterization,

$$J = A^2\lambda^6\eta\left(1-\lambda^2/2\right) + \mathcal{O}(\lambda^{10}) \approx 3\times 10^{-5}\,. \tag{12}$$

The empirical value of J is small compared with its mathematical maximum of $1/(6\sqrt{3}) \approx 0.1$, showing that CP violation is suppressed as a consequence of the strong hierarchy exhibited by the CKM matrix elements. Remarkably, to account for CP violation (see Eq. (9)) requires not only a nonzero J, but also nondegenerate masses of the up-type and down-type quarks.

Physically meaningful quantities are phase-convention invariant. Such invariants are the moduli, $|V_{ij}|$, and the quadri-products $V_{ij}V_{kl}V_{il}^*V_{kj}^*$ (e.g., the Jarlskog invariant J). Higher-order invariants can be rewritten as functions of these [15]. The Wolfenstein parameters $\lambda = |V_{us}|/\sqrt{|V_{ud}|^2+|V_{us}|^2}$ and $A = |V_{cb}/V_{us}|/\lambda$ are phase-convention invariant, whereas ρ and η with $\rho + i\eta = V_{ub}^*/(A\lambda^3)$ are not. We use phase-invariant representations and formulas throughout this review.

1.3.3 Unitarity Triangles

The allowed region for the CKM phase can be elegantly displayed by means of the Unitarity Triangle (UT) described by the *rescaled* unitarity relation between the first column of the CKM matrix and the complex conjugate of the third column (i.e., corresponding to the B_d meson system[3])

$$0 = \frac{V_{ud}V_{ub}^*}{V_{cd}V_{cb}^*} + \frac{V_{cd}V_{cb}^*}{V_{cd}V_{cb}^*} + \frac{V_{td}V_{tb}^*}{V_{cd}V_{cb}^*} = \mathcal{O}(1) + 1 + \mathcal{O}(1)\,, \tag{13}$$

Note that twice the area of the *non-rescaled* UT equals the Jarlskog parameter J (this is true for any one of the six UTs, because they all have the same area). This provides a geometrical interpretation of the phase-convention invariance of J: A phase redefinition of the CKM matrix rotates the UT while leaving its area, and hence J, invariant. It is a remarkable property of the UT in the B system that its three sides are proportional to the same power of λ (so all sides of the rescaled UT (13) are of order one), which predicts large observable CP violation. In comparison, the corresponding UT for the kaon sector is strongly flattened

$$0 = \frac{V_{ud}V_{us}^*}{V_{cd}V_{cs}^*} + \frac{V_{cd}V_{cs}^*}{V_{cd}V_{cs}^*} + \frac{V_{td}V_{ts}^*}{V_{cd}V_{cs}^*} = \mathcal{O}(1) + 1 + \mathcal{O}(\lambda^4)\,, \tag{14}$$

[3]The subscript in B_d is omitted in the following.

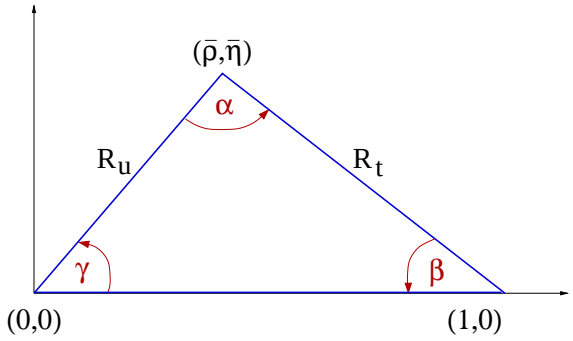

Figure 1: *The rescaled Unitarity Triangle.*

implying small observable *CP* violation.

The UT (13) is sketched in Fig. 1 in the complex plane, where the apex is given by the following phase-convention independent definition [16],

$$\overline{\rho} + i\overline{\eta} \equiv -\frac{V_{ud}V_{ub}^*}{V_{cd}V_{cb}^*}\,. \tag{15}$$

When the above equation is expressed in the Wolfenstein parameterization, one finds to all orders in λ [13][4]

$$\rho + i\eta \;=\; \frac{\sqrt{1-A^2\lambda^4}(\overline{\rho}+i\overline{\eta})}{\sqrt{1-\lambda^2}\,[1-A^2\lambda^4(\overline{\rho}+i\overline{\eta})]}\,. \tag{16}$$

The sides R_u and R_t of the UT (the third side along the real axis is normalized to unity) read to all orders,

$$R_u = \left|\frac{V_{ud}V_{ub}^*}{V_{cd}V_{cb}^*}\right| = \sqrt{\overline{\rho}^2+\overline{\eta}^2}\,, \qquad R_t = \left|\frac{V_{td}V_{tb}^*}{V_{cd}V_{cb}^*}\right| = \sqrt{(1-\overline{\rho})^2+\overline{\eta}^2}\,. \tag{17}$$

The three angles of the UT, α, β, γ, are defined by

$$\alpha = \arg\left(-\frac{V_{td}V_{tb}^*}{V_{ud}V_{ub}^*}\right), \qquad \beta = \arg\left(-\frac{V_{cd}V_{cb}^*}{V_{td}V_{tb}^*}\right), \qquad \gamma = \arg\left(-\frac{V_{ud}V_{ub}^*}{V_{cd}V_{cb}^*}\right), \tag{18}$$

and the KM phase in the standard parameterization (6) is $\delta = \gamma + A^2\lambda^4\eta + \mathcal{O}(\lambda^6)$.

At hadron machines there is copious production of B_s^0 mesons. Here the corresponding Unitarity Triangle, UT_s, is obtained by multiplying the second column of the CKM matrix by the complex conjugate of the third column, which is equivalent to replacing all d-quarks with s-quarks. Appropriately rescaled, one has

$$0 = \frac{V_{us}V_{ub}^*}{V_{cs}V_{cb}^*} + \frac{V_{cs}V_{cb}^*}{V_{cs}V_{cb}^*} + \frac{V_{ts}V_{tb}^*}{V_{cs}V_{cb}^*} = \mathcal{O}(\lambda^2) + 1 + \mathcal{O}(1)\,, \tag{19}$$

The apex of the UT_s is defined accordingly by

$$\overline{\rho}_s + i\overline{\eta}_s \equiv -\frac{V_{us}V_{ub}^*}{V_{cs}V_{cb}^*}\,, \tag{20}$$

[4]Expanding Eq. (15) in λ leads to the well-known approximation

$$\overline{\rho} = \rho(1-\lambda^2/2) + \mathcal{O}(\lambda^4)\,, \qquad \overline{\eta} = \eta(1-\lambda^2/2) + \mathcal{O}(\lambda^4)\,.$$

which is a short vector of order λ^2. The small angle β_s opposing the short side is given by

$$\beta_s = \arg\left(-\frac{V_{ts}V_{tb}^*}{V_{cs}V_{cb}^*}\right). \tag{21}$$

The quantity $\sin 2\beta_s$ can be determined from a time-dependent analysis of $B_s^0 \to J/\psi\phi$ decays.

1.4 *CP* Violation and Neutral-Meson Mixing

The most precise and among the theoretically cleanest information about the phase of the CKM matrix stems at present from the measurements of time-dependent CP asymmetries in B decays, so we need to review briefly the relevant formalism. We use the B^0 system as an example. In general, all forms of CP violation are related to interference phenomena, because CP violation is due to irreducible phases in the Lagrangian, which are observable only in interference experiments.

The conceptually simplest form of CP violation, which can occur in both charged- and neutral-meson as well as baryon decays, is *CP violation in decay*. If at least two amplitudes with nonzero relative weak (ϕ_k) and strong (δ_k) phases (that are odd and even under CP, respectively) contribute to a decay,

$$A_f = \langle f|H|B\rangle = \sum_k A_k\, e^{i\delta_k}\, e^{i\phi_k}\,, \qquad \overline{A}_{\overline{f}} = \langle \overline{f}|H|\overline{B}\rangle = \sum_k A_k\, e^{i\delta_k}\, e^{-i\phi_k}\,. \tag{22}$$

Then it is possible that $|\overline{A}_{\overline{f}}/A_f| \neq 1$, and thus CP symmetry is violated. If there are two contributing amplitudes then $|\overline{A}_{\overline{f}}|^2 - |A_f|^2 \propto \sin(\phi_1 - \phi_2)\sin(\delta_1 - \delta_2)$. Because these kinds of CP asymmetries depend on strong phases, their interpretation is usually model dependent (unless the strong phase can be eliminated by relating several decays to each other). The best established observations of this type of CP violation are $\mathrm{Re}\,\varepsilon'_K$ and the charge asymmetry in $B^0 \to K^+\pi^-$.

In neutral-meson decays there are other possibilities in which CP violation can occur. The two B-meson mass eigenstates are linear combinations of the flavor eigenstates,

$$|B_{L,H}\rangle = p|B^0\rangle \pm q|\overline{B}^0\rangle\,, \tag{23}$$

with two complex parameters p and q. The CP symmetry is violated if the mass eigenstates are not equal to the CP eigenstates (*CP violation in mixing*). This happens if $|q/p| \neq 1$, i.e., if the physical states are not orthogonal, $\langle B_H|B_L\rangle \neq 0$, which could not occur in a classical system. The theoretical prediction of $|q/p|$ requires the calculation of inclusive nonleptonic rates, which is feasible in the heavy-quark limit, but in practice the uncertainties may be sizable. This type of CP violation is well established in the charge asymmetry of semileptonic K_L^0 decay (given by $\delta_L \approx 2\mathrm{Re}\,\varepsilon_K$) or the asymmetry between $K^0_{t=0} \to e^+X$ and $\overline{K}^0_{t=0} \to e^-X$ (given by $4\,\mathrm{Re}\,\varepsilon_K$) [17]. The latter asymmetry measuring CP violation in mixing is denoted by A_{SL} in the B system, where it is expected to be below the 10^{-3} level.

When both B^0 and $\overline{B}^0$ can decay to the same final state, f, the time-dependent CP asymmetry can be studied:

$$A_f(t) = \frac{\Gamma[\overline{B}^0(t) \to f] - \Gamma[B^0(t) \to f]}{\Gamma[\overline{B}^0(t) \to f] + \Gamma[B^0(t) \to f]} = S_f \sin(\Delta m\, t) - C_f \cos(\Delta m\, t)\,, \tag{24}$$

where $\Delta m = m_{B_H} - m_{B_L}$ and t is the proper decay time of the B, and where we have assumed CPT invariance and neglected lifetime differences in the neutral B-meson system (see Refs. [16] and [18] for a more general formulation of the time dependence). The S and C coefficients can be calculated in terms of the $B^0\overline{B}^0$ mixing parameters and the decay amplitudes,

$$S_f = \frac{2\,\mathrm{Im}\,\lambda_f}{1+|\lambda_f|^2}\,, \qquad C_f = \frac{1-|\lambda_f|^2}{1+|\lambda_f|^2}\,, \qquad \lambda_f = \frac{q}{p}\,\frac{\overline{A}_f}{A_f}\,. \tag{25}$$

It is possible that $|q/p| = 1$ and $|\lambda_f| = 1$, i.e., there is no CP violation in either mixing or decay, but the CP asymmetry in Eq. (24) is nonzero, because $\mathrm{Im}\lambda_f \neq 0$ (*CP violation in the interference between decay with and without mixing*, or *mixing-induced CP violation*).

For decays in which the final state is a CP eigenstate and amplitudes with one weak phase dominate, $A_{f_{CP}}$ measures a phase in the Lagrangian theoretically cleanly, independent of hadronic matrix elements. (However, f does not have to be a CP eigenstate for this type of CP violation to occur, nor for it to have a clean interpretation.) For such decays, the CP symmetry of QCD implies $A_{f_{CP}} = \eta_{f_{CP}} A_{\overline{f}_{CP}}$, where $\eta_{f_{CP}}$ is the CP eigenvalue of f, simplifying the evaluation of λ_f. In such cases $C_{f_{CP}} = 0$ and $S_{f_{CP}} = \mathrm{Im}\,\lambda_{f_{CP}} = \sin(\arg\lambda_{f_{CP}})$, where $\arg\lambda_{f_{CP}}$ is the phase difference between the $\overline{B}^0 \to f$ and $\overline{B}^0 \to B^0 \to f$ decay paths. For the generic case, where several amplitudes with different weak phases contribute, detailed knowledge of $\overline{A}_f/A_f$ is necessary to interpret the experimental measurements. In particular, the strong phases of the amplitudes, which usually result in hadronic uncertainties in the interpretation of S_f, and may also give rise to $C_f \neq 0$, must be determined. Note that if C_f is small, it does not imply that S_f provides clean information on short-distance physics. If there are amplitudes with different weak but small relative strong phases, then $C_f \approx 0$, but S_f still depends on the hadronic physics.

1.5 Physics Beyond the Standard Model

There are many reasons to believe that there is physics beyond the SM. The evidence for dark matter implies not-yet-seen particles, the observed matter-antimatter asymmetry of the Universe implies not-yet-observed CP violation, and neutrino masses make the existence of heavy right-handed neutrinos an appealing scenario. More aesthetic reasons include the gauge hierarchy problem that requires new physics to stabilize the huge $M_{\rm Planck}/M_{\rm weak}$ ratio, grand unification of the electroweak- and strong-interaction couplings (that appears naturally with Supersymmetry (SUSY) at the TeV scale), the strong CP problem that may imply the existence of an axion, and the evidence for dark energy that may simply be a cosmological constant in the Einstein equations. Some of these may also relate to new flavor physics that could have observable effects in low-energy experiments.

It is interesting to probe the flavor sector, because it is not well understood. In the SM, the origin of quark-mass and mixing-angle hierarchies are not understood. And if there is new physics at the TeV scale, as conjectured from the gauge hierarchy problem and grand unification, we do not understand why it does not show up in flavor physics experiments. A four-quark operator $(s\overline{d})^2/\Lambda^2_{\rm NP}$ with $\mathcal{O}(1)$ coefficient would give a contribution exceeding the measured value of ε_K unless $\Lambda_{\rm NP} \gtrsim 10^4$ TeV. Similarly, $(d\overline{b})^2/\Lambda^2_{\rm NP}$ yields Δm_d above its measured value unless $\Lambda_{\rm NP} \gtrsim 10^3$ TeV. Extensions of the SM typically have many new sources of CP violation and

flavor-changing neutral-current interactions, and in most scenarios, to satisfy the experimental constraints, specific mechanisms must be introduced to suppress these.

Supersymmetric models are a good example. Compared with the SM, their flavor sector contains 59 new *CP*-conserving parameters and 41 new *CP*-violating phases [19, 20], and many of them have to be suppressed to not contradict the experimental data. The smallness of ε_K and Δm_K have driven SUSY model building to a large extent, and have given rise to several mechanisms that constrain the relevant soft SUSY-breaking terms. Generic models with superpartner masses at the TeV scale also violate the current bounds on electric dipole moments, and fine tuning at the 1% level is required to avoid conflict with the data.

We do not know whether there is new flavor physics at the TeV scale, so it is hard, if not impossible, to make firm predictions. If the new flavor scale is at the TeV scale (where the hierarchy problem suggests that some new physics should exist), it could have observable effects in the (low-energy) flavor sector. If the flavor scale is much above the TeV scale, as is the case for example in models with gauge-mediated SUSY breaking, then we expect no significant deviations from the CKM picture. In any case, if we see new particles at the Large Hadron Collider (LHC), it will be much clearer how to use flavor physics to learn about the new couplings.

2 Theoretical Framework and Tools

With the remarkable exception of the UT angles, the experimental observables presently used to constrain $\overline{\rho}$ and $\overline{\eta}$ depend on hadronic matrix elements. QCD is well established as the theory of strong interaction, and it has been tested to high precision in the perturbative regime where the coupling constant α_s is small. However, presently it is difficult to obtain quantitative predictions in the low-energy regime, except for a few special cases. Although it is beyond the scope of this review to discuss the wealth of approaches to nonperturbative QCD, it is useful to recall a few general techniques to evaluate the matrix elements relevant to quark-flavor physics.

The methods reviewed below all give controllable systematic errors, by which we mean that the uncertainties can be incrementally improved in a well-defined way, expanding in small parameters order by order. Most of the model-independent theoretical tools utilize that some quark masses are smaller while others are greater than $\Lambda_{\rm QCD}$ (throughout this review $\Lambda_{\rm QCD}$ denotes a typical hadronic scale, of order 500 MeV). Expanding in the resulting small ratios can be used to simplify some of the hadronic physics. However, depending on the process under consideration, the relevant hadronic scale may or may not be much smaller than m_b. For example, f_π, m_ρ, and m_K^2/m_s are all of order $\Lambda_{\rm QCD}$, but their numerical values span an order of magnitude. In most cases experimental guidance is necessary to determine how well the expansions work.

2.1 Effective Hamiltonians for Weak Decays

All flavor-changing interactions (except that of the top quark) are due to tree and loop diagrams involving heavy virtual particles: W bosons in the SM, or not-yet-discovered particles in its extensions. These particles propagate over much shorter distances than $1/m_b$, so their interactions can be described by local operators. In principle, there is an infinite number of

such operators. The contributions of the higher dimensional ones are however suppressed by increasing powers of m_b/m_W, so it is sufficient to consider the first few operators. The effective weak Hamiltonian can be written as $H_W = \sum C_i(\mu)\, O_i(\mu)$, where O_i are the lowest dimensional operators contributing to a certain process and C_i are their Wilson coefficients, with perturbatively calculable scale dependences. It is possible to sum the large logarithms of m_W^2/m_b^2 by first calculating $C_i(\mu \sim m_W)$ (matching) and then evolving the effective Hamiltonian down to a scale $\mu \sim m_b$ using the renormalization group (running). This shifts the large logarithms from the matrix elements of O_i to C_i. In this last step the operators can in general mix; for example, $C_2(m_W)$ affects all of $C_{1-9}(m_b)$ below.

The simplest examples are semileptonic decays, where integrating out the virtual W in $b \to c\ell\bar{\nu}$, for instance, gives

$$H_W = \frac{G_F}{\sqrt{2}}\, V_{cb}\, (\bar{c}b)_{V-A}\, (\bar{\ell}\nu)_{V-A}\,, \tag{26}$$

where $V-A$ denotes the Dirac structure $\gamma^\mu(1-\gamma_5)$ between the fermion fields. In this case there is only one operator, and its coefficient is scale independent because the (axial) vector current is (partially) conserved. Semileptonic decays involving a $\bar{\ell}\ell$ pair and nonleptonic decays are more complicated. The $\Delta B = 1$ effective Hamiltonian has both $\Delta S = 0$ and 1 terms. The $\Delta S = 1$ part,

$$H_W = \frac{G_F}{\sqrt{2}} \sum_{p=u,c} V_{pb} V_{ps}^* \left[C_1 O_1^p + C_2 O_2^p + \sum_{i\geq 3} C_i O_i \right], \tag{27}$$

contains the operators

$$\begin{array}{ll}
O_1^u = (\bar{u}_\beta b_\alpha)_{V-A}\, (\bar{s}_\alpha u_\beta)_{V-A}\,, & O_2^u = (\bar{u}b)_{V-A}\, (\bar{s}u)_{V-A}\,, \\
O_1^c = (\bar{c}_\beta b_\alpha)_{V-A}\, (\bar{s}_\alpha c_\beta)_{V-A}\,, & O_2^c = (\bar{c}b)_{V-A}\, (\bar{s}c)_{V-A}\,, \\
O_3 = \sum_q (\bar{s}b)_{V-A}\, (\bar{q}q)_{V-A}\,, & O_4 = \sum_q (\bar{s}_\beta b_\alpha)_{V-A}\, (\bar{q}_\alpha q_\beta)_{V-A}\,, \\
O_5 = \sum_q (\bar{s}b)_{V-A}\, (\bar{q}q)_{V+A}\,, & O_6 = \sum_q (\bar{s}_\beta b_\alpha)_{V-A}\, (\bar{q}_\alpha q_\beta)_{V+A}\,, \\
O_7 = -\frac{e}{8\pi^2}\, m_b\, \bar{s}\, \sigma^{\mu\nu} F_{\mu\nu} (1+\gamma_5) b\,, & O_8 = -\frac{g}{8\pi^2}\, m_b\, \bar{s}\, \sigma^{\mu\nu} G^a_{\mu\nu} T^a (1+\gamma_5) b\,, \\
O_9 = \frac{e^2}{8\pi^2}\, (\bar{s}b)_{V-A}\, (\bar{\ell}\ell)_V\,, & O_{10} = \frac{e^2}{8\pi^2}\, (\bar{s}b)_{V-A}\, (\bar{\ell}\ell)_A\,.
\end{array} \tag{28}$$

The $\Delta S = 0$ part is obtained by replacing $s \to d$ in Eqs. (27) and (28). Here $O^u_{1,2}$ and $O^c_{1,2}$ are current-current operators, O_{3-6} are penguin operators with a sum over $q = u, d, s, c, b$ flavors (α, β are color indices). The C_i coefficients in Eq. (27) are known at next-to-leading logarithmic order [21]. In nonleptonic B decays, four more operators corresponding electroweak penguin diagrams contribute to H_W:

$$\begin{array}{ll}
O_7^{\rm ew} = \sum_q \frac{3}{2}\, e_q\, (\bar{s}b)_{V-A}\, (\bar{q}q)_{V+A}\,, & O_8^{\rm ew} = \sum_q \frac{3}{2}\, e_q\, (\bar{s}_\beta b_\alpha)_{V-A}\, (\bar{q}_\alpha q_\beta)_{V+A}\,, \\
O_9^{\rm ew} = \sum_q \frac{3}{2}\, e_q\, (\bar{s}b)_{V-A}\, (\bar{q}q)_{V-A}\,, & O_{10}^{\rm ew} = \sum_q \frac{3}{2}\, e_q\, (\bar{s}_\beta b_\alpha)_{V-A}\, (\bar{q}_\alpha q_\beta)_{V-A}\,.
\end{array} \tag{29}$$

Non-SM physics can either modify the coefficients C_i at the weak scale, or give rise to additional operators (for example, those obtained by replacing $(\bar{s}b)_{V-A}$ by $(\bar{s}b)_{V+A}$). The goal is to find out if the data show evidence for either type of modification. The largest source of theoretical uncertainty usually stems from our limited ability to compute the hadronic matrix elements of such operators, and the rest of this section introduces methods that allow calculating them, or relating them between various observables.

2.2 Chiral Symmetry

The u, d and s-quark masses are small compared with $\Lambda_{\rm QCD}$, so it is useful to consider the $m_q \to 0$ limit ($q = u, d, s$) and treat corrections perturbatively. This is known as the chiral limit, because the Lagrangian for the light quarks has a $\mathrm{SU}(3)_L \times \mathrm{SU}(3)_R$ chiral symmetry, under which the left- and right-handed quarks transform differently. This symmetry is spontaneously broken to $\mathrm{SU}(3)_V$ by the vacuum expectation value of the quark bilinears, $\langle \bar{q}^i_R q^j_L \rangle = v\delta^{ij}$. The eight broken generators are related to Goldstone bosons, the three pions, four kaons, and the η (for now, we neglect η-η'-π^0 mixing). Chiral symmetry relates different hadronic matrix elements to one another, and has very diverse applications in flavor physics.

Because the u and d-quark masses are small, the SU(2) isospin symmetry between the u and d is usually a very good approximation. The corrections to the chiral limit are suppressed by $(m_d - m_u)/\Lambda_{\chi\rm SB}$—where $\Lambda_{\chi\rm SB} \approx 1\,\mathrm{GeV}$ (of order m_ρ or $4\pi f_\pi$) is the chiral symmetry breaking scale—and are usually not larger than a few percent at the amplitude level. There are also explicit violations of chiral symmetry, for example, due to weak or electromagnetic interactions. In certain cases these effects can be enhanced as is the case, e.g., in the neutral versus charged B (or D) meson lifetimes. The full SU(3) symmetry is broken by $m_s/\Lambda_{\chi\rm SB}$, and is known to have typically $20 - 30\%$ corrections. (The same is true for its u-spin and d-spin SU(2) subgroups, which act on the ds and us pairs, respectively.)

Some of the most prominent cases of isospin symmetry in the context of the CKM matrix include relations between amplitudes involving charged and neutral pions, the determination of $|V_{ud}|$ (Sec. 3.1), and the extraction of the UT angle α from $B \to \pi\pi$ decays (Sec. 5.2). Similarly, SU(3) symmetry and chiral perturbation theory are key ingredients in determining $|V_{us}|$ (Sec. 3.2.2). It also relates form factors and certain matrix elements involving pions and kaons to one another, a relation that has many applications. Recently, the SU(3) relations between nonleptonic decays have been extensively studied, because the $\pi\pi$, $K\pi$, and KK amplitude relations give sensitivity to the UT angle γ and possibly to new physics. SU(3) has also been used as a bound on the SM-induced deviations of the time-dependent CP asymmetries from $\sin 2\beta$ in the penguin-dominated modes (see Sec. 7.2).

2.3 Heavy-Quark Symmetry and Heavy-Quark Effective Theory

In mesons composed of a heavy quark and a light antiquark (plus gluons and $q\overline{q}$ pairs), the energy scale of strong interactions is small compared with the heavy-quark mass. The heavy quark acts as a static point-like color source with fixed four-velocity, which cannot be altered by the soft gluons responsible for confinement. Hence the configuration of the light degrees of freedom (the so-called "brown muck") becomes independent of the spin and flavor (mass) of the heavy quark, which, for N_f heavy-quark flavors, results in a $\mathrm{SU}(2N_f)$ heavy-quark spin-flavor symmetry [22].

Heavy-quark spin-flavor symmetry has many important implications for the spectroscopy and strong decays of B and D mesons (for a review, see e.g. [23]). It is especially predictive for exclusive $B \to D^{(*)}\ell\overline{\nu}$ semileptonic decays, which are relevant for the determination of $|V_{cb}|$

(Sec. 3.2.4). When the weak current suddenly changes the flavor (on a time scale $\ll \Lambda_{\rm QCD}^{-1}$), momentum, and possibly the spin of the b-quark to a c-quark, the brown muck only notices that the four-velocity of the static color source has changed, $v_b \to v_c$. Therefore, the form factors that describe the wave-function overlap between the initial and final mesons become independent of the Dirac structure of weak current, and depend only on a scalar quantity, $w = v_b{\cdot}v_c$. Thus all six $B \to D^{(*)}\ell\overline{\nu}$ form factors are related to a single Isgur-Wise function, $\xi(v_b \cdot v_c)$, which contains all the low-energy nonperturbative hadronic physics relevant for these decays. Moreover, $\xi(1) = 1$ because at zero recoil—where the c quark is at rest in the b quark's rest frame—the configuration of the brown muck does not change at all.

Deviations from the heavy-quark limit can be included using the heavy-quark effective theory (HQET) [24], which provides a systematic expansion in powers of $\alpha_s(m_Q)$ and $\Lambda_{\rm QCD}/m_Q$ ($Q = b, c$). The former type of corrections are calculable perturbatively, whereas the latter ones can be parameterized by a minimal set of hadronic matrix elements that can be extracted from data and/or estimated using nonperturbative techniques. Heavy-quark spin symmetry also implies relations, in combination with chiral symmetry, between, for example, $B \to \rho\ell\overline{\nu}$ and $B \to K^*\ell^+\ell^-$ form factors [25].

2.4 Factorization and Soft-Collinear Effective Theory

Researchers have long known that in the decay $B \to M_1M_2$, if the meson M_1 that inherits the spectator quark from the B is heavy and M_2 is light then "color transparency" can justify factorization [26, 27]. Traditionally, naive factorization refers to the hypothesis that matrix elements of the four-quark operators can be estimated by grouping the quark fields into a pair that can mediate $B \to M_1$ transition and into another pair that describes vacuum $\to M_2$ transition.

Recently the development of the soft collinear effective theory (SCET) [28, 29] put these notions on a firmer footing. SCET is designed to describe the interactions of energetic and low invariant-mass partons in the $Q \gg \Lambda_{\rm QCD}$ limit. It introduces distinct fields for the relevant degrees of freedom, and a power-counting parameter λ. There are two distinct theories, $\rm SCET_I$ in which $\lambda = \sqrt{\Lambda_{\rm QCD}/Q}$ and $\rm SCET_{II}$ in which $\lambda = \Lambda_{\rm QCD}/Q$. They are appropriate for final states with invariant mass $Q\lambda$; i.e., $\rm SCET_I$ for jets and inclusive $B \to X_s\gamma$, $X_u\ell\overline{\nu}$, $X_s\ell^+\ell^-$ decays ($m_X^2 \sim \Lambda_{\rm QCD}Q$), and $\rm SCET_{II}$ for exclusive hadronic final states ($m^2 \sim \Lambda_{\rm QCD}^2$). It is convenient to use light-cone coordinates, decomposing momenta as

$$p^\mu = (\bar{n}\cdot p)\frac{n^\mu}{2} + p_\perp^\mu + (n\cdot p)\frac{\bar{n}^\mu}{2} = p_-\frac{n^\mu}{2} + p_\perp + p_+\frac{\bar{n}^\mu}{2}, \tag{30}$$

where $n^2 = \bar{n}^2 = 0$ and $n\cdot\bar{n} = 2$. For a light quark moving near the n direction, $p_- \gg p_\perp \gg p_+$, and this hierarchy can be used to successively integrate out the less and less off-shell momenta. Factorization has been proven in ($B \to D\pi^\pm$)-type decays [30] to all orders in α_s and at leading order in $\Lambda_{\rm QCD}/Q$ by decoupling the ultrasoft $[(p_-, p_+, p_\perp) \sim Q(\lambda^2, \lambda^2, \lambda^2)]$ gluons from the collinear $[(p_-, p_+, p_\perp) \sim Q(1, \lambda^2, \lambda)]$ Lagrangian at leading order in λ.

The study of heavy to light transitions, which are particularly important for CP violation and CKM measurements, is complicated by the fact that one has to work to subleading order in λ.

This is because collinear and ultrasoft quarks cannot interact at leading order, only via the mixed ultrasoft-collinear Lagrangian, $\mathcal{L}^{(1)}_{\xi q}$, which is suppressed by one power of λ and allowed to couple an ultrasoft and a collinear quark to a collinear gluon [31]. This is relevant for all processes in which the spectator quark in the B ends up in an energetic light meson. So far, maybe the most surprising model-independent result at subleading order is proof of factorization in the previously intractable $B \to D^0\pi^0$ type "color-suppressed" decays [32]. In this case factorization means the systematic separation of the physics associated with different momentum scales, and the factorization theorem can even accommodate a nonperturbative strong phase.

Other important applications include the exclusive semileptonic form factors, and factorization in charmless two-body decays, both of which are subject to intense discussions. For semileptonic $B \to \pi\ell\overline{\nu}$ and $\rho\ell\overline{\nu}$ decays, there are two contributions of the same order in $\Lambda_{\rm QCD}/Q$. It is not yet clear whether or not the factorizable parts that violate the form factor relations [33] are smaller than the nonfactorizable contributions. For charmless decays [34,35], an additional complication is that the power counting appropriate for the charm penguins has not been settled [36, 37].

2.5 The Operator Product Expansion for Inclusive Decays

In the large m_b limit, there is a simple argument based on a separation of scales, that inclusive rates may be modeled by the decay of a free b-quark. The weak decay takes place on a time scale much shorter than the time it takes the quarks in the final state to hadronize. Once the b-quark has decayed, the probability that the decay products hadronize is equal to unity, and the (unknown) probabilities of hadronization to specific final states can be ignored.

This argument can be formalized using an operator product expansion (OPE) [38]. To calculate the semileptonic rates, the leptonic and the hadronic parts of the $\langle X\ell\overline{\nu}\,|H\,|B\rangle$ matrix element can be separated. Nonperturbative strong-interaction effects enter the rate via the hadronic tensor,

$$W^{\mu\nu} = \sum_X (2\pi)^3\,\delta^4(p_B - q - p_X)\,\frac{\langle B|J^{\mu\dagger}|X\rangle\,\langle X|J^\nu|B\rangle}{2m_B}\,, \tag{31}$$

where $J^\mu = \overline{q}\,\gamma^\mu P_L\,b$ for semileptonic B decay. The optical theorem implies that $W^{\mu\nu}$ can be related to the discontinuity across the cut of the forward-scattering matrix element of the time-ordered product,

$$T^{\mu\nu} = -i\int {\rm d}^4x\, e^{-iq\cdot x}\,\frac{\langle B|\,T[J^{\mu\dagger}(x)\,J^\nu(0)]\,|B\rangle}{2m_B}\,, \tag{32}$$

i.e., $W^{\mu\nu} = -\frac{1}{\pi}\,{\rm Im}\,T^{\mu\nu}$. When the energy release to the hadronic final state is large, the time-ordered product can be expanded in local operators, whose B-meson matrix elements can be parameterized using HQET. $T^{\mu\nu}$ is an analytic function with singularities that correspond to on-shell hadronic intermediate states. For semileptonic decays one can deform the integration contour away from the physical region in the complex $q\cdot v$ plane (see Fig. 2), and asymptotic freedom ensures that $T^{\mu\nu}$ can be reliably calculated far from its singularities.

In the $m_b \gg \Lambda_{\rm QCD}$ limit, the OPE reproduces the b-quark decay result, and shows that the leading power-suppressed corrections occur at order $\Lambda^2_{\rm QCD}/m_b^2$ and can be parameterized by two

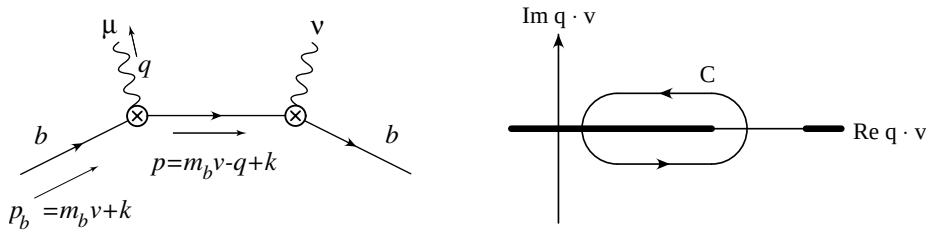

Figure 2: *(Left) Forward-scattering amplitude whose imaginary part gives the decay rate. (Right) Analytic structure of the correlation function in the complex $q\cdot v$ plane and the integration contour that gives the total rate.*

matrix elements, usually denoted by λ_1 and λ_2. The result is of the form

$$\mathrm{d}\Gamma = \begin{pmatrix} b\text{-quark} \\ \text{decay} \end{pmatrix} \times \left[1 + \frac{0}{m_b} + \frac{\mathcal{O}(\lambda_1, \lambda_2)}{m_b^2} + \dots\right]. \tag{33}$$

Most decay rates of interest have been computed including the $\Lambda_{\rm QCD}^3/m_b^3$ corrections (which are parameterized by six additional hadronic matrix elements), whereas the b-quark decay rates have been computed including perturbative corrections at order α_s and $\alpha_s^2\beta_0$ ($\beta_0 = 11 - 2n_f/3$ is the first coefficient of the QCD β-function, and the terms proportional to it often dominate at order α_s^2).

The OPE can also be used to calculate inclusive nonleptonic decays, such as heavy hadron lifetimes, the B_s width difference, $\Delta\Gamma_s$, and the semileptonic CP asymmetry, $A_{\rm SL}$. Whereas the structure of the results is the same as for semileptonic decays, there is no "external" current to the strong interaction in these cases, so there is no variable that can be used to move the integration contour away from the cuts. Therefore, the OPE is performed directly in the physical region, and we expect the accuracy of these calculations to be worse than those for semileptonic decays. Experimental data are crucial to validate each of the applications; in particular, the unexpected smallness of the Λ_b to B lifetime ratio may indicate that the nonleptonic calculations are more difficult to control.

2.6 Lattice QCD

In lattice QCD (LQCD), the functional integral for correlation functions is computed using numerical Monte Carlo integration. To keep the degrees of freedom and the required computational power at an acceptable level, a finite lattice spacing, a, is introduced to discretize space-time, and the calculation is performed within a finite volume. The finite lattice spacing (finite volume) is an ultraviolet (infrared) cutoff, which can be dealt with using field theory techniques to extract cutoff-independent quantities from the results of the computations. In practical calculations the ultraviolet cutoff is typically approximately $a^{-1} \sim$ (2–3) GeV. Consequently, b-quarks can be simulated only using actions based on HQET and nonrelativistic QCD, where m_b is removed from the dynamics using the effective theory. The matching between the lattice and the continuum is in principle straightforward, but in practice it often introduces a significant uncertainty, because $\alpha_s(a^{-1})$ is not small, and few matching calculations have been done beyond one loop.

The most difficult issues are related to how the fermionic part of the action is computed. Until a few years ago, to make the computations manageable, most calculations used the quenched approximation, which amounts to neglecting virtual quark loops. It is not a systematic approximation to QCD and the error associated with it is difficult to estimate. Recent advances in algorithms and computers have allowed an increasing number of quantities to be computed with dynamical u, d, and s-quarks. A remaining source of systematic uncertainty is often the chiral extrapolation. The simulations with light u and d-quarks are computationally expensive, so the use of $m_{u,d}/m_s \sim 1/2$ is not uncommon. To date only the MILC collaboration has used $m_{u,d}/m_s \sim 1/8$, which still has to be extrapolated to the physical values, $m_{u,d}/m_s \sim 1/25$. The results based on MILC's gauge configurations use improved "staggered" quarks. There are several ways to discretize the quark action, and the cost of simulations with light quarks is sensitive to this choice. Unquenched calculations with staggered quarks are much faster than with the Wilson, domain wall, or overlap formulations. In the staggered formulation each field produces four quark "tastes", so there are 16 light mesons. The unphysical ones are removed by taking the fourth root of the fermion determinant. The validity of this fourth-root trick has so far been proven only in perturbation theory.

Recently many new results have emerged in which all these systematic effects are studied in detail. The gold-plated quantities are those that contain at most one hadron in both the initial and final state, not moving with large velocities. These include decay constants, bag parameters, and semileptonic form factors, which are important for flavor physics. For most of these quantities, the currently available calculations using staggered fermions obtain significantly smaller errors than those with Wilson and other formulations. The fastest LQCD computers now run at a computation rate of a few tens of TeraFLOPs, and the PetaFLOP barrier is expected to be passed by the end of this decade. This may allow LQCD to make predictions approaching the percent level, especially if all ingredients of the calculation can be performed numerically (including matching from the lattice to the continuum). With such precision, several measurements in exclusive decays, which are sensitive to new physics but are presently dominated by theoretical uncertainties in the corresponding matrix elements, could become precise tests of the SM (such as $B \to \rho\gamma$, $B \to \pi\ell\bar{\nu}$, ε_K, etc.).

3 Determining Magnitudes of CKM Elements

Determining of the magnitudes of CKM elements uses a number of sophisticated theoretical and experimental techniques, the complete discussion of which is beyond the scope of this review. We concentrate on topics where recent developments have occurred.

3.1 $|V_{ud}|$ from β-Decays

The CKM matrix element $|V_{ud}|$ has been extracted by three different methods: superallowed nuclear β-decays with pure Fermi transitions ($0^+ \to 0^+$), neutron β-decay ($n \to pe\overline{\nu}_e$), and pion β-decay ($\pi^+ \to \pi^0 e^+ \nu_e(\gamma)$). All three methods involve the hadronic form factor of the vector current $\langle f|\overline{u}\gamma_\mu d|i\rangle$, where $|i\rangle$ and $|f\rangle$ are the initial and final states of the transitions.

The neutron β-decay also involves an axial-vector form factor, which requires external input for the ratio of the axial-vector to the vector coupling constants. The form factors describe the long-distance hadronic effects that confine the quarks within hadrons. The normalization of the vector current is fixed at the kinematic endpoint of zero-momentum transfer between initial and final states, and at the exact isospin limit ($m_u = m_d$). Isospin-breaking corrections are suppressed by the quark mass difference divided by the hadronic scale.

Superallowed nuclear β-decays give the best experimental precision. The product of the integral over the emitted electron energy spectrum and the neutron lifetime is proportional to $|V_{ud}|^{-2}$. Radiative and charge symmetry breaking corrections, which depend in part on the nuclear structure of the nucleus under consideration must be applied. They lie between 3.1% and 3.6% for the nine superallowed transitions that give the best sensitivity [39]. Recent theoretical improvements in the calculation of loop contributions, notably for the problematic γW box diagram, and a detailed error analysis achieved a reduction in uncertainty by a factor of two to 1.9×10^{-4} [40]. With this, the world average is $|V_{ud}|_{0^+\to 0^+} = 0.97377 \pm 0.00027$ [41].

From a theoretical point of view, the neutron β-decay, or ultimately the pion β-decay, represent the cleanest determination of $|V_{ud}|$, because they are free from nuclear structure effects. Because no other decay channels exist, the decay rate can be obtained from lifetime measurements. The PERKEO-II experiment achieved significant improvement in this $|V_{ud}|$ determination owing to the precise measurement of $g_A/g_V = -1.2739 \pm 0.0019$ [42] (confirmed in Ref. [43]), a value that is, however, significantly larger than earlier measurements. Several new experiments are planned or are in construction to remeasure this quantity. Unfortunately, there is currently a problem with the second input to determine $|V_{ud}|$ from neutron β-decays, namely a large discrepancy between a new neutron lifetime measurement [44] and the PDG average [45]. Such a discrepancy, if confirmed, would significantly impact the extracted value for $|V_{ud}|$, and hence CKM unitarity. Ignoring this measurement, the present world average from neutron β-decays is $|V_{ud}|_{n_\beta} = 0.9730 \pm 0.0004 \pm 0.0012 \pm 0.0002$ [41], where the errors arise from the neutron lifetime, from g_A/g_V, and from radiative corrections, respectively. Note that the change induced by the new lifetime measurement, if confirmed, would be as large as three times the total error quoted.

The pion β-decay $\pi^+ \to \pi^0 e^+ \nu_e$ is an attractive candidate to extract $|V_{ud}|$ from the branching ratio of the decay and the pion lifetime. It is mediated by a pure vector transition. Unfortunately, because of the small branching ratio of 10^{-8}, the statistical precision is not yet competitive with the other methods: $|V_{ud}| = 0.9748 \pm 0.0025$ [46, 41].

3.2 CKM Elements from (Semi)Leptonic Decays

3.2.1 Leptonic Decays

The decay rate of the lightest pseudoscalar meson, M—which is composed of the quarks $q_d \bar{q}_u$—to a lepton antineutrino pair is given by

$$\Gamma\left(M^- \to \ell^- \overline{\nu}_\ell\right) = \frac{G_F^2}{8\pi} |V_{q_u q_d}|^2 f_M^2 m_M m_\ell^2 \left(1 - \frac{m_\ell^2}{m_M^2}\right)^2 , \tag{34}$$

where the decay constant f_M, defined by $i f_M p^\mu = \langle 0 | \bar{q}_u \gamma^\mu \gamma_5 q_d | M(p) \rangle$, contains all the nonperturbative strong-interaction physics. If f_M is known, then leptonic π, K, D, D_s, B, and B_c

decay rates determine $|V_{ud}|$, $|V_{us}|$, $|V_{cd}|$, $|V_{cs}|$, $|V_{ub}|$, and $|V_{cb}|$, respectively.

Owing to the m_ℓ^2 suppression, however, these rates are small for $\ell = \mu$ or e, and the τ final state is harder to reconstruct experimentally. The current errors of the LQCD determinations of the decay constants are around the 10% level, so the observed leptonic K, D, D_s and B decays do not give competitive direct determinations of the corresponding CKM elements. However, ratios of decay constants are easier to determine in LQCD, and a recent calculation of $f_K/f_\pi = 1.198 \pm 0.003^{+0.016}_{-0.005}$ [47] allows $|V_{us}/V_{ud}|$ to be extracted from the ratio of leptonic K and π decays, yielding $|V_{us}| = 0.2245^{+0.0012}_{-0.0031}$ [48]. The ratios f_{D_s}/f_D and f_{B_s}/f_B are also known much more precisely than the individual decay constants. However, the experimental errors are still sizable for $D \to \ell\overline{\nu}$, and because the B_s meson is neutral, it cannot decay to a $\ell\overline{\nu}$ pair.[5]

Metrologically useful experimental information exists for the decay $B^+ \to \tau^+\nu_\tau$, where averaging the experimental likelihoods from Belle (reporting a 4.2σ evidence for this decay) and *BABAR* [50] gives $(10.4\,^{+3.0}_{-2.7}) \times 10^{-5}$ for the branching fraction, which is consistent with the prediction, $(9.6 \pm 1.5) \times 10^{-5}$, from the global CKM fit (not including the direct measurement) [51]. It is interesting to study the constraint obtained from this measurement in conjunction with the measurement of the $B^0\overline{B}^0$ oscillation frequency, Δm_d, which also depends on f_B, so that f_B cancels in the combination. The allowed regions obtained in the $(\overline{\rho}, \overline{\eta})$ plane are shown in Fig. 3. The remaining theoretical uncertainty stems from the bag parameter, B_B, that enters the SM prediction of Δm_d [see Eq. (45)].

3.2.2 $|V_{us}|$

Traditionally, the magnitude of V_{us} has been extracted from semileptonic K decays, which can be analyzed using chiral perturbation theory. The $K \to \pi\ell\nu$ amplitude can be expanded in powers of the K and π momenta and the quark masses divided by a scale of order $\Lambda_{\chi\mathrm{SB}}$. The decay rates for $K = K^\pm, K^0$ and $\ell = e, \mu$ can be written as [41]

$$\Gamma(K \to \pi\ell\overline{\nu}) = \frac{G_F^2 m_K^5}{128\pi^3}\, C\, I^{K\ell}\, |V_{us}|^2 \left| f_+^{K^0\pi^-}(0) \right|^2 (1 + \ldots)\,, \tag{35}$$

where $C = 1$ (1/2) for K^0 ($K^\pm$) decays, $I^{K\ell}$ is a phase-space integral depending on the shape of the form factor, $f_+(q^2)$, and the dots stand for isospin-breaking and electroweak corrections. It is convenient to factor out $f_+^{K^0\pi^-}(0) \equiv f_+(0)$, because the Ademolo-Gatto theorem [52] implies that there is no $\mathcal{O}(p^2)$ correction to $f_+(0)$, i.e., $f_+(0) = 1 + f_{p^4} + f_{p^6}$. Most of the $\mathcal{O}(p^4)$ corrections are known in terms of physical parameters, and beyond this the estimates are model dependent. The original value, $f_+(0) = 0.961 \pm 0.008$ [53], is still broadly accepted, although some other calculations differ by as much as 2%, with uncertainties around 1% [41]. It will be interesting to see whether unquenched LQCD results confirm this estimate. Significant progress on the experimental side has taken place recently. After a high-statistics measurement of the $\mathcal{B}(K^+ \to \pi^0 e^+ \nu)$ [54], a suite of measurements of neutral-kaon branching ratios [55],

[5] The hadronic physics relevant to the rare decay $B_s \to \ell^+\ell^-$ is also governed by f_{B_s}, and once the decay is measured at the LHC, it will give a precise determination of $|V_{ub}|$ from the double ratio $[\mathcal{B}(B \to \ell\overline{\nu})/\mathcal{B}(B_s \to \ell^+\ell^-)] \times [\mathcal{B}(D_s \to \ell\overline{\nu})/\mathcal{B}(D \to \ell\overline{\nu})]$ [49]. This double ratio can also give a precise SM prediction for $B_s \to \ell^+\ell^-$, and $B \to \ell\overline{\nu}$ can even be replaced by $B \to \ell^+\ell^-$.

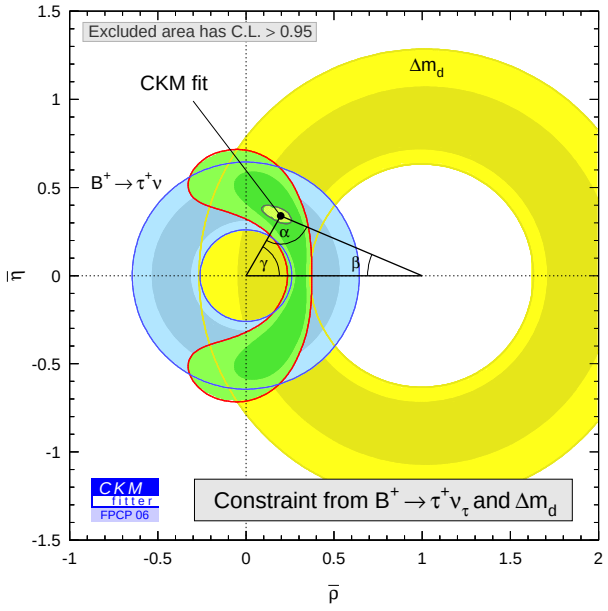

Figure 3: *Constraints of 95% C.L. in the* $(\overline{\rho},\overline{\eta})$ *plane from the* $B^+ \to \tau^+\nu_\tau$ *branching fraction,* Δm_d*, and the combined use of these [51] (darker shades indicate 68%* C.L. *regions) [50]. The results are compared with the global CKM fit (cf. Sec. 6).*

of form factors [56], and of lifetime [57] followed. From semileptonic kaon decays one obtains $|V_{us}| = 0.2257 \pm 0.0021$.

The τ spectral function into $|\Delta S| = 1$ final states can be used to determine the s-quark mass and the CKM element $|V_{us}|$ [58]. Although the determination of $\overline{m}_s(m_\tau)$ is strongly model dependent, the determination of $|V_{us}|$ appears on safe grounds, because it relies on the non-weighted spectral function with maximum inclusiveness and a better control of the perturbative expansion. Present data give [59] $|V_{us}| = 0.2204 \pm 0.0028 \pm 0.0003 \pm 0.0001$, where the first error is experimental, the second theoretical and the third due to m_s (taken from LQCD).

3.2.3 $|V_{cs}|$ and $|V_{cd}|$

For the dominant semileptonic D decays, $D \to K^{(*)}\ell\nu$, neither heavy-quark nor chiral symmetry is particularly useful. Hence, until recently, the only precise direct constraint involving $|V_{cs}|$ was from the leptonic branching ratio of the W, which measured the sum of CKM elements in the first two rows (corrected for effects from perturbative QCD), $\sum_{i,j\in\{u,c,d,s,b\}} |V_{ij}|^2 = 1.999 \pm 0.026$ [60] (compared with the expected value of two), providing a precise test of unitarity.

Fortunately, the $D \to K\ell\nu$ and $\pi\ell\nu$ decays are well suited for LQCD calculations, because the charm quark is neither too heavy nor too light, and the maximal momenta of the final state K or π is not too large. Together with the CLEO-c program, it promises significant advances both in the measurements of $|V_{cs}|$ and $|V_{cd}|$ as well as in our understanding of the robustness of LQCD calculations from which B physics will also benefit.

The direct determination of $|V_{cs}|$ and $|V_{cd}|$ is possible from semileptonic D or leptonic D_s decays, relying on the form factors (which depend on the invariant mass of the lepton pair, q^2).

Recently, the first three-flavor unquenched LQCD calculations for $D \to K\ell\overline{\nu}$ and $D \to \pi\ell\overline{\nu}$ were published [61]. Using these calculations, and the isospin-averaged charm semileptonic widths measured by CLEO-c, one obtains [62]

$$|V_{cd}| = 0.213 \pm 0.008 \pm 0.021\,, \qquad |V_{cs}| = 0.957 \pm 0.017 \pm 0.093\,, \tag{36}$$

where the first errors are experimental, and the second theoretical due to the form factors.[6] Note that both $|V_{cs}|$ and $|V_{cd}|$ are determined much more precisely if CKM unitarity is assumed, with uncertainties around 0.0002 and 0.001, respectively (see Table 3 on p. 43). Therefore, these measurements do not affect the global CKM fit at present.

3.2.4 $|V_{cb}|$

The CKM element $|V_{cb}|$ can be extracted from exclusive and inclusive semileptonic B decays. The determination from exclusive $B \to D^{(*)}\ell\overline{\nu}$ uses an extrapolation of the measured rates to zero recoil, $w = 1$ (i.e., maximal momentum transfer to the leptons, $q^2_{\rm max}$). The rates can be written schematically as

$$\frac{{\rm d}\Gamma(B \to D^{(*)}\ell\overline{\nu})}{{\rm d}w} = (\text{known terms}) \times |V_{cb}|^2 \times \begin{cases} (w^2-1)^{1/2}\,\mathcal{F}_*^2(w)\,, & \text{for } B \to D^*, \\ (w^2-1)^{3/2}\,\mathcal{F}^2(w)\,, & \text{for } B \to D\,. \end{cases} \tag{37}$$

Heavy-quark symmetry (see Sec. 2.3) determines the rate at $w = 1$, that is, in the $m_Q \gg \Lambda_{\rm QCD}$ limit ($Q = b, c$), $\mathcal{F}(w) = \mathcal{F}_*(w) = \xi(w)$, and in particular $\mathcal{F}_{(*)}(1) = 1$, allowing for a model-independent determination of $|V_{cb}|$. The corrections to the heavy-quark limit can be organized in expansions in $\alpha_s(m_Q)$ and $\Lambda_{\rm QCD}/m_Q$, which take the form

$$\begin{aligned} \mathcal{F}_*(1) &= 1 + c_A(\alpha_s) + \frac{0}{m_Q} + \frac{(\text{LQCD or models})}{m_Q^2} + \dots\,, \\ \mathcal{F}(1) &= 1 + c_V(\alpha_s) + \frac{(\text{LQCD or models})}{m_Q} + \dots\,. \end{aligned} \tag{38}$$

Heavy-quark symmetry implies that the leading-order results are unity, whereas the absence of the $\Lambda_{\rm QCD}/m_Q$ correction to $\mathcal{F}_*(1)$ is due to Luke's theorem [63]. The perturbative corrections $c_A = -0.04$ and $c_V = 0.02$ are known to order α_s^2 [64], and higher-order terms are below the 1% level. The terms indicated by "LQCD or models" are known only from quenched LQCD [65] or phenomenological models. The experimental results for the rates, extrapolated to $w = 1$ are [66]

$$|V_{cb}|\,\mathcal{F}_*(1) = (37.6 \pm 0.9) \times 10^{-3}\,, \qquad |V_{cb}|\,\mathcal{F}(1) = (42.2 \pm 3.7) \times 10^{-3}\,. \tag{39}$$

Using $\mathcal{F}_*(1) = 0.91 \pm 0.04$, yields $|V_{cb}| = (41.3 \pm 1.0_{\rm exp} \pm 1.8_{\rm th}) \times 10^{-3}$. The $B \to D\ell\overline{\nu}$ data are consistent with this, but to make a real test, smaller experimental errors and unquenched LQCD calculations are needed.

The inclusive determination of $|V_{cb}|$ is based on the OPE (see Sec. 2.5). The state of the art is that the semileptonic rate, as well as moments of the lepton energy and the hadronic

[6] The most precise measurement of $|V_{cd}|$ still comes from charm production in neutrino scattering. The PDG quotes $|V_{cd}| = 0.230 \pm 0.011$ [48], an uncertainty that will be hard to reduce, whereas that from Eq. (36) will improve with better LQCD calculations and data.

invariant-mass spectra with varying cuts have been computed to orders $\Lambda^3_{\rm QCD}/m_b^3$ and $\alpha_s^2\beta_0$. Their dependence on $m_{b,c}$ and the parameters that occur at subleading orders in $\Lambda_{\rm QCD}/m_b$ are different. The expressions for a large number of observables are of the form

$$\begin{aligned}\Gamma(B\to X_c\ell\overline{\nu}) = {} & \frac{G_F^2|V_{cb}|^2}{192\pi^3}\left(\frac{m_\Upsilon}{2}\right)^5(0.534)\Big[1-0.22\Big(\frac{\Lambda_{1S}}{500\ \text{MeV}}\Big)\\ & -0.011\Big(\frac{\Lambda_{1S}}{500\ \text{MeV}}\Big)^2-0.052\Big(\frac{\lambda_1}{(500\ \text{MeV})^2}\Big)-0.071\Big(\frac{\lambda_2}{(500\ \text{MeV})^2}\Big)\\ & +0.096\varepsilon-0.030\varepsilon^2_{\rm BLM}+0.015\varepsilon\Big(\frac{\Lambda_{1S}}{500\ \text{MeV}}\Big)+\ldots\Big],\end{aligned} \tag{40}$$

where m_Υ is the $\Upsilon(1S)$ mass. The precise determination of $|V_{cb}|$ requires the use of an appropriate short-distance quark mass, the so-called "threshold" mass [67, 68], and $\Lambda_{1S}\equiv m_\Upsilon/2-m_b^{1S}$ is related to one of these, m_b^{1S} [67, 69]. The $\Lambda^2_{\rm QCD}/m_b^2$ corrections are parameterized by $\lambda_{1,2}$. The $\Lambda^3_{\rm QCD}/m_b^3$ terms are known and are parameterized by six more nonperturbative matrix elements. For the perturbative corrections $\varepsilon\equiv 1$ shows the order in the expansion, and the BLM subscript shows that only the terms with the highest power of β_0 are known [70]. Such formulas are fit to approximately 90 (correlated) observables obtained from the lepton energy and hadronic invariant-mass spectra. The fits determine $|V_{cb}|$ and the hadronic parameters, and their consistency provides a powerful test of the theory. The fits have been performed in several schemes and give [71, 72],

$$|V_{cb}| = (41.7\pm 0.7)\times 10^{-3}, \tag{41}$$

where the central values were averaged and the errors quoted in each paper were retained. The same fits simultaneously determine the quark masses, $m_b^{1S}=(4.68\pm0.03)$ GeV and $\overline{m}_c(\overline{m}_c)=(1.22\pm0.06)$ GeV [71, 73], which correspond to $\overline{m}_b(\overline{m}_b)=(4.18\pm0.04)$ GeV and $m_c^{1S}=(1.41\pm0.05)$ GeV. The m_b-m_c mass difference is even better constrained [71, 72].

3.2.5 $|V_{ub}|$

Of the measurements of $|V_{ub}|$ from exclusive decays, $B\to\pi\ell\overline{\nu}$ is the most advanced, as both experiment and LQCD calculations are under the best control. The determination relies on measuring the rate and calculating the form factor $f_+(q^2)$,

$$\frac{{\rm d}\Gamma(\overline{B}^0\to\pi^+\ell\overline{\nu})}{{\rm d}q^2} = \frac{G_F^2|\vec{p}_\pi|^3}{24\pi^3}\,|V_{ub}|^2\,|f_+(q^2)|^2\,. \tag{42}$$

Unquenched calculations of f_+ exist only for $q^2>16$ GeV^2 (small $|\vec{p}_\pi|$) [74, 75], where the available statistics is reduced because the phase space is proportional to $|\vec{p}_\pi|^3$. Averaging the LQCD calculations, and using data only in the $q^2>16$ GeV^2 region, gives $|V_{ub}|=(4.13\pm0.62)\times 10^{-3}$ [66, 76].

Some of the current $|V_{ub}|$ determinations use model-dependent parameterizations of $f_+(q^2)$ to extend the LQCD results to a larger part of the phase space, or to combine them with QCD sum-rule calculations at small q^2 (which tend to give smaller values for $|V_{ub}|$ [77]). These model-dependent ingredients can be avoided using constraints on the shape of $f_+(q^2)$ that follow from dispersion relations and the knowledge of $f_+(q^2)$ at a few values of q^2 [78]. The recent

LQCD results revitalized this area [79,80]. Using the LQCD calculations of f_+ at large q^2, the experimental measurements, and the dispersion relation to constrain the shape of $f_+(q^2)$, gives $|V_{ub}| = (3.92 \pm 0.52) \times 10^{-3}$ [79], using the full q^2 range.

The determination of $|V_{ub}|$ from inclusive semileptonic B decay is more complicated than that of $|V_{cb}|$, because of the large $B \to X_c \ell \overline{\nu}$ background. Much of the recent experimental progress is related to the fact that the B-factories produce pure $B\overline{B}$ pairs, where the full reconstruction of one B allows the measurement of the energy and momenta of both the leptonic and the hadronic systems in the $X_u \ell \overline{\nu}$ decay of the other B (the so-called "B-beam" technique). This provides several handles to suppress the $B \to X_c \ell \overline{\nu}$ background. The total $B \to X_u \ell \overline{\nu}$ rate is known theoretically at the 5% level [67,68], but the cuts used in most experimental analyses to remove the $B \to X_c \ell \overline{\nu}$ background complicate the theory. The local OPE used to extract $|V_{cb}|$ is applicable for $B \to X_u \ell \overline{\nu}$ if the typically allowed m_X and E_X of the final state satisfy

$$m_X^2 \gg E_X \Lambda_{\rm QCD} \gg \Lambda_{\rm QCD}^2 \,. \tag{43}$$

However, most of the current $|V_{ub}|$ determinations restrict the phase space to (a subset of) the $m_X < m_D$ region. As a result, there are three qualitatively different regions.

If $m_X \sim \Lambda_{\rm QCD}$, the final state is dominated by resonances, and it is not possible to compute inclusive quantities reliably. If $m_X^2 \sim E_X \Lambda_{\rm QCD} \gg \Lambda_{\rm QCD}^2$, the OPE becomes an expansion in terms of b-quark light-cone distribution functions (sometimes termed shape functions). This is the case for many measurements to date, such as the rate for $E_\ell > (m_B^2 - m_D^2)/(2m_B)$, $m_X < m_D$, or $P_X^+ (\equiv E_X - |\vec{p}_X|) < m_D^2/m_B$. At leading order one such nonperturbative function occurs [81,82], which can be determined from the $B \to X_s \gamma$ photon spectrum. At order $\Lambda_{\rm QCD}/m_b$ there are several new functions [83], which cannot be extracted from the data, and are modelled. The hadronic physics parameterized by functions is a significant complication compared with the determination of $|V_{cb}|$, where it is encoded in a few hadronic matrix elements. Moreover, at order α_s, moments of the shape function are no longer given simply by local hadronic matrix elements [84, 85]. One can either fit the shape function from $B \to X_s \gamma$, or directly relate the $B \to X_u \ell \overline{\nu}$ partial rates to weighted integrals of the $B \to X_s \gamma$ spectrum [86]. Finally, if $m_X^2 \gg E_X \Lambda_{\rm QCD} \gg \Lambda_{\rm QCD}^2$, the OPE converges, and the first few terms give reliable results. This is the case for the rate for $q^2 > (m_B - m_D)^2$ [87], but the expansion parameter is then $\Lambda_{\rm QCD}/m_c$. The dependence on the shape function can be kept under control by combining q^2 and m_X cuts. The shape-function dependence can also be reduced by extending the measurements into the $B \to X_c \ell \overline{\nu}$ region. Recent analyses could measure the $B \to X_u \ell \overline{\nu}$ rates for $|\vec{p}_e| \geq 1.9\,\text{GeV}$ [88] and for $m_X < 2.5$ GeV [89]. Averaging these inclusive measurements, the Heavy Flavor Averaging Group (HFAG) obtains $|V_{ub}| = (4.38 \pm 0.19 \pm 0.27) \times 10^{-3}$ [66] using [85], which indicates a slight tension with the CKM fit for $|V_{ub}|$ dominated by the $\sin 2\beta$ measurement (cf. Table 3 on p. 43).

3.3 CKM Elements from Rare Loop-Mediated B Decays

To measure $|V_{td}|$ and $|V_{ts}|$, one has to rely on loop-mediated rare B decays, or rare K decays discussed in Sec. 4.3, or $B\overline{B}$ oscillations discussed in Sec. 3.4. All of them provide important

tests of the SM, as different transitions can receive different contributions from new physics.

The inclusive branching fraction $\mathcal{B}(B \to X_s\gamma) = (3.39\,^{+0.30}_{-0.27}) \times 10^{-4}$ [66] is sensitive to $|V_{tb}V_{ts}^*|$ via penguin diagrams with a top quark. A large contribution to the rate stems from the $b \to c\bar{c}s$ four-quark operator, O_2^c in Eq. (28), mixing into the electromagnetic penguin operator, O_7. Using unitarity, $V_{cb}V_{cs}^* = -V_{tb}V_{ts}^* - V_{ub}V_{us}^*$, the measured rate implies $|V_{tb}V_{ts}^*| = (39.0 \pm 3.1) \times 10^{-3}$ [48].

The theoretical uncertainties can be reduced by taking ratios of processes that are equal in the flavor SU(3) limit to determine $|V_{td}/V_{ts}|$. The exclusive rare decays suffer from larger theoretical uncertainties owing to unknown hadronic form factors, but exclusive branching fractions are easier to measure. Recently, Belle observed the first $b \to d\gamma$ signals in $B \to (\rho/\omega)\gamma$ decays. We define the ratios of branching fractions

$$\frac{\mathcal{B}(B \to \rho\gamma)}{\mathcal{B}(B \to K^*\gamma)} = \left|\frac{V_{td}}{V_{ts}}\right|^2 \left(\frac{m_B - m_\rho}{m_B - m_{K^*}}\right)^3 \times \begin{cases} \frac{1}{2}(\xi_{V^0\gamma})^{-2}\,, & \text{for } V^0\gamma\,, \\ (\xi_{V^\pm\gamma})^{-2}\,, & \text{for } V^\pm\gamma\,, \end{cases} \tag{44}$$

where $\xi_{V^0\gamma}$ and $\xi_{V^\pm\gamma}$ denote SU(3)-breaking corrections. The ratio of the neutral rates gives the theoretically cleaner determination of $|V_{td}/V_{ts}|$, because weak annihilation enters in the $\rho^\pm\gamma$ mode, but only W exchange contributes to $\rho^0\gamma$. (Although both annihilation and exchange are suppressed by $\Lambda_{\rm QCD}/m_b$, they are hard to estimate, and exchange is color-suppressed compared with annihilation.) Averaging the results from *BABAR* and Belle [90, 66] gives $\mathcal{B}(B^0 \to \rho^0\gamma)/\mathcal{B}(B^0 \to K^{*0}\gamma) = 0.0095 \pm 0.0045$ [66]. Using the estimate $\xi_{V^0\gamma} = 1.2 \pm 0.1$ for this average [91] implies $|V_{td}/V_{ts}| = 0.16 \pm 0.05$. Although the theoretical uncertainty for this determination of $|V_{td}/V_{ts}|$ will not compete with that for $\Delta m_d/\Delta m_s$, it provides an important test of the SM, as new physics could contribute differently to these decays and to $B\overline{B}$ mixing (cf. right plot of Fig. 4).

3.4 Neutral B-Meson Oscillation

The $B^0\overline{B}^0$ oscillation frequency is governed by the mass difference Δm_d between the two B^0 mass eigenstates, B_H and B_L. It is defined as a positive number and has been measured by many experiments leading to an overall 1% precision, $\Delta m_d = (0.507 \pm 0.005)\,\text{ps}^{-1}$ (dominated by the measurements at the B-factories) [66]. In analogy to $|\varepsilon_K|$ (see below), $B^0\overline{B}^0$ oscillation in the SM is described by FCNC box diagrams. However, in contrast to $|\varepsilon_K|$, where the large quark-mass-dependent hierarchy in the FCNC amplitude is offset by the tiny CKM matrix element $|V_{td}V_{ts}^*|$, the $\Delta B = 2$ box diagrams are dominated by intermediate top quarks. This implies that Δm_d is determined by short-distance physics up to the matrix element of the $(\overline{d}\gamma^\mu(1-\gamma_5)b)^2$ operator, parameterized by $f_{B_d}^2 B_d$,

$$\Delta m_d = \frac{G_{\rm F}^2}{6\pi^2}\eta_B m_{B_d} f_{B_d}^2 B_d m_W^2 S(x_t)\,|V_{td}V_{tb}^*|^2\,. \tag{45}$$

Here $\eta_B = 0.551 \pm 0.007$ is a perturbative QCD correction to the Inami-Lim function $S(x_t)$ (with $x_t = \overline{m}_t^2/m_W^2$) [92], and $f_{B_d}\sqrt{B_d}$ is taken from LQCD. Much progress has been achieved in this domain with unquenched calculations becoming available (see Sec. 2.6). A fixed value of the CKM factor $|V_{td}V_{tb}^*|^2$ occurring in Eq. (45) describes approximately a circle around $(1,0)$ in the $(\overline{\rho},\overline{\eta})$ plane, to which an elliptic distortion appears only at order λ^6.

In the SM, the mass difference Δm_s between the heavy and the light B_s^0 mass eigenstates has only $\mathcal{O}(\lambda^2)$ dependence on the Wolfenstein parameters $\overline{\rho}$, $\overline{\eta}$. A measurement of Δm_s is nevertheless useful for CKM metrology within the SM, because it leads to an improvement in the constraint from the Δm_d measurement on $|V_{td}V_{tb}^*|^2$. Its SM prediction is given by

$$\Delta m_s = \frac{G_{\rm F}^2}{6\pi^2}\eta_B m_{B_s}\xi^2 f_{B_d}^2 B_d m_W^2 S(x_t)\,|V_{ts}V_{tb}^*|^2\ , \tag{46}$$

where the parameter $\xi = f_{B_s}\sqrt{B_s}/f_{B_d}\sqrt{B_d}$ quantifies SU(3)-breaking corrections to the matrix elements, which can be calculated more accurately in LQCD than the matrix elements themselves. Hence a measurement of Δm_s reduces the uncertainty of $f_{B_d}\sqrt{B_d}$. LQCD calculations using Wilson fermions have to work with light-quark masses of order 100 MeV, so calculations for B^0 mesons need to be extrapolated to the chiral (massless) limit. This is not necessary for the B_s^0 due to the relatively heavy strange quark. The use of staggered fermions allows LQCD calculations to be performed with significantly smaller light-quark masses, which implicates smaller systematic uncertainties.

Because of the large ratio $|V_{ts}/V_{td}|^2$ and SU(3)-breaking corrections, $B_s^0\overline{B}_s^0$ oscillation occurs approximately 35 times faster than $B^0\overline{B}^0$ oscillation. Also, measurements of the time-integrated mixing probability χ_s indicate a value close to its maximum, 1/2, requiring very fast oscillation. Excellent proper-time resolution and large data samples are needed to resolve $B_s^0\overline{B}_s^0$ oscillation in the detector. Because only pairs of the two lightest B mesons can be produced in $\Upsilon(4S)$ decays, $B_s^0\overline{B}_s^0$ oscillation can be probed only at high-energy e^+e^- or hadron colliders.

Lower limits on Δm_s have been obtained by the LEP, SLD and Tevatron experiments. A convenient approach to averaging the various results is the amplitude method ([93]; see also the studies in Refs. [13, 94]). It consists of introducing an ad hoc amplitude coefficient, $\mathcal{A}$, placed in front of the cosine modulation term that describes the time-dependent mixing asymmetry $(N_{\rm unmixed}(t) - N_{\rm mixed}(t))/(N_{\rm unmixed}(t) + N_{\rm mixed}(t)) = \mathcal{A}\cdot\cos(\Delta m_s t)$. The advantage of this indirect probe for oscillation is that the dependence on $\mathcal{A}$ is linear so that $\mathcal{A}$ is Gaussian distributed. The measured amplitude must reach $\mathcal{A} = 1$ at the true values of Δm_s (if within reach of the experimental sensitivity), and zero elsewhere. The preliminary combined 95% C.L. lower limit was $\Delta m_s > 16.6\,{\rm ps}^{-1}$ [66].

Shortly before finalizing this review, the DØ and CDF Collaborations reported new preliminary results on $B_s^0\overline{B}_s^0$ oscillation using data samples corresponding to an integrated luminosity of $1\,{\rm fb}^{-1}$. Using the charge of the muon in a partially reconstructed $B_s^0 \to D_s^-\mu^+\nu_\mu$ decay to tag the flavor of the B_s^0 meson, DØ sets the 90% C.L. interval $17\,{\rm ps}^{-1} < \Delta m_s < 21\,{\rm ps}^{-1}$ [95]. Because the upper bound is close to the sensitivity limit of the measurement, larger Δm_s values are excluded only at the 2.1σ level. Using hadronic and semileptonic B_s^0 decays, CDF finds [96]

$$\Delta m_s = \left(17.31\,^{+0.33}_{-0.18} \pm 0.07\right)\ {\rm ps}^{-1}\,, \tag{47}$$

where the first error is statistical and the second is systematic. The probability that the observed signal is a background fluctuation is quoted as 0.2% (5%) for CDF (DØ). The value of Δm_s is in agreement with the prediction from the global CKM fit, $(21.7\,^{+5.9}_{-4.2})\,{\rm ps}^{-1}$, obtained without using the measurement in the fit (cf. Table 2 on p. 42). The preliminary world-average amplitude

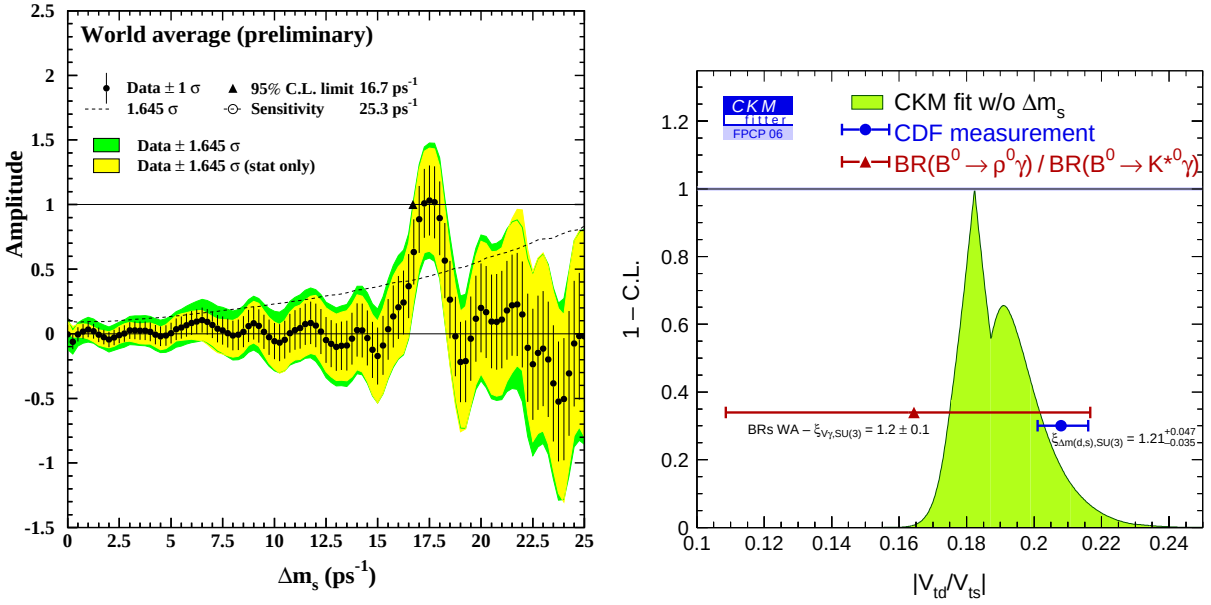

Figure 4: *Left: preliminary world-average amplitude spectrum as a function of Δm_s [66], dominated by the recent CDF measurement [96]. Right: $|V_{td}/V_{ts}|$ determined by CDF from the ratio $\Delta m_d/\Delta m_s$ (full circle) [96], from the ratio $\mathcal{B}(B^0 \to \rho^0\gamma)/\mathcal{B}(B^0 \to K^{*0}\gamma)$ (triangle) (see Sec. 3.3), and from the global CKM fit (shaded region; not including Δm_s in the fit (see Sec. 6).*

scan is shown in the left plot of Fig. 4. The combined signal significance amounts to 3.8σ at $17.5\,\mathrm{ps}^{-1}$ [66]. CDF infers from its measurement of Δm_s that the ratio of CKM elements $|V_{td}/V_{ts}| = 0.208\,^{+0.008}_{-0.006}$ (dominated by the theoretical uncertainty on $\xi = 1.21\,^{+0.047}_{-0.035}$, used by CDF). A comparison with the CKM fit is given in the right plot of Fig. 4. This measurement provides the first strong indication that $B_s^0\overline{B}_s^0$ mixing is probably SM-like.

4 CKM Matrix Constraints from Kaon Physics

The neutral-kaon system constrains the UT through $K^0\overline{K}^0$ mixing, through indirect and direct *CP* violation,[7] and through the rare decays $K^+ \to \pi^+\nu\overline{\nu}$ and the yet unobserved $K_L^0 \to \pi^0\nu\overline{\nu}$. In this case, contrary to Eq. (23), the convention is to label the states by their lifetimes, $|K_{S,L}^0\rangle = p_K|K^0\rangle \pm q_K|\overline{K}^0\rangle$ (experimentally, $m_{K_L^0} > m_{K_S^0}$). The SM prediction for Δm_K suffers from badly controlled long-distance contributions to the mixing amplitudes. Nonperturbative physics with large hadronic uncertainties also impede a reliable SM prediction of direct *CP* violation. The above-mentioned rare decays are cleaner and will give precise constraints as soon as they are measured with sufficient accuracy. They are discussed in Sec 4.3.

[7] "Indirect" *CP* violation refers to situations in which the *CP*-violating phase can be chosen to appear only in the mixing amplitudes, whereas "direct" *CP* violation occurs when a *CP* violating phase must appear in decay amplitudes. The observables $\mathrm{Im}\,\varepsilon_K$ and $\mathrm{Im}\,\varepsilon'_K$ measure *CP* violation in the interference between decays with and without mixing, whereas $\mathrm{Re}\,\varepsilon_K$ and $\mathrm{Re}\,\varepsilon'_K$, measure *CP* violation in mixing and in decay, respectively.

4.1 Indirect *CP* Violation

The most precise measurement of the *CP*-violation parameter ε_K uses η_{+-} and η_{00}—which are the ratios of K_L^0 and K_S^0 amplitudes to a pair of pions, $\eta_{ij} = A(K_L^0 \to \pi^i\pi^j)/A(K_S^0 \to \pi^i\pi^j)$—so that

$$\varepsilon_K = \frac{2}{3}\,\eta_{+-} + \frac{1}{3}\,\eta_{00}\,. \tag{48}$$

This is motivated by the so-called $\Delta I = \frac{1}{2}$ rule, i.e., that the amplitude to two pions in an $I = 0$ state is approximately 20 times larger than the amplitude to two pions in $I = 2$. The definition of ε_K ensures that only the dominant hadronic amplitude contributes, so *CP* violation in decay gives negligible contribution to ε_K, and so $\varepsilon_K \approx [1 - \lambda_{\pi\pi(I=0)}]/2$ (and $2\mathrm{Re}\,\varepsilon_K \approx 1 - |q_K/p_K|$). The phase of ε_K is independent of CKM elements (and of new physics), and is approximately $\pi/4$ owing to to $2\Delta m_K \approx \Delta\Gamma_K$. The current world average is $|\varepsilon_K| = (2.221 \pm 0.008) \times 10^{-3}$ [55]. Other observables measure $|\varepsilon_K|$ with less precision. Among these are the charge asymmetry in semileptonic K_L^0 decays, δ_L, or decay-plane asymmetry in $K_L^0 \to \pi^+\pi^-e^+e^-$ decays.

Within the SM, ε_K is induced by $\Delta S = 2$ transitions mediated by box diagrams. They are related to the CKM elements via a local hadronic matrix element, parameterized by the bag parameter B_K,

$$\langle \overline{K}^0 | (\overline{s}\gamma^\mu(1-\gamma_5)d)^2 | K^0\rangle = \frac{8}{3}\, m_K^2 f_K^2 B_K(\mu)\,, \tag{49}$$

where μ is the renormalization scale, usually chosen to be 2 GeV. Note that $B_K = 1$ corresponds to the vacuum insertion approximation. The renormalization scale and scheme-independent bag parameter (sometimes denoted by $\widehat{B}_K$) is hereafter denoted by B_K, which differs from $B_K(\mu)$ by a series in α_s that cancels the scale and scheme dependences (similar to B_d introduced in Sec. 3.4). The kaon decay constant, $f_K = (159.8 \pm 1.5)$ MeV [45], is extracted from the leptonic decay rate $\Gamma(K^+ \to \mu^+\nu_\mu)$. The most reliable prediction of B_K is obtained from LQCD. At present, calculations are performed assuming SU(3) symmetry and using mostly the quenched approximation. The world average is $B_K = 0.79 \pm 0.04 \pm 0.09$ [97, 98], where the first error combines statistical and accountable systematic uncertainties[8] and the second is theoretical. Analytical approaches based on the large-N_c expansion of QCD find a smaller value for B_K in the chiral limit [99]. Large chiral corrections could be the origin of this difference. At present, B_K is the primary source of theoretical uncertainty in the SM prediction of ε_K.

Neglecting the real part of the off-diagonal element, M_{12}, of the neutral-kaon mixing matrix, one obtains [21].

$$|\varepsilon_K| = \frac{G_F^2 m_W^2 m_K f_K^2}{12\sqrt{2}\,\pi^2 \Delta m_K}\, B_K \Big\{ \eta_{cc} S(x_c, x_c) \mathrm{Im}[(V_{cs}V_{cd}^*)^2] + \eta_{tt} S(x_t, x_t) \mathrm{Im}[(V_{ts}V_{td}^*)]^2 + 2\eta_{ct} S(x_c, x_t)\, \mathrm{Im}[V_{cs}V_{cd}^* V_{ts}V_{td}^*] \Big\}\,, \tag{50}$$

where $\Delta m_K = (3.490 \pm 0.006) \times 10^{-12}$ MeV [45], and $S(x_i, x_j)$, with $x_i = m_i^2/m_W^2$ $(i = c, t)$, are Inami-Lim functions [92]. The running quark masses are evaluated in the $\overline{\mathrm{MS}}$ scheme.

[8] The term "accountable systematic uncertainties" denotes uncertainties that have been evaluated in a systematic manner. Most of the experimental systematic uncertainties fall into this category. An example of an unaccountable (i.e., to a large extent arbitrary) theoretical uncertainty is the quenched approximation used in some LQCD calculations.

The parameters η_{ij} in Eq. (50) are next-to-leading-order QCD corrections to the Inami-Lim functions [100], where η_{cc} is the parameter with the largest uncertainty.

4.2 Direct *CP* Violation

A nonzero value for the *CP*-violation parameter ε'_K, defined by

$$\varepsilon'_K = \frac{1}{3}\left(\eta_{+-} - \eta_{00}\right) \tag{51}$$

establishes direct *CP* violation, because $\varepsilon'_K \approx (\lambda_{\pi^0\pi^0} - \lambda_{\pi^+\pi^-})/6$. The experimentally convenient observable $\mathrm{Re}(\varepsilon'_K/\varepsilon_K)$ is determined by the measurement of the double ratio

$$\frac{\Gamma(K_L^0 \to \pi^0\pi^0)}{\Gamma(K_L^0 \to \pi^+\pi^-)}\frac{\Gamma(K_S^0 \to \pi^+\pi^-)}{\Gamma(K_S^0 \to \pi^0\pi^0)} = \left|\frac{\eta_{00}}{\eta_{+-}}\right|^2 \simeq 1 - 6\,\mathrm{Re}\left(\frac{\varepsilon'_K}{\varepsilon_K}\right), \tag{52}$$

which cancels many experimental uncertainties. Evidence for direct *CP* violation was first seen by the NA31 Collaboration [101], and was firmly established by NA48 [102] and KTeV [103], with the world average $\mathrm{Re}(\varepsilon'_K/\varepsilon_K) = (16.7 \pm 1.6) \times 10^{-4}$.

Because $\mathrm{Re}(\varepsilon'_K/\varepsilon_K)$ is proportional to $\mathrm{Im}(V_{td}V_{ts}^*) = A^2\lambda^5\overline{\eta} + \mathcal{O}(\lambda^7)$, it measures $\overline{\eta}$. However, the SM prediction of $\mathrm{Re}(\varepsilon'_K/\varepsilon_K)$ suffers from large uncertainties, because the dominant gluonic and electromagnetic penguin contributions tend to cancel each other [104]. Detailed calculations at next-to-leading order [105,106] have been carried out for the coefficients of the two dominant hadronic parameters, $B_6^{(1/2)}$ (gluonic penguins) and $B_8^{(3/2)}$ (electroweak penguins), where the superscripts denote the isospin change in the $K \to \pi\pi$ transition. Because no reliable LQCD calculation for $B_6^{(1/2)}$ is available, the measurement of $\mathrm{Re}(\varepsilon'_K/\varepsilon_K)$ is usually not used to constrain CKM elements.

4.3 $K^+ \to \pi^+\nu\overline{\nu}$ and $K_L^0 \to \pi^0\nu\overline{\nu}$

The E787 experiment at the Brookhaven National Laboratory (BNL) observed two events of the very rare decay $K^+ \to \pi^+\nu\overline{\nu}$, resulting in $\mathcal{B}(K^+ \to \pi^+\nu\overline{\nu}) = (1.57^{+1.75}_{-0.82}) \times 10^{-10}$ [107], which, owing to the small expected background rate (0.15 ± 0.03 events), effectively excludes the null hypothesis. One additional event was observed near the upper kinematic limit by the successor experiment, BNL-E949 [108]. They quote the combined branching fraction $\mathcal{B}(K^+ \to \pi^+\nu\overline{\nu}) = (1.47^{+1.30}_{-0.89}) \times 10^{-10}$.

In the SM, the branching fraction at next-to-leading order is given by [109]

$$\mathcal{B}(K^+ \to \pi^+\nu\overline{\nu}) = r_{K^+}\frac{3\alpha^2\,\mathcal{B}(K^+ \to \pi^0 e^+\nu)}{2\pi^2\,|V_{us}|^2\sin^4\theta_{\mathrm{W}}}\left|X(x_t)V_{td}V_{ts}^* + X_cV_{cd}V_{cs}^*\right|^2, \tag{53}$$

where $r_{K^+} = 0.901$ corrects for isospin breaking [110]. $X(x_t) = \eta_X X_0(x_t)$ is an Inami-Lim function for the dominant top-quark contribution, X_0, corrected by a perturbative QCD factor, η_X. The second term contains the charm-quark contribution.

Expressing Eq. (53) in terms of the Wolfenstein parameters gives

$$\mathcal{B}(K^+ \to \pi^+\nu\overline{\nu}) = \kappa_+ A^4 X(x_t)^2 \frac{1}{\sigma}\left[(\sigma\overline{\eta})^2 + (\rho_0 - \overline{\rho})^2\right], \tag{54}$$

with $\sigma = 1 + \lambda^2 + \mathcal{O}(\lambda^4)$ and

$$\rho_0 = 1 + \frac{P_0}{A^2 X(x_t)}\,. \tag{55}$$

It provides an almost elliptic constraint in the $(\overline{\rho}, \overline{\eta})$ plane, centered near $(\overline{\rho} = 1, \overline{\eta} = 0)$. The parameter $\kappa_+ = \lambda^8\,[3\alpha^2 \mathcal{B}(K^+ \to \pi^0 e^+ \nu)]/[2\pi^2 \sin^4\theta_{\rm W})$ is such that $\mathcal{B}(K^+ \to \pi^+ \nu\overline{\nu})$ depends on $(A\lambda^2)^4$, which is constrained by $|V_{cb}|$. The parameter $P_0 = P_c + \delta P_c$ quantifies the charm-quark contribution, which until recently provided the largest theoretical error owing to the m_c and scale dependences. The short-distance part, $P_c = 0.38 \pm 0.04$, is now calculated to next-to-next-to-leading order [111]. The long distance contributions of c and u loops are estimated to be $\delta P_c = 0.04 \pm 0.02$ and are expected to be under good control [112].

In the SM, the decay $K_L^0 \to \pi^0 \nu\overline{\nu}$ is theoretically clean, because the final state is almost completely CP-even [113], so the decay proceeds dominantly through CP violation in the interference of decay with and without mixing [114, 115]. The amplitude is dominated by the top-quark contribution. The theoretical prediction of the branching fraction is given by [109]

$$\mathcal{B}(K_L^0 \to \pi^0 \nu\overline{\nu}) = \kappa_L \left[\frac{{\rm Im}(V_{td} V_{ts}^*)}{\lambda^5}\, X(x_t)\right]^2 = \kappa_L A^4 \overline{\eta}^2 X^2(x_t) + \mathcal{O}(\lambda^4)\,, \tag{56}$$

where $\kappa_L = \kappa_+ (r_{K_L} \tau_{K_L})/(r_{K^+} \tau_{K^+}) = (2.12 \pm 0.03) \times 10^{-10}$ [116], and $r_{K_L} = 0.944$ accounts for isospin breaking [110]. As for the charged mode, the branching fraction is proportional to $(A\lambda^2)^4$, which would, however, cancel in the ratio of rates. The constraint in the $(\overline{\rho}, \overline{\eta})$ plane from a future measurement of $\mathcal{B}(K_L^0 \to \pi^0 \nu\overline{\nu})$ would correspond to two horizontal bands at a certain value of $\pm|\overline{\eta}|$.

The interpretation of rare K decays involving lepton pairs is more complicated than for the similar B decays, because in most channels long-distance contributions are important. For example, $K^\pm \to \pi^\pm \ell^+ \ell^-$ is dominated by a virtual photon converting into $\ell^+\ell^-$, whereas $K_L^0 \to \ell^+\ell^-$ is dominated by virtual two-photon contribution. More interesting are the $K^0 \to \pi^0 \ell^+ \ell^-$ modes. Similar to $K_L^0 \to \pi^0 \nu\overline{\nu}$, the CP-violating amplitude dominates in $K_L^0 \to \pi^0 e^+ e^-$, whereas there are comparable CP-violating and CP-conserving contributions in $K_L^0 \to \pi^0 \mu^+ \mu^-$ [117]. A more precise measurement of $\mathcal{B}(K_S^0 \to \pi^0 e^+ e^-)$ would allow the clean extraction of the relevant short-distance physics from $K_L^0 \to \pi^0 e^+ e^-$.

5 Unitarity Triangle Angle Measurements

The observation of a nonzero Jarlskog parameter [14] in the SM leads to the requirement that the angles of the UT (and equivalently of all six unitarity triangles of the CKM matrix) be nonzero (modulo π). The UT angles α, β and γ (18) are all accessible from the B sector, albeit with different sensitivity and purity. Whereas the measurements of β (the leading experimental observable here is $\sin 2\beta$) and γ, through B decays in charmonium and open charm, respectively, are theoretically clean, the measurement of α in charmless B decays relies on theoretical assumptions. Because the measurements of α and γ involve interference with transitions governed by the small CKM matrix element V_{ub}, they require larger data samples than when measuring $\sin 2\beta$.

The experimental techniques to measure the UT angles also change radically from one to another. The measurements of α and β require $B^0\overline{B}^0$ mixing and therefore use neutral B mesons, whereas the measurements of γ use interference between $b \to u$ and $b \to c$ decay amplitudes, and can be done with both neutral and charged B decays.

In the following we neglect CP violation in B^0 mixing, which has been searched for with both flavor-specific and inclusive B^0 decays in samples where the initial flavor state is tagged. The current world average is $|q/p| = 1.0018 \pm 0.0017$ [118, 119], whereas the deviation from unity is expected to be $|q/p| - 1 \approx 0.0003$ [120], and around λ^2 times smaller in B_s^0 mixing. See Sec. 7 for an application of this search in the context of new physics studies.

5.1 β from B Decays to Charmonium Final States

In $b \to c\bar{c}s$ quark-level decays, the time-dependent CP violation parameters measured from the interference between decays with and without mixing are $S_{c\bar{c}s} = -\eta_C P \sin 2\beta$ and $C_{c\bar{c}s} = 0$, to a very good approximation. The theoretically cleanest case if $B \to J/\psi K^0_{S,L}$, where

$$\lambda_{\psi K^0_{S,L}} = \mp \left(\frac{V_{tb}^* V_{td}}{V_{tb} V_{td}^*}\right)\left(\frac{V_{cb} V_{cs}^*}{V_{cb}^* V_{cs}}\right)\left(\frac{V_{cs} V_{cd}^*}{V_{cs}^* V_{cd}}\right) = \mp e^{-2i\beta}\,, \tag{57}$$

and so $\mathrm{Im}\lambda_{\psi K^0_{S,L}} = S_{\psi K^0_{S,L}} = \pm \sin 2\beta$ (see Sec. 1.4). The sign is from $\eta_{\psi K^0_{S,L}} = \mp 1$, the first factor is the SM value of q/p in $B^0\overline{B}^0$ mixing, the second is $\overline{A}/A$, and the last one is p_K/q_K. In the absence of $K^0\overline{K}^0$ mixing there could be no interference between $\overline{B}^0 \to \psi\overline{K}^0$ and $B^0 \to \psi K^0$.

BABAR [121] and Belle [122] have both used the $\eta_C P = -1$ modes $J/\psi\, K^0_S$, $\psi(2S)K^0_S$, $\chi_{c1}K^0_S$ and $\eta_c K^0_S$, as well as $J/\psi\, K^0_L$, which has $\eta_C P = +1$, and $J/\psi\, K^{*0}(892)(\to K^0_S\pi^0)$, which is found from an angular analysis to have $\eta_C P$ close to $+1$ (the CP-odd fraction amounts to 0.217 ± 0.010 [66]). In the latest result from Belle, only $J/\psi\, K^0_S$ and $J/\psi\, K^0_L$ are used. The world average reads [66]

$$\sin 2\beta = 0.687 \pm 0.032\,, \tag{58}$$

giving for the angle β within $[0, \pi]$ the solutions $(21.7\,^{+1.3}_{-1.2})^\circ$ and $(68.3\,^{+1.2}_{-1.3})^\circ$, where the first number is compatible with the result from the global CKM fit without the measurement of β, $(24.4^{+2.6}_{-1.5})^\circ$ and $\sin 2\beta_{\rm CKM} = 0.752\,^{+0.057}_{-0.035}$ (cf. Sec. 6). As expected in the SM, no direct CP violation has been observed in these modes.

In $b \to c\bar{c}d$ quark-level decays, such as $B^0 \to J/\psi\,\pi^0$ or $B^0 \to D^{(*)}D^{(*)}$, unknown contributions from (not CKM suppressed) penguin-type diagrams, carrying a different weak phase than the tree-level diagram, compromises the clean extraction of $\sin 2\beta$. Consequently, they are not included in the $\sin 2\beta$ average.

5.1.1 Resolving the four-fold ambiguity

Despite the agreement of Eq. (58) with the SM, it is still possible that, because of contributions from new physics, the correct value of β is one of the three solutions not compatible with the SM. The measurement of the sign of $\cos 2\beta$ eliminates two of the solutions.[9] B-meson decays to the vector-vector final state $J/\psi K^{*0}$, where three helicity states of the vector mesons mix

[9] The invariance $\beta \to \pi + \beta$ remains. It cannot be lifted without theoretical input on a strong phase [123].

CP-even and *CP*-odd amplitudes, are also mediated by the $b \to c\overline{c}s$ transition. When the final state $K^{*0} \to K^0_S\pi^0$ is used, a time-dependent transversity analysis can be performed allowing sensitivity to both sin2β and cos2β [124]. Here, cos2β enters as a factor in the interference between the *CP*-even and *CP*-odd amplitudes. In principle, the sign of cos2β in this analysis is ambiguous owing to an incomplete determination of the strong phases occurring in the three transversity amplitudes. *BABAR* resolves this ambiguity by inserting the known variation [125] of the rapidly changing P-wave phase relative to the slowly changing S-wave phase with the invariant mass of the $K\pi$ system in the vicinity of the $K^{*0}(892)$ resonance.[10] The result from *BABAR*, $\cos2\beta = 3.32\,^{+0.76}_{-0.96} \pm 0.27$, although seemingly significant, exhibits a strongly non-Gaussian behavior, and the confidence level for a positive value (as expected in the SM) is only 86% [127]. The result from Belle is compatible with zero [128].

Bondar *et al.* [129] suggested another idea to resolve the four-fold ambiguity of β. For quark-level transitions $b \to c\overline{u}d$, where the final state is a *CP* eigenstate (such as $D_{CP}\pi^0$), the time dependence is given by the usual formulas, with the sine coefficient sensitive to sin2β. When a multibody D decay, such as $D \to K^0_S\pi^+\pi^-$ is used instead, a time-dependent analysis of the Dalitz plot of the neutral D decay allows the extraction of both sin2β and cos2β. The Belle Collaboration [130] has perfomed such an analysis, giving $\beta = (16 \pm 21 \pm 12)^\circ$, which rules out the non-SM solution at 97% C.L.. Although HFAG has not attempted a combination of the two results on cos2β, it is not premature to conclude that the SM solution is largely favored by the data.

5.2 α from Charmless B Decays

Unlike $B^0 \to J/\psi\, K^0$, for which amplitudes with weak phases different from the dominant tree phase are doubly CKM suppressed, multiple weak phases must be considered in most of the analyses of B decays to final states without charm. This complication makes the extraction of the CKM couplings from the experimental observables considerably more difficult, although richer. The decays most sensitive to α are $B^0 \to \pi^+\pi^-$, $\rho^\pm\pi^\mp$, and $\rho^+\rho^-$ (α measures $\pi - \beta - \gamma$ in the SM and in any model with unitary 3×3 CKM matrix). The extraction of α in the presence of unknown penguin amplitudes requires an isospin analysis [131] for $\pi\pi$, $\rho\rho$, and a Dalitz-plot analysis [132] for $\rho^\pm\pi^\mp$, which are briefly introduced below. Relying on flavor symmetries, in particular SU(2), does not represent a severe theoretical limitation. However, it certainly creates model-dependent uncertainties from flavor-symmetry breaking so that — neglecting statistical considerations — the measurement of α is not of the same quality as the measurements of sin2β and γ.

In naive factorization, there is a hierarchy between penguins in modes where the B^0 decays to two pseudoscalar particles (such as $\pi^+\pi^-$), to a pseudoscalar and a vector particle ($\rho^\pm\pi^\mp$), and to two vector particles ($\rho^+\rho^-$) [133]. This is due to the Dirac structure of the $(V-A)\times(V+A)$ penguin operators, which do not contribute when the meson that does not receive the spectator quark (the "upper" meson) is a vector, as in $B^0 \to \rho^+\pi^-$ and $B^0 \to \rho^+\rho^-$. Similarly, these

[10] The result for the strong phase is in agreement with the prediction obtained from s-quark helicity conservation [126].

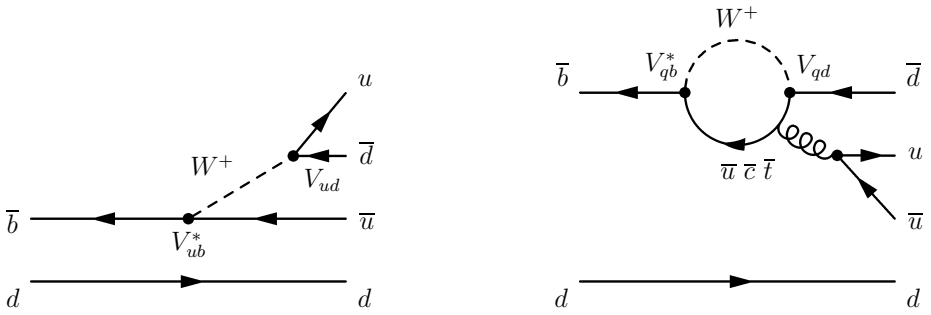

Figure 5: *Tree (left) and penguin (right) diagrams for the decay* $B^0 \to \pi^+\pi^-$.

operators interfere constructively (destructively) with $(V-A)\times(V-A)$ penguin operators when the upper meson is a pseudoscalar and the lower meson is a pseudoscalar (vector), as in $B^0 \to \pi^+\pi^-$ ($B^0 \to \rho^-\pi^+$). This qualitative picture[11] reproduces quite well the experimental results. Using the value of α from the global CKM fit, the penguin-to-tree ratios are $0.23^{+0.41}_{-0.10}$, $0.05^{+0.07}_{-0.05}$, $0.03^{+0.09}_{-0.03}$ and $0.10^{+0.02}_{-0.03}$, for $\pi^+\pi^-$, $\rho^+\rho^-$, $\rho^+\pi^-$ and $\rho^-\pi^+$, respectively [13], where penguin and tree correspond to the P^{+-} and T^{+-} amplitudes defined in Eq. (60) below.

5.2.1 Relations Between Transition Amplitudes

The general form of the $B^0 \to \pi^+\pi^-$ decay amplitude, accounting for the tree and penguin diagrams that correspond to the three up-type quark flavors (u,c,t) occurring in the W loop (see Fig. 5), reads

$$A^{+-} \equiv A(B^0 \to \pi^+\pi^-) = V_{ud}V_{ub}^* M_u + V_{cd}V_{cb}^* M_c + V_{td}V_{tb}^* M_t\,, \tag{59}$$

and the CP-conjugated amplitude can be similarly written. Using unitarity, this can be written as[12]

$$A^{+-} = V_{ud}V_{ub}^* T^{+-} + V_{td}V_{tb}^* P^{+-}\,, \tag{60}$$

with $T^{+-} = M_u - M_c$ and $P^{+-} = M_t - M_c$. We refer to the T^{+-} and P^{+-} amplitudes as "tree" and "penguin", respectively, although it is implicitly understood that both of them receive various contributions of distinct topologies, which are mixed under hadronic rescattering. The time-dependent CP-violating asymmetry is given by Eqs. (24) and (25), with the CP-violation parameter $\lambda_{\pi^+\pi^-} = (q/p)(\overline{A}^{+-}/A^{+-})$, since $\pi^+\pi^-$ is a CP eigenstate with eigenvalue $+1$. In the absence of penguin contributions $\lambda_{\pi^+\pi^-} = e^{2i\alpha}$, and hence $S_{\pi^+\pi^-} = \sin 2\alpha$ and $C_{\pi^+\pi^-} = 0$. In general, however, the phase of $\lambda_{\pi^+\pi^-}$ is modified by the interference between the penguin and the tree amplitudes, which can also lead to direct CP violation. It is customary to define an effective angle $\alpha_{\rm eff}$ that incorporates the penguin-induced phase shift $\lambda_{\pi^+\pi^-} = |\lambda_{\pi^+\pi^-}|\, e^{2i\alpha_{\rm eff}}$, so

[11] Because $(V-A)\times(V+A)$ operators are power suppressed in the QCD factorization approach, the naive hierarchy may receive large corrections [134].

[12] In Eq. (60), the c-quark loop is eliminated using the unitarity relation. In Charles *et al.*'s [13] definition, this corresponds to the c-convention. Note that the particular choice of which amplitude to remove in the definition of a total transition amplitude is arbitrary and does not have observable physical implications.

that the sine coefficient becomes $S_{\pi^+\pi^-} = \sqrt{1 - C^2_{\pi^+\pi^-}}\,\sin 2\alpha_{\rm eff}$. Twice the effective angle $\alpha_{\rm eff}$ corresponds to the relative phase between $e^{-2i\beta}\overline{A}^{+-}$ and A^{+-}.

The isospin invariance of the strong interaction relates the amplitudes of the various $B \to \pi\pi$ decays to each other. A pair of pions in a $B \to \pi\pi$ decay must be in a zero angular momentum state, and then, because of Bose statistics, they must have even isospin. Consequently, $\pi^\pm\pi^0$ is in a pure isospin-2 state, free of QCD penguin amplitudes, which contribute only to the isospin-0 final states. Gronau & London showed that the measurements of rates and *CP*-violating asymmetries of the charged and two neutral $\pi\pi$ final states provide sufficient information to extract the angle α as well as the various tree and penguin amplitudes [131]. Unfortunately, this isospin analysis is plagued by a 16-fold ambiguity for $\alpha \in [0, 2\pi]$, i.e., 16 (not necessarily) different values of α reproduce the same set of observables.

Using the same convention as in Eq. (60), one can write for the remaining $B \to \pi\pi$ decays

$$\begin{aligned}\sqrt{2}A^{+0} &\equiv \sqrt{2}A(B^+ \to \pi^+\pi^0) = V_{ud}V^*_{ub}T^{+0} + V_{td}V^*_{tb}P_{\rm EW}\,,\\ \sqrt{2}A^{00} &\equiv \sqrt{2}A(B^0 \to \pi^0\pi^0) = V_{ud}V^*_{ub}T^{00}_{\rm C} + V_{td}V^*_{tb}P^{00}\,,\end{aligned} \tag{61}$$

and the *CP*-conjugated modes can be similarly written. The subscript C stands for a color-suppressed amplitude, and the subscript EW stands for the electroweak penguin amplitude contributing to $\pi^+\pi^0$. The $P_{\rm EW}$ contributions are usually neglected in the amplitude fits performed by the experiments, so that the $\Delta I = 3/2$ decay $B^+ \to \pi^+\pi^0$ is mediated by a pure tree amplitude.[13] Applying the isospin relations [131]

$$A^{+0} = \frac{1}{\sqrt{2}}A^{+-} + A^{00}\,, \quad \text{and} \quad \overline{A}^{+0} = \frac{1}{\sqrt{2}}\overline{A}^{+-} + \overline{A}^{00}\,, \tag{62}$$

the amplitudes (61) can be rearranged and, e.g., T^{+0} and P^{00} eliminated. Isospin-breaking effects have been examined in Refs. [138] and are expected to be smaller than the current experimental precision on α.

Applying the isospin relations reduces the number of unknowns in the $B \to \pi\pi$ isospin analysis to six, which aligns with the number of experimental observables: three branching ratios, one mixing-induced *CP* asymmetry ($S_{\pi^+\pi^-}$), and two direct *CP* asymmetries ($C_{\pi^+\pi^-}$ and $C_{\pi^0\pi^0}$). Owing to the missing tracks in most of the $B^0 \to \pi^0\pi^0$ events, $S_{\pi^0\pi^0}$ cannot be measured in the foreseeable future. In absence of isospin breaking, direct *CP* violation cannot occur in $B^+ \to \pi^+\pi^0$. A small value for the branching fraction to $\pi^0\pi^0$ would indicate that the penguin contribution cannot be large [139]. This observation led to the development of isospin bounds on $\Delta\alpha = \alpha - \alpha_{\rm eff}$ [140, 141]. Applying the optimal bound is equivalent to constraining α using the isospin relations without using the measurement of $C_{\pi^0\pi^0}$.

5.2.2 Isospin Analysis of $B \to \pi\pi$ Decays

All six observables used in the isospin analysis have been measured in $B \to \pi\pi$ decays. The past disagreement between *BABAR* and Belle for the *CP* asymmetries in $B^0 \to \pi^+\pi^-$ (Belle

[13] The bulk part of the shift of α due to $P_{\rm EW}$ can be estimated model independently [135,136,137], and amounts to -2.1° [13].

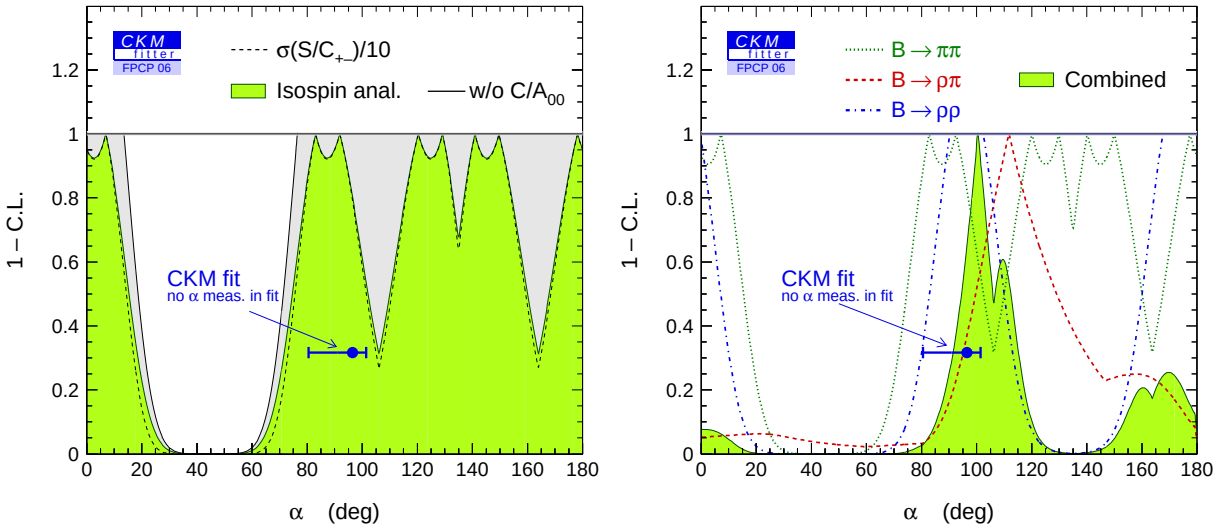

Figure 6: *Left: confidence level for the UT angle α obtained from the $B \to \pi\pi$ isospin analysis under various conditions: full isospin analysis (dark shaded), isospin analysis without using $C_{\pi^0\pi^0}$ (light shaded), and full isospin analysis assuming perfect knowledge of the parameters $S_{\pi^+\pi^-}$ and $C_{\pi^+\pi^-}$ (dashed line). Right: confidence level for the UT angle α from the isospin analyses of $B \to \pi\pi$ (dotted) and $B \to \rho\rho$ (dashed-dotted), and the Dalitz plot analysis of $B \to \rho\pi$ (dashed). The shaded region shows the combined constraint from all three measurements [51].*

saw evidence for both mixing-induced and direct *CP* asymmetries, whereas *BABAR* did not) has been alleviated recently. The world averages for the *CP* asymmetries and branching fractions measured by *BABAR*, Belle and CLEO (for the branching fractions) have been compiled by the HFAG [142, 66]. A large $\mathcal{B}^{00}_{\pi\pi}/\mathcal{B}^{+-}_{\pi\pi}$ ratio is found, indicating significant penguin or color-suppressed tree contributions, and representing a challenge for the theoretical understanding of the decay dynamics. This ratio implies only a loose upper bound $|\Delta\alpha| < 40^\circ$ at 95% C.L., if $C_{\pi^0\pi^0}$ is not used [51].

The confidence level for α from $B \to \pi\pi$ is shown in the left plot of Fig. 6. Three cases are distinguished: *a*) the full isospin analysis using the present world averages (shaded), *b*) the incomplete isospin analysis without $C_{\pi^0\pi^0}$ (solid line), and *c*) the full isospin analysis assuming perfect knowledge of $S_{\pi^+\pi^-}$ and $C_{\pi^+\pi^-}$ (dashed line). The present constraint on α from $\pi^+\pi^-$ is weak, and future improvement will be driven almost entirely by the measurement of $C_{\pi^0\pi^0}$.

5.2.3 Isospin Analysis of $B \to \rho\rho$ Decays

Similar to $B \to \pi\pi$, the angle α can be extracted from the measurement of time-dependent *CP* asymmetries in $B^0 \to \rho^+\rho^-$, together with an isospin analysis including the full $B \to \rho\rho$ system, to determine the penguin pollution. The specific interest of this mode is the potentially small penguin contribution, which is suggested by the smallness of the experimental upper bound on the $B^0 \to \rho^0\rho^0$ branching fraction when compared with the branching fractions of $B^0 \to \rho^+\rho^-$ and $B^+ \to \rho^+\rho^0$ [143,66]. In addition, both direct and mixing-induced *CP*-violating asymmetries

of the $B^0 \to \rho^0\rho^0$ decays are experimentally accessible once the decay has been seen.

The analysis is complicated by the presence of three helicity states for the two vector mesons. One corresponds to longitudinal polarization (A_0) and is *CP*-even. Two helicity states ($A_\pm$) are transversely polarized and are admixtures of *CP*-even and *CP*-odd amplitudes. Because helicity flips are suppressed in these decays, the relative proportions of the helicity amplitudes in naive factorization are expected to be [144]

$$A_0 : A_- : A_+ \approx 1 : \frac{\Lambda_{\rm QCD}}{m_b} : \left(\frac{\Lambda_{\rm QCD}}{m_b}\right)^2 . \tag{63}$$

The dominance of the longitudinal polarization has been confirmed by experiment in the measured $B \to \rho\rho$ decays. The isospin analysis can therefore, without significant loss of sensitivity, be applied to the longitudinally polarized states only.[14]

The confidence level obtained from the $B \to \rho\rho$ system for α is given in the right plot of Fig. 6 (dashed-dotted line). The reduction of $\mathcal{B}(B^+ \to \rho^+\rho^0)$ by the latest *BABAR* measurement improved the consistency of the isospin analysis, which now exhibits a closed isospin triangle, and deteriorated somewhat the resulting constraint on α. Choosing the solution consistent with the SM gives $\alpha_{\rho\rho} = (100\,^{+13}_{-20})^\circ$ [51]. Also shown in the plot is the prediction from the CKM fit, where the direct measurement of α has been excluded from the fit. It exhibits excellent agreement with the measurement. The 95% C.L. bound on $\Delta\alpha$ is $|\Delta\alpha| < 17^\circ$, reflecting a small penguin pollution.

5.2.4 Dalitz Plot Analysis of $B \to \rho\pi$ Decays

Unlike $\pi^+\pi^-$ and $\rho^+\rho^-$, the final state $\rho^\pm\pi^\mp$ is not a *CP* eigenstate, and four flavor-charge configurations ($B^0(\overline{B}^0) \to \rho^\pm\pi^\mp$) must be considered. The corresponding isospin analysis [146] is unfruitful with the present statistics, because two pentagonal amplitude relations with a total of 12 unknowns have to be solved. However, as Snyder and Quinn [132] pointed out, the necessary degrees of freedom to constrain α without ambiguity (except for the irreducible $\alpha \to \alpha + \pi$), can be obtained by including in the analysis the (known) strong-phase modulations of the interfering ρ resonances in the Dalitz plot.

The *BABAR* [147] Collaboration has performed such an analysis, where the interfering B^0 decay amplitudes into $\rho^+\pi^-$, $\rho^-\pi^+$ and $\rho^0\pi^0$ have been included. To avoid mirror solutions for the fit parameters and non-Gaussian observables, *BABAR* fits 16 interdependent coefficients that are bilinears of the charged and neutral ρ form factors.[15] Each coefficient is related in a unique way to the quantities of interest, the tree-level and penguin-type amplitudes, and α. These are obtained in a least-squares fit to the measured coefficients. Systematic uncertainties are dominated by the lack of knowledge of the tails of the ρ form factor, where higher ρ excitations occur and precise B decay data are scarce. Ignoring the mirror solution at $\alpha + 180^\circ$, *BABAR*

[14] Owing to the finite width of the ρ meson, $I = 1$ contributions can occur in $B \to \rho\rho$ decays [145]. Although no explicit calculation is available, one expects these effects to be of order $(\Gamma_\rho/m_\rho)^2 \sim 4\%$. At present the experiments also neglect effects from the interference with the radial excitations of the ρ, with other $\pi\pi$ resonances, and with a nonresonant component. The latter two effects are included in the systematic errors quoted by the experiments.

[15] The full set of bilinears comprises 27 observables out of which *BABAR* neglects nine related to *CP* asymmetries in $B^0 \to \rho^0\pi^0$, which has only a small event yield.

finds $\alpha_{\rho\pi} = (113\,^{+27}_{-17} \pm 6)^\circ$, whereas only a marginal constraint on α is obtained beyond two standard deviations.

The confidence level for α obtained from the $B \to \rho\pi$ Dalitz analysis is given in the right plot of Fig. 6 (dashed line). Also shown is the combined constraint from all three measurements (shaded), giving

$$\alpha = \left(100\,^{+15}_{-9}\right)^\circ \tag{64}$$

for the SM solution. This measurement is in agreement with the expectation $\alpha_{\rm CKM} = (97\,^{+5}_{-16})^\circ$ from the global CKM fit (see Table 2 on p. 42) [51].

5.3 γ from B Decays to Open Charm

The golden methods to determine γ at the B-factories utilize the measurement of direct CP violation in $B^+ \to DK^+$ decays, where the neutral D meson can be both D^0 and $\overline{D}^0$ (and where D^0 also stands for D^{*0}). The D^0 corresponds to the leading $\overline{b} \to \overline{c}$ transition, whereas the $\overline{D}^0$ is produced by a CKM- and color-suppressed $\overline{b} \to \overline{u}$ transition. If the final state is chosen so that both D^0 and $\overline{D}^0$ can contribute, the two amplitudes interfere, and the resulting observables are sensitive to the UT angle γ, the relative weak phase between the two B decay amplitudes.

Among the many methods that exploit this interference, the experiments concentrate on the reconstruction of the neutral D in a CP eigenstate (GLW) [148], in other final states common to D^0 and $\overline{D}^0$ such as $K^\mp\pi^\pm$ (ADS) [149], or in the self-conjugate three-body final state $K^0_S\pi^+\pi^-$ (GGSZ) [150]. All variations are sensitive to the same B decay parameters and can therefore be treated in a combined fit to extract γ. For the GLW analysis, the relations between the experimental observables, the rates $R_{CP^\pm}$ and charge asymmetries $A_{CP^\pm}$ of the CP-even and CP-odd modes, and the model parameters are

$$R_{CP^\pm} = 1 + r_B^2 \pm 2r_B\cos\delta_B\cos\gamma\,, \qquad A_{CP^\pm} = \pm\frac{2r_B\sin\delta_B\sin\gamma}{R_{CP^\pm}}\,, \tag{65}$$

where δ_B is the (CP-conserving) relative strong phase between the interfering amplitudes, and $r_B^{(*)} = |A(B^+ \to D^{0(*)}K^+)/A(B^+ \to \overline{D}^{0(*)}K^+)|$ is the ratio of the B decay amplitudes. The same relations apply for the GGSZ analysis, where the variations of additional strong phases and amplitude ratios throughout the Dalitz plot of the three-body decay are extracted from high statistics D decay data and modeled by the experiments. For the ADS analysis two additional unknowns (phase and amplitude ratio) appear because the neutral D mesons do not decay to CP eigenstates. High-statistics charm decays can be used as external constraints for the amplitude ratio. Moreover, only two observables (rate and asymmetry) per B decay mode exist for ADS. The above equations show that the feasibility of the γ measurement depends crucially on the size of r_B (expected to be roughly $r_B \sim 0.1$, if naive color suppression holds). Instead of fitting the model parameters (γ, r_B, δ_B) directly, the experiments proceed by determining the Cartesian coordinates $(x_\pm, y_\pm) = (r_B\cos(\delta_B \pm \gamma), r_B\sin(\delta_B \pm \gamma))$, which have the advantage of being Gaussian distributed, uncorrelated and unbiased (the parameter r_B is positive definite and hence exhibits a fit bias toward larger values, if its central value is in the vicinity of zero within errors), and simplify the averaging of the various measurements.

Results are available from both *BABAR* and Belle on the GLW analysis using the decay modes $B^+ \to DK^+$, $B^+ \to D^*K^+$ and $B^+ \to DK^{*+}$ [151]. For ADS [152] only *BABAR* uses all three decays. Here, the decays $D^* \to D\pi^0$ and $D^* \to D\gamma$ have a relative strong-phase shift and must be studied separately [153]. The world averages for the GLW and ADS measurements are provided by the HFAG [66]. So far none of these measurements have obtained a significant signal for the suppressed amplitude.

Both experiments have studied the GGSZ analysis using the same B decay modes as for the GLW and ADS analyses, and using in all cases the subsequent decay $D^0(\overline{D}^0) \to K^0_S\pi^+\pi^-$. Both experiments perform a full frequentist statistical analysis to determine the physical parameters. Exploiting the three-body Dalitz plot enhances the sensitivity to the suppressed amplitude compared to the (quasi-)two-body decays used for GLW and ADS. This leads to a significant determination of r_B and hence γ with this method. Using the same three modes $D^{(*)}K^{(*)+}$, the experiments report the GGSZ measurements $\gamma = (67 \pm 28 \pm 13 \pm 11)^\circ$ (*BABAR* [154]) and $\gamma = (53\,^{+15}_{-18} \pm 3 \pm 9)^\circ$ (Belle [155]), where the first errors are statistical, the second are systematic, and the third are due to the Dalitz plot model.

The CKMfitter Group has performed a combined analysis of all GLW, ADS and GGSZ results using a frequentist statistical framework. Including the former two methods leads to a reduction in the average r_B values of all modes, which are $r_B(DK) = 0.10 \pm 0.03$, $r_B(D^*K) = 0.10\,^{+0.03}_{-0.05}$ and $r_B(DK^*) = 0.11\,^{+0.08}_{-0.11}$ [51]. All values are in agreement with the naive expectation from CKM and color suppression. The smaller r_B values deteriorate the constraint on γ obtained from the GGSZ analyses. The preliminary overall γ average is [51]

$$\gamma = \left(62\,^{+35}_{-25}\right)^\circ , \tag{66}$$

which is in agreement with the prediction $\gamma_{\rm CKM} = (60\,^{+5}_{-4})^\circ$ from the global CKM fit (where the direct γ measurement has been excluded from the fit) [51]. The GLW, ADS and GGSZ confidence levels for γ as well as the combined constraint are shown in Fig. 7. Also shown is the expectation from the global CKM fit.

5.4 $2\beta + \gamma$ from B Decays to Open Charm

Similar to the decay $B^0 \to \rho^\pm\pi^\mp$, which is not a CP eigenstate but sensitive to α because both final states can be reached by both neutral B flavors, interference between decays with and without mixing can occur in $B^0 \to D^{(*)\pm}\pi^\mp(\rho^\pm)$. A time-dependent analysis of these decays is sensitive to $\sin(2\beta+\gamma)$, because the CKM-favored $\overline{b} \to \overline{c}$ decay amplitude interferes with the CKM-suppressed $b \to u$ decay amplitude with a relative weak-phase shift γ. In these $\overline{b} \to \overline{c}(u\overline{d})$, $\overline{u}(c\overline{d})$ quark-level transitions no penguin contributions are possible, because all quarks in the final state are different. Hence there is no direct CP violation. Furthermore, owing to the smallness of the ratio of the magnitudes of the CKM-suppressed and CKM-favored amplitudes (denoted r_f), to a very good approximation, $C_f = -C_{\overline{f}} = 1$ (using $f = D^{(*)-}h^+$, $\overline{f} = D^{(*)+}h^-$ $h = \pi, \rho$), and the coefficients of the sine terms are given by

$$S_f = -2r_f \sin(2\beta+\gamma-\delta_f)\,, \qquad S_{\overline{f}} = -2r_f \sin(2\beta+\gamma+\delta_f), \tag{67}$$

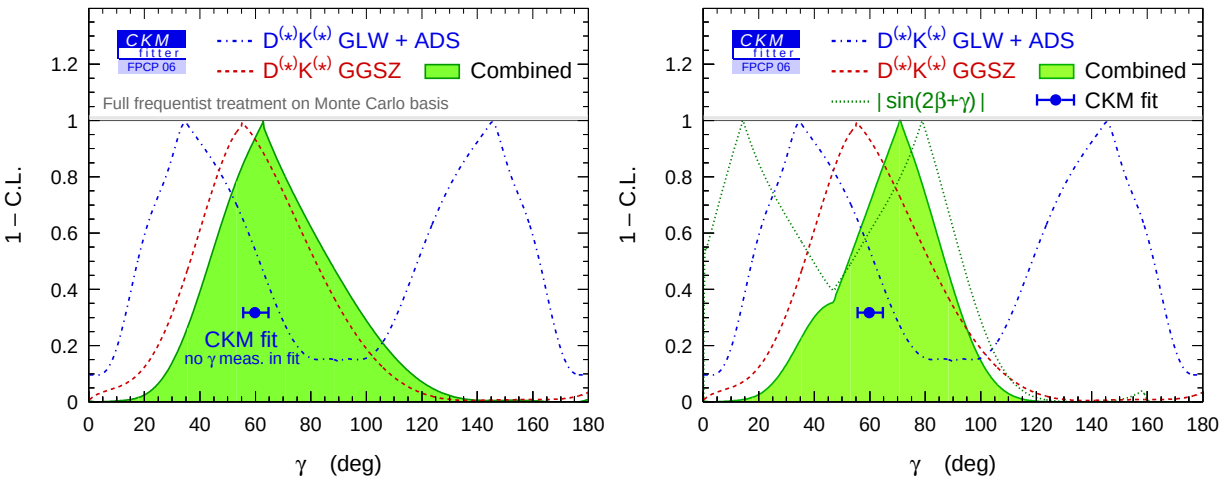

Figure 7: *Left: confidence level for the UT angle γ from the measurement of direct CP asymmetries in $B \to D^{(*)}K^{(*)}$ decays (left). Shown are the individual results for the combined GLW and ADS analysis (dashed-dotted), for GGSZ (dashed), and the combination of both analyses (shaded). Right: adding to these the measurement of $2\beta+\gamma$ from time-dependent analyses of neutral B decays to open charm, together with the precise* $\sin 2\beta$ *measurement. A theoretical error of* 15% *has been used to account for SU(3) breaking. The plots are taken from Ref. [51].*

where δ_f is the strong-phase shift due to final-state interaction between the decaying mesons. Hence, the weak phase $2\beta+\gamma$ can be cleanly obtained from measurements of S_f and $S_{\overline{f}}$, although external information on at least r_f or δ_f is necessary. It can be obtained from the corresponding flavor-tagged branching fractions, or from similar modes that are easier to measure. These can be ratios of branching fractions of the charged $B^+ \to D^{(*)+}\pi^0$ to the neutral CKM-favored decay, or ratios involving self-tagging decays with strangeness like $B^0 \to D_s^{(*)+}\pi^-$. Corrections for SU(3) breaking in the latter case generate a significant theoretical uncertainty, which is in general hard to quantify. Naively, one can estimate $r^{(*)} \sim |V_{cd}^* V_{ub}/V_{ud}V_{cb}^*| \simeq 0.02$. At present, the most precise estimate of r_f obtained from SU(3)-corrected ratios are [156] $r_{D\pi} = 0.013 \pm 0.002$ and $r_{D^*\pi} = 0.019 \pm 0.0029$, where a 15–30% theoretical uncertainty is usually added to account for SU(3) breaking.

The constraint on $2\beta+\gamma$ obtained using these amplitude ratios (assuming a 15% uncertainty on SU(3) breaking), and the world averages of the experimental observables [157,66], is depicted by the dotted line in the right plot of Fig. 7. The measured values for $\sin 2\beta$ (and $\cos 2\beta$) have been used to infer γ from this. The shaded curve gives the overall constraint on γ obtained when averaging these results with those given in Sec. 5.3. The $2\beta+\gamma$ measurements help to exclude large values of γ.

5.5 Weak-Phase Information from Direct *CP* Violation in *B* Decays

The KM mechanism causes "direct" *CP* violation in the decay, as soon as at least two amplitudes with different strong and weak phases contribute. Because virtual loops are present in all meson

decays, "some" (possibly unobservable) amount of direct *CP* violation *always* occurs. Owing to the large weak phases arising in B decays, direct *CP* violation should be more prominent here than, e.g., in the kaon system. This has been confirmed by the measurement of the direct *CP* asymmetry $A_{K^+\pi^-} = -0.115 \pm 0.018$ in $B^0 \to K^+\pi^-$ decays [158]. Evidence for direct *CP* violation in neutral B decays also exists for $B^0 \to \pi^+\pi^-$ (3.7σ significance) and $B^0 \to \rho^\pm\pi^\mp$ (3.4σ significance) [66]. Recently, the first evidence for direct *CP* violation in charged B decays emerged from the mode $B^+ \to K^+\rho^0$ with a charge asymmetry of $0.31\,^{+0.12}_{-0.11}$ [159]. With the data samples at the B-factories increasing, we expect the discovery of more and more rare-decay modes with significant *CP* violation in the decay.

From the point of view of the weak-phase extraction, the required conspiracy between competing amplitudes of similar size and the occurrence of strong phases, represent serious obstacles. A reliable and model-independent calculation of direct *CP* violation is not possible at present, and estimates based on factorization are plagued by large uncertainties. However, flavor symmetries in particular isospin can be exploited to (essentially) assess model independently direct *CP* violation. In B decays to $\pi\pi$, $\rho\pi$ and $\rho\rho$, the measurements of direct *CP*-violating asymmetries (independent of whether they are compatible with zero or not) are essential inputs to the isospin analyses. In the $K\pi$ system the corresponding isospin analysis used to extract γ [146] is fruitless at present, and affected by possibly large isospin-breaking corrections from electroweak penguins, which cannot be taken into account model independently as is the case in the $\pi\pi$ and $\rho\rho$ isospin analyses.

Although a quantitative prediction is difficult, direct *CP* violation can be a powerful probe for new physics in decays where negligible *CP* asymmetries are expected. This is the case for all B decays dominated by a single decay amplitude. Prominent examples are penguin-dominated decays, such as $b \to s\gamma$ or $B \to K^{(*)}\ell^+\ell^-$, where a significant nonzero direct *CP* violation would unambiguously indicate new physics.

6 The Global CKM Fit

The global CKM fit consists of maximizing a likelihood built upon relevant experimental measurements and their SM predictions, which depend on the parameters of the theory. Some of these parameters, such as quark masses or matrix elements, are experimentally or theoretically constrained, whereas others are unknown. These unknowns contain the four Wolfenstein parameters, but also, for instance, hadronic quantities that occur in the determination of the UT angles α and γ. To avoid uncontrolled biases, the unknown parameters should be treated as free parameters of the theory in a frequentist statistical sense. Such an approach has been adopted by the CKMfitter Group [160, 13], whose results we use here.

Many of the observables presently used to constrain the CKM matrix depend on hadronic matrix elements and hence are subject to significant theoretical uncertainties. The treatment of these theoretical uncertainties has a large amount of arbitrariness, and different choices lead to different results. The CKMfitter Group advocates the Rfit approach [160, 13]. In this approach the ranges spanned by the model-dependent theoretical errors are scanned to maximize the agreement between theory and experiment, which corresponds to a minimization of the exclusion

confidence level at a given point in parameter space that is to be tested. Other approaches exist in the literature [161, 162].

6.1 Fit Inputs and Initial Tests of Unitarity

What is often termed the "standard global CKM fit" includes only those observables for which the SM predictions can be considered quantitatively under control, and that lead to a significant constraint on the CKM parameters. These comprise the measurements of $|V_{ud}|$, $|V_{us}|$, $|V_{ub}|$, $|V_{cb}|$, $|\varepsilon_K|$, Δm_d, Δm_s,[16] $\sin 2\beta$, $\cos 2\beta$, α, γ and $\mathcal{B}(B^+ \to \tau^+ \nu_\tau)$. The inputs used by the fit are given in Table 1.

Using the independently measured moduli of the CKM elements mentioned in the previous sections, the unitarity of the CKM matrix can be checked. We obtain $|V_{ud}|^2 + |V_{us}|^2 + |V_{ub}|^2 - 1 = -0.0008 \pm 0.0011$ (first row), $|V_{cd}|^2 + |V_{cs}|^2 + |V_{cb}|^2 - 1 = -0.03 \pm 0.18$ (second row), and $|V_{ud}|^2 + |V_{cd}|^2 + |V_{td}|^2 - 1 = 0.001 \pm 0.005$ (first column). The sum in the second column, $|V_{us}|^2 + |V_{cs}|^2 + |V_{ts}|^2$ is practically identical to that in the second row, as the errors in both cases are dominated by $|V_{cs}|$. For the second row, a more stringent test is obtained from the measurement of $\sum_{u,c,d,s,b} |V_{ij}|^2$ minus the sum in the first row, giving $|V_{cd}|^2 + |V_{cs}|^2 + |V_{cb}|^2 = 1.000 \pm 0.026$.

It is an unexpected success of the B-factory experiments that, beyond the precision measurement of $\sin 2\beta$, measurements of α and γ became available. Remarkably, the most powerful determinations of the latter two angles involve measurements that were not considered before the data became available. Choosing the SM solution for each of the angles, their sum reads [51]

$$\alpha + \beta + \gamma = \left(186\,^{+38}_{-27}\right)^\circ \,, \tag{68}$$

which corresponds to a closed triangle verifying the three-generation KM mechanism.

Various theory parameters enter the SM predictions that relate the measurements to the fundamental CKM parameters determined by the fit. Those with the largest uncertainties are hadronic matrix elements obtained with LQCD, quark masses determined using LQCD and QCD sum-rule analyses, and coefficients calculated in perturbative QCD. The values used for these parameters in the CKM fit are also given in Table 1.

6.2 Fit Results

The global CKM fit results in the Wolfenstein parameters are given in Table 2 (top four lines). The goodness-of-fit, evaluated with the use of Monte Carlo methods [13], is satisfying, so one can assume the correctness of the SM and proceed with the metrology of the CKM parameters and the related quantities. It is interesting to compare the direct measurements of the UT angles with the predictions from the CKM fit that do not include these measurements. The measurement of $\sin 2\beta$ outperforms by far the indirect prediction. Also, the precision of the α measurement exceeds that of the CKM prediction so that its inclusion in the fit improves the knowledge of the apex of the UT. For γ, the experimental precision is not yet sufficient to

[16] The results shown in this section include the new DØ and CDF analyses of $B_s^0 \overline{B}_s^0$ mixing [95, 96].

Parameter	Value ± Error(s)	Reference	Errors GS	Errors TH
$\|V_{ud}\|$ (β-decays)	0.97377 ± 0.00027	[98]	$\star$	–
$\|V_{us}\|$ ($K_{\ell 3}$ and $K_{\mu 2}$)	0.2257 ± 0.0021	[45]	$\star$	–
$\|V_{ub}\|$ (inclusive)	$(4.45 \pm 0.23 \pm 0.39) \times 10^{-3}$	[66, 51]	$\star$	$\star$
$\|V_{ub}\|$ (exclusive)	$(3.94 \pm 0.28 \pm 0.51) \times 10^{-3}$	[45]	$\star$	$\star$
$\|V_{cb}\|$ (inclusive)	$(41.70 \pm 0.70) \times 10^{-3}$	[45]	$\star$	–
$\|V_{cb}\|$ (exclusive)	$(41.2 \pm 1.7) \times 10^{-3}$	[66]	$\star$	–
$\|\varepsilon_K\|$	$(2.221 \pm 0.008) \times 10^{-3}$	[55, 51]	$\star$	–
Δm_d	(0.507 ± 0.004) ps^{-1}	[66]	$\star$	–
Δm_s	Amplitude spectrum (incl. DØ), and CDF $\log \mathcal{L}$ parameterization	[98]	$\star$	–
$\sin 2\beta_{[c\bar{c}]}$	0.687 ± 0.032	[66]	$\star$	–
$S^{+-}_{\pi\pi}$, $C^{+-}_{\pi\pi}$, $C^{00}_{\pi\pi}$, $\mathcal{B}_{\pi^{+/0}\pi^{-/0}}$	Inputs to isospin analysis	[66]	$\star$	–
$S^{+-}_{\rho\rho,L}$, $C^{+-}_{\rho\rho,L}$, $\mathcal{B}_{\rho^{+/0}\rho^{-/0},L}$	Inputs to isospin analysis	[66]	$\star$	–
$B^0 \to (\rho\pi)^0 \to 3\pi$	Time-dependent Dalitz plot analysis	[163]	$\star$	–
$B^- \to D^{(*)}K^{(*)-}$	Inputs to GLW analysis	[66]	$\star$	–
$B^- \to D^{(*)}K^{(*)-}$	Inputs to ADS analysis	[66]	$\star$	–
$B^- \to D^{(*)}K^{(*)-}$	GGSZ Dalitz plot analysis	[66]	$\star$	–
$\mathcal{B}(B^- \to \tau^- \overline{\nu}_\tau)$	Experimental likelihoods	[50]	$\star$	–
$\overline{m}_c(m_c)$	$(1.24 \pm 0.037 \pm 0.095)$ GeV	[72]	$\star$	$\star$
$\overline{m}_t(m_t)$	(162.3 ± 2.2) GeV	[164]	$\star$	–
f_K	(159.8 ± 1.5) MeV	[45]	–	–
B_K	$0.79 \pm 0.04 \pm 0.09$	[98]	$\star$	$\star$
$\alpha_s(m_Z^2)$	0.1176 ± 0.0020	[45]	–	$\star$
η_{ct}	0.47 ± 0.04	[100]	–	$\star$
η_{tt}	0.5765 ± 0.0065	[100]	–	–
$\eta_B(\overline{\rm MS})$	0.551 ± 0.007	[21]	–	$\star$
f_{B_d}	(191 ± 27) MeV	[98]	$\star$	–
B_d	1.37 ± 0.14	[98]	$\star$	–
$\xi^{(a)}$	$1.24 \pm 0.04 \pm 0.06$	[98]	$\star$	$\star$

$^{(a)}$anticorrelated theory error with $f_{B_d}\sqrt{B_d}$.

Table 1: *Inputs to the standard CKM fit. If not stated otherwise, when two errors given, the first is statistical and accountable systematic and the second stands for theoretical uncertainties. The last two columns indicate whether errors are treated Gaussian (GS) or theoretical (TH) within Rfit [13]. Table taken from Ref. [51].*

improve the CKM metrology. It is remarkable that the prediction of $\sin 2\beta_s$ has an absolute precision of 0.002 (owing to its CKM suppression), so a measurement of it at the LHC will represent a very sensitive probe for physics beyond the SM. Also given are the sides of the UT, and the angles of the standard parameterization of the CKM matrix.

Once the Wolfenstein parameters are fit, determining fully consistent confidence levels for all related observables is straightforward. It is also possible to derive constraints on the matrix

Observable	central ± C.L. ≡ 1σ	± C.L. ≡ 2σ	± C.L. ≡ 3σ
λ	$0.2272\,^{+0.0010}_{-0.0010}$	$^{+0.0020}_{-0.0020}$	$^{+0.0030}_{-0.0030}$
A	$0.809\,^{+0.014}_{-0.014}$	$^{+0.029}_{-0.028}$	$^{+0.044}_{-0.042}$
$\overline{\rho}$	$0.197\,^{+0.026}_{-0.030}$	$^{+0.050}_{-0.087}$	$^{+0.074}_{-0.133}$
$\overline{\eta}$	$0.339\,^{+0.019}_{-0.018}$	$^{+0.047}_{-0.037}$	$^{+0.075}_{-0.057}$
J $[10^{-5}]$	$3.05\,^{+0.18}_{-0.18}$	$^{+0.45}_{-0.36}$	$^{+0.69}_{-0.54}$
$\sin 2\alpha$	$-0.25\,^{+0.17}_{-0.15}$	$^{+0.49}_{-0.28}$	$^{+0.71}_{-0.42}$
$\sin 2\alpha$ (meas. not in fit)	$-0.23\,^{+0.55}_{-0.16}$	$^{+0.72}_{-0.32}$	$^{+0.83}_{-0.45}$
$\sin 2\beta$	$0.716\,^{+0.024}_{-0.024}$	$^{+0.048}_{-0.049}$	$^{+0.074}_{-0.075}$
$\sin 2\beta$ (meas. not in fit)	$0.752\,^{+0.057}_{-0.035}$	$^{+0.105}_{-0.073}$	$^{+0.135}_{-0.112}$
α (deg)	$97.3\,^{+4.5}_{-5.0}$	$^{+8.7}_{-14.0}$	$^{+13.7}_{-20.7}$
α (deg) (meas. not in fit)	$96.5\,^{+4.9}_{-16.0}$	$^{+9.9}_{-21.2}$	$^{+14.6}_{-25.3}$
α (deg) (direct meas. only)	$100.2\,^{+15.0}_{-8.8}$	$^{+22.7}_{-18.2}$	$^{+32.0}_{-28.1}$
β (deg)	$22.86\,^{+1.00}_{-1.00}$	$^{+2.03}_{-1.97}$	$^{+3.22}_{-2.93}$
β (deg) (meas. not in fit)	$24.4\,^{+2.6}_{-1.5}$	$^{+5.1}_{-3.0}$	$^{+6.9}_{-4.5}$
β (deg) (direct meas. only)	$21.7\,^{+1.3}_{-1.2}$	$^{+2.6}_{-2.4}$	$^{+4.1}_{-3.6}$
$\gamma \simeq \delta$ (deg)	$59.8\,^{+4.9}_{-4.1}$	$^{+13.9}_{-7.9}$	$^{+20.8}_{-12.1}$
$\gamma \simeq \delta$ (deg) (meas. not in fit)	$59.8\,^{+4.9}_{-4.2}$	$^{+14.1}_{-8.0}$	$^{+21.0}_{-12.3}$
$\gamma \simeq \delta$ (deg) (direct meas. only)	$62\,^{+35}_{-25}$	$^{+61}_{-39}$	$^{+100}_{-54}$
β_s (deg)	$1.045\,^{+0.061}_{-0.057}$	$^{+0.151}_{-0.114}$	$^{+0.238}_{-0.177}$
$\sin(2\beta_s)$	$0.0365\,^{+0.0021}_{-0.0020}$	$^{+0.0053}_{-0.0040}$	$^{+0.0083}_{-0.0062}$
R_u	$0.391\,^{+0.015}_{-0.015}$	$^{+0.031}_{-0.029}$	$^{+0.049}_{-0.044}$
R_t	$0.872\,^{+0.033}_{-0.028}$	$^{+0.095}_{-0.054}$	$^{+0.143}_{-0.082}$
Δm_d (ps^{-1}) (meas. not in fit)	$0.394\,^{+0.097}_{-0.097}$	$^{+0.219}_{-0.132}$	$^{+0.361}_{-0.162}$
Δm_s (ps^{-1})	$17.34\,^{+0.49}_{-0.20}$	$^{+0.65}_{-0.35}$	$^{+0.78}_{-0.49}$
Δm_s (ps^{-1}) (meas. not in fit)	$21.7\,^{+5.9}_{-4.2}$	$^{+9.7}_{-6.8}$	$^{+13.1}_{-9.1}$
ε_K $[10^{-3}]$ (meas. not in fit)	$2.46\,^{+0.63}_{-0.88}$	$^{+1.05}_{-1.05}$	$^{+1.50}_{-1.20}$
f_{B_d} (MeV) (lattice value not in fit)	$183\,^{+10}_{-10}$	$^{+21}_{-20}$	$^{+34}_{-28}$
ξ (lattice value not in fit)	$1.061\,^{+0.122}_{-0.047}$	$^{+0.213}_{-0.083}$	$^{+0.324}_{-0.119}$
B_K (lattice value not in fit)	$0.722\,^{+0.251}_{-0.084}$	$^{+0.348}_{-0.157}$	$^{+0.461}_{-0.216}$
m_c (GeV/c^2) (meas. not in fit)	$0.81\,^{+0.93}_{-0.36}$	$^{+1.08}_{-0.36}$	$^{+1.23}_{-0.81}$
m_t (GeV/c^2) (meas. not in fit)	$150\,^{+27}_{-21}$	$^{+57}_{-35}$	$^{+79}_{-46}$
$\mathcal{B}(K_{\mathrm{L}}^0 \to \pi^0 \nu\overline{\nu})$ $[10^{-11}]$	$2.58\,^{+0.48}_{-0.40}$	$^{+1.01}_{-0.68}$	$^{+1.53}_{-0.93}$
$\mathcal{B}(K^+ \to \pi^+ \nu\overline{\nu})$ $[10^{-11}]$	$7.5\,^{+1.8}_{-2.0}$	$^{+2.5}_{-2.4}$	$^{+3.2}_{-2.7}$
$\mathcal{B}(B^+ \to \tau^+ \nu_\mu)$ $[10^{-5}]$	$9.7\,^{+1.3}_{-1.3}$	$^{+2.9}_{-2.5}$	$^{+4.6}_{-3.6}$
$\mathcal{B}(B^+ \to \tau^+ \nu_\mu)$ $[10^{-5}]$ (direct meas. only)	$10.4\,^{+3.0}_{-2.7}$	$^{+3.0}_{-5.1}$	$^{+3.0}_{-7.1}$
$\mathcal{B}(B^+ \to \mu^+ \nu_\mu)$ $[10^{-7}]$	$4.32\,^{+0.58}_{-0.57}$	$^{+1.27}_{-1.12}$	$^{+2.05}_{-1.62}$

Table 2: *Numerical results of the global CKM fit (I) [51]. The errors correspond to one, two and three standard deviations, respectively.*

Observable	central $\pm$ C.L. $\equiv 1\sigma$	$\pm$ C.L. $\equiv 2\sigma$	$\pm$ C.L. $\equiv 3\sigma$
$\lvert V_{ud}\rvert$	$0.97383^{+0.00024}_{-0.00023}$	$^{+0.00047}_{-0.00047}$	$^{+0.00071}_{-0.00071}$
$\lvert V_{us}\rvert$	$0.2272^{+0.0010}_{-0.0010}$	$^{+0.0020}_{-0.0020}$	$^{+0.0030}_{-0.0030}$
$\lvert V_{ub}\rvert$ $[10^{-3}]$	$3.82^{+0.15}_{-0.15}$	$^{+0.31}_{-0.29}$	$^{+0.49}_{-0.44}$
$\lvert V_{ub}\rvert$ $[10^{-3}]$ (meas. not in fit)	$3.64^{+0.19}_{-0.18}$	$^{+0.39}_{-0.36}$	$^{+0.60}_{-0.55}$
$\lvert V_{cd}\rvert$	$0.22712^{+0.00099}_{-0.00103}$	$^{+0.00199}_{-0.00205}$	$^{+0.00300}_{-0.00307}$
$\lvert V_{cs}\rvert$	$0.97297^{+0.00024}_{-0.00023}$	$^{+0.00048}_{-0.00047}$	$^{+0.00071}_{-0.00071}$
$\lvert V_{cb}\rvert$ $[10^{-3}]$	$41.79^{+0.63}_{-0.63}$	$^{+1.26}_{-1.27}$	$^{+1.89}_{-1.90}$
$\lvert V_{cb}\rvert$ $[10^{-3}]$ (meas. not in fit)	$44.9^{+1.2}_{-2.8}$	$^{+2.4}_{-5.7}$	$^{+3.8}_{-7.7}$
$\lvert V_{td}\rvert$ $[10^{-3}]$	$8.28^{+0.33}_{-0.29}$	$^{+0.92}_{-0.57}$	$^{+1.38}_{-0.86}$
$\lvert V_{ts}\rvert$ $[10^{-3}]$	$41.13^{+0.63}_{-0.62}$	$^{+1.25}_{-1.24}$	$^{+1.87}_{-1.86}$
$\lvert V_{tb}\rvert$	$0.999119^{+0.000026}_{-0.000027}$	$^{+0.000052}_{-0.000054}$	$^{+0.000078}_{-0.000082}$
$\lvert V_{td}/V_{ts}\rvert$	$0.2011^{+0.0081}_{-0.0065}$	$^{+0.0230}_{-0.0127}$	$^{+0.0345}_{-0.0195}$
$\lvert V_{ud}V_{ub}^*\rvert$ $[10^{-3}]$	$3.72^{+0.15}_{-0.14}$	$^{+0.30}_{-0.29}$	$^{+0.48}_{-0.43}$
$\arg\left[V_{ud}V_{ub}^*\right]$ (deg)	$59.8^{+4.9}_{-4.0}$	$^{+13.9}_{-7.8}$	$^{+20.9}_{-12.1}$
$\arg\left[-V_{ts}V_{tb}^*\right]$ (deg)	$1.043^{+0.061}_{-0.057}$	$^{+0.151}_{-0.114}$	$^{+0.238}_{-0.176}$
$\lvert V_{cd}V_{cb}^*\rvert$ $[10^{-3}]$	$9.49^{+0.15}_{-0.15}$	$^{+0.30}_{-0.30}$	$^{+0.45}_{-0.45}$
$\arg\left[-V_{cd}V_{cb}^*\right]$ (deg)	$0.0339^{+0.0021}_{-0.0020}$	$^{+0.0050}_{-0.0040}$	$^{+0.0077}_{-0.0060}$
$\lvert V_{td}V_{tb}^*\rvert$ $[10^{-3}]$	$8.27^{+0.33}_{-0.29}$	$^{+0.93}_{-0.57}$	$^{+1.38}_{-0.85}$
$\arg\left[V_{td}V_{tb}^*\right]$ (deg)	$-22.84^{+1.00}_{-0.99}$	$^{+1.98}_{-2.02}$	$^{+2.93}_{-3.21}$
$\sin\theta_{12}$	$0.2272^{+0.0010}_{-0.0010}$	$^{+0.0020}_{-0.0020}$	$^{+0.0030}_{-0.0030}$
$\sin\theta_{13}$ $[10^{-3}]$	$3.82^{+0.15}_{-0.15}$	$^{+0.31}_{-0.30}$	$^{+0.49}_{-0.44}$
$\sin\theta_{23}$ $[10^{-3}]$	$41.78^{+0.63}_{-0.63}$	$^{+1.26}_{-1.26}$	$^{+1.90}_{-1.89}$

Table 3: *Numerical results of the global CKM fit (II) [51]. The errors correspond to one, two and three standard deviations, respectively.*

elements of neutral K and B mixing, which in turn are in agreement with the LQCD results. The determination of ξ through the Δm_s measurement in the CKM fit is not yet competitive with the LQCD determination, owing to the currently insufficient precision of the γ and α measurements. It represents a remarkable success of flavor physics to correctly reproduce the scales of the charm and top masses through FCNC loop processes only. Also listed in Table 2 are the predictions for the rare kaon decays to pions and neutrino-antineutrino pairs (including the next-to-next-to-leading-order calculation of the charm contribution to the charged decay [111]) and for rare leptonic B decays. (The comment "meas. (or lattice value) not in fit" in some rows indicates that for the corresponding determination the direct measurement of the quantity (or the LQCD prediction) has been excluded from the fit.)

Finally, Table 3 gives the standard CKM fit results for the absolute values of the CKM elements and the magnitudes and phases of the sides of the non-rescaled UT. The results of the fit are shown in the $(\overline{\rho}, \overline{\eta})$ plane in Fig. 8. The outer contour of the combined fit corresponds to 95% C.L. exclusion. Also shown are the 95% C.L. regions for the individual constraints entering the fit (the constraint from $B^+ \to \tau^+\nu_\tau$ is not shown, although it is included in the fit).

The global CKM fit performed so far contains all relevant information collected by the ex-

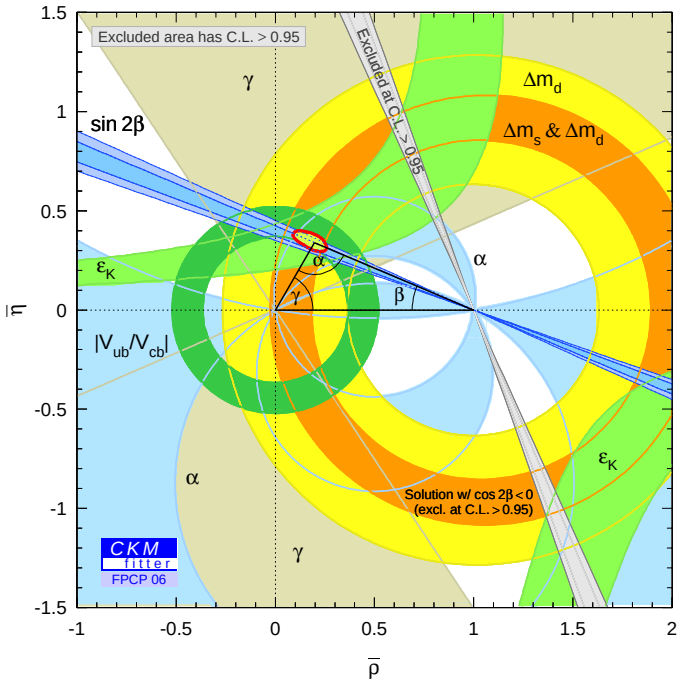

Figure 8: *Confidence levels in the* $(\overline{\rho},\overline{\eta})$ *plane for the global CKM fit. The shaded areas indicate* 95% C.L. *allowed regions [51].*

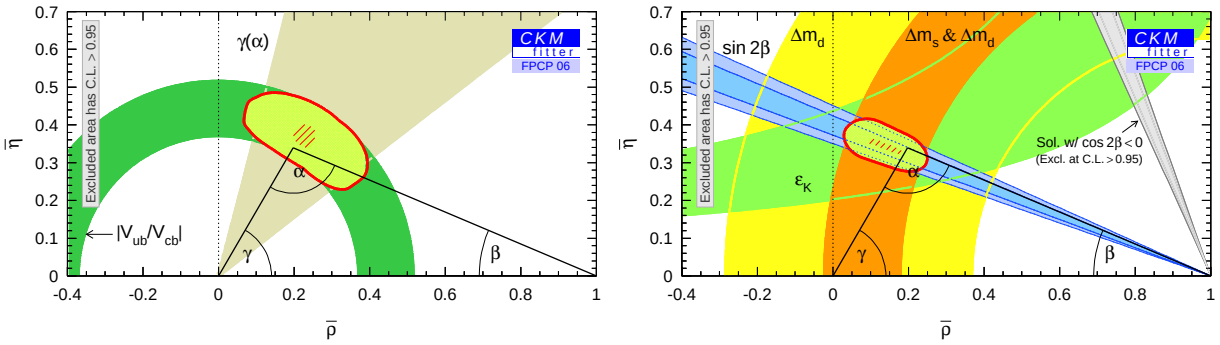

Figure 9: *Confidence levels in the* $(\overline{\rho},\overline{\eta})$ *plane for global CKM fits using only tree-level (left) and loop-induced (right) inputs. The shaded areas indicate* 95% C.L. *allowed regions.*

periments. From the new physics perspective, it is interesting to confront the measurements according to their sensitivity to new physics contributions. Figure 9 shows on the left plot the constraints that originate from mainly tree-level processes, together with their combined fit. The right plot shows the constraints from loop-induced processes. To fix the length scale of the UT and the constraints on λ and A from the tree-level determinations of the CKM elements $|V_{ud}|$, $|V_{us}|$ and $|V_{cb}|$ are used. If γ is extracted from the measurement of α using β from mixing-induced CP violation as input, it is effectively a tree-level quantity, because the isospin analysis isolates the $\Delta I = 3/2$ component in the decay amplitude, which is assumed to be standard (this corresponds to the SM4FC case defined in Ref. [13]). Consequently, the constraint for γ that

enters the tree-level plot is the average of the direct measurement of γ via open-charm processes, and the value obtained from $\pi - \alpha - \beta$, from which new physics in mixing cancels. This provides the first determination of $(\overline{\rho},\overline{\eta})$ from (effectively) tree-level processes. Good agreement is observed between the tree-level and loop-induced constrained fits.

7 The CKM Matrix and the Search for New Physics

7.1 New Physics Extensions of the Standard Model and their Relation to CKM

If the constraints of the SM are lifted, K, B, and D decays are described by many more parameters than just the four CKM parameters and the W, Z and quark masses. The most general effective Lagrangian at lowest order contains approximately one hundred flavor-changing operators, and the observable effects of any short-distance, high-energy physics are encoded in their Wilson coefficients. Therefore, all measurements sensitive to different short-distance physics are important, and overconstraining the magnitudes and phases of CKM elements could detect deviations from the SM. For example, Δm_d, $\Gamma(B \to \rho\gamma)$, and $\Gamma(B \to X_d\ell^+\ell^-)$ are all proportional to $|V_{td}V_{tb}^*|^2$ in the SM, however, they may receive unrelated contributions from new physics. Similar to the measurements of $\sin 2\beta$ from tree- and loop-dominated modes, testing such correlations, and not simply the unitarity of the CKM matrix, provides the best sensitivity to new physics.

In the kaon sector both CP-violating observables, ε_K and ε'_K, are tiny, so models in which all sources of CP violation are small are viable. Owing to the measurement of $\sin 2\beta$ we know that CP violation is an $\mathcal{O}(1)$ effect and only the flavor mixing is suppressed between the three quark generations. Hence, many models with spontaneous CP violation that predicted small CP-violating effects are excluded. However, model-independent statements for the constraints imposed by the CKM measurements on new physics are hard to make because most models that allow new flavor physics contain a large number of new parameters.

There are large classes of models in which the biggest effects of new physics occur in transitions involving second- and third-generation fermions, thus escaping the bounds from kaon physics (see, e.g., Refs. [165] and [166]). For example, in SUSY GUTs, the observed near-maximal $\nu_\mu - \nu_\tau$ mixing may imply large mixing between s_R and b_R, and between their supersymmetric partners $\tilde{s}_R$ and $\tilde{b}_R$ [167]. Although the mixing of the right-handed quarks does not enter the CKM matrix, the mixing among the right-handed squarks is physical. It may entail sizable deviations of the time-dependent CP asymmetries in penguin-dominated modes from $\sin 2\beta$ discussed in the next section, and an enhancement, compared with the SM value, of Δm_s. Another recently popular scenario with large effects in flavor physics involves Higgs-mediated FCNCs in the large $\tan\beta$ region of SUSY ($\tan\beta$ is the ratio of the vacuum expectation values of the two Higgs doublets, and $\tan\beta \sim m_t/m_b$ is motivated by the unification of top and bottom Yukawa couplings predicted by some GUT models). Neutral Higgs-mediated FCNC couplings that occur at one loop increase rapidly with $\tan\beta$ and can exceed other SUSY contributions by more than an order of magnitude, giving an enhancement of $\mathcal{B}(B_{d,s} \to \mu^+\mu^-)$ proportional to

$\tan^6\beta$ [168]. This scenario also predicts a suppression of Δm_s proportional to $\tan^4\beta$ [169]. As discussed below (see Fig. 11), $B^0\overline{B}^0$ mixing may still receive a significant positive or negative new physics contribution even after the measurement of Δm_s.

The existing data on rare B decays set severe constraints on (SUSY) model building. In particular $\mathcal{B}(B \to X_s\gamma)$ provides strong parameter bounds. Both the SUSY and the SM contributions enter at the one-loop level, and the charged Higgs diagrams always enhance the rate, whereas the chargino contributions can reduce it if $\mu > 0$ (μ is the coefficient of the H_uH_d term in the superpotential, and $H_{u,d}$ are the Higgs fields that couple to the up- and down-type fermions). One reason that $B \to X_s\gamma$ is the only B decay that enters the bounds in many analyses (e.g., the constraints on dark matter candidates [170], usually the lightest neutralino) is because such studies often assume the constrained MSSM (MSUGRA), which implies minimal flavor violation [171], and relate the charged Higgs and the chargino contributions to each other. The $B \to X_s\gamma$ rate can be enhanced significantly even without new sources of flavor violation, i.e., with all flavor changing interactions proportional to CKM matrix elements. Nontrivial flavor physics due to TeV-scale new physics would indicate deviations from this parameterization, which could weaken the bounds from $B \to X_s\gamma$. Then the constraints can become more complex, and other B decays would also be important in constraining the new physics parameters.

As mentioned above, not all CP-violating measurements can be interpreted as constraints on the $(\overline{\rho},\overline{\eta})$ plane. For example, probing with $B_s^0 \to J/\psi\phi$ whether β_s, the order λ^2 angle of the squashed UT defined in Eq. (21), agrees with its SM prediction is an important independent test of the theory. Other comparisons between the SM correlations in B and K physics can come from future measurements of $K_L^0 \to \pi^0\nu\overline{\nu}$ and $K^+ \to \pi^+\nu\overline{\nu}$. These loop-induced decays are sensitive to new physics and will allow a determination of β independent of its value measured in B decays [172].

7.2 *CP* Asymmetries in Loop-Dominated Modes

The FCNC $b \to s$ transition is mediated by penguin diagrams. It can have any up-type quark in the loop, so its amplitude can be written as

$$\begin{aligned} A_{b\to s} &= m_t V_{tb}V_{ts}^* + m_c V_{cb}V_{cs}^* + m_u V_{ub}V_{us}^* \\ &= (m_c - m_t)V_{cb}V_{cs}^* + (m_u - m_t)V_{ub}V_{us}^* = \mathcal{O}(\lambda^2) + \mathcal{O}(\lambda^4)\,, \end{aligned} \tag{69}$$

where the unitarity of the CKM matrix has been used in the second step. In the SM, the amplitude is dominated by the first, $V_{cb}V_{cs}^*$, term, which has the same weak phase as the amplitude in $B^0 \to J/\psi K^0$ decay. We expect $||\overline{A}/A| - 1| = \mathcal{O}(\lambda^2)$, and the time-dependent CP asymmetry parameters are given to a similar accuracy by $S_{b\to sq\overline{q}} \approx -\eta_{f_{CP}}\sin 2\beta$ and $C_{b\to sq\overline{q}} \approx 0$.

Owing to the large mass scale of the virtual particles that can occur in the loops, additional diagrams from physics beyond the SM, with heavy particles in the loops, may contribute. The measurement of CP violation in these channels and the comparison with the B-to-charmonium reference value is therefore a sensitive probe for physics beyond the SM. A discrepancy between $S_{b\to sq\overline{q}}$ and $\sin 2\beta$ can provide an indication of new physics. If the SM and new physics contributions are both significant, the deviations of the CP asymmetries from $\sin 2\beta$ become mode

dependent, because they depend on the relative size and phase of the contributing amplitudes, which are determined by the quantum numbers of the new physics and by strong interactions.

The important question is how well can we bound the contribution of the second, CKM-suppressed, term to the $b \to sq\overline{q}$ transition in Eq. (69)? This term has a different weak phase than the dominant first term, so its impact on $S_{b\to sq\overline{q}}$ depends on both its magnitude and relative strong phase. Naive factorization suggests that for $q = s$ the λ^2 suppression of the second term is likely to hold because it would require an enhancement of rescattering effects to upset this. However, for $q = u$, there is a color-suppressed $b \to u$ tree diagram, which has a different weak (and possibly strong) phase than the leading λ^2 penguin amplitude. For $q = d$, any light neutral meson formed from $d\overline{d}$ also has a $u\overline{u}$ component, and there is "tree pollution" again. The B^0 decays to $\pi^0 K^0_S$ and ωK^0_S belong to this category. The mesons η' and $f_0(980)$ have significant $s\overline{s}$ components, which may reduce the tree pollution. Neglecting rescattering, the three-body final state $K^0\overline{K}^0 K^0$ (reconstructed as $K^0_S K^0_S K^0_S$) has no tree pollution, whereas $B^0 \to K^+K^-K^0$ (excluding ϕK^0) does.

Recently QCD factorization [173, 174] and SCET [175] was used to calculate the deviations from sin2β in some of the two-body penguin modes. It was found that the deviations are the smallest ($\lesssim 0.02$) for ϕK^0 and $\eta' K^0$. This is fortunate because these are also the modes in which the experimental errors are the smallest. The SM shifts enhance $-\eta_f S_f$ (except for ρK^0_S) using [173,174], while suppress $S_{\eta' K_S}$ using [175]. SU(3) flavor symmetry has also been used to bound the SM-induced deviations from sin2β [176, 177]. Owing to the lack of information on strong phases and the weak experimental bounds on some $b \to dq\overline{q}$ mediated rates, the resulting bounds tend to be weak. An exception is $\pi^0 K^0_S$, where SU(3) relates the relevant amplitudes to $\pi^0\pi^0$ and K^+K^- [177]. The theoretical understanding of factorization in three-body decays does not yet allow accurate bounds on $-\eta_f S_f - \sin 2\beta$ to be computed.

There has been considerable excitement about these measurements in the past few years, which has been somewhat damped by recent updates from the experiments. The results for the measurement of $\sin 2\beta_{\rm eff}$ (which is equal to $-\eta_f S_f$ for the final states with unique CP content) from the various penguin modes are compiled in Fig. 10. If one restricts the modes to those with the potentially smallest theoretical uncertainties, i.e., the final states ϕK^0, $\eta' K^0$, and $K^0\overline{K}^0 K^0$, and attempts to average the effective sin2β results, $\langle \sin 2\beta_{\rm eff} \rangle = 0.50 \pm 0.08$, which is within 2.2σ reach of the charmonium reference value. Beginning of 2005, this s-penguin average was 0.40 ± 0.09, and because the charmonium result was larger at that time, the discrepancy between the sin2β numbers was at the 3.2σ level, which explains the popularity of the results. Better statistics are required to clarify the situation.[17]

Another interesting measurement in the penguin sector is the time-dependent CP asymmetry in $B \to K^0_S \pi^0 (K^{*0})\gamma$. *BABAR* and Belle have measured it exclusively and inclusively, with the averages $S_{K^*\gamma} = -0.13 \pm 0.32$ and $S_{K_S\pi^0\gamma} = 0.00 \pm 0.28$ [179, 66]. Although the $B \to X_s\gamma$ rate is correctly predicted by the SM at the 10% level, that measurement sums over the rates to left- and right-handed photons, and their ratio is also sensitive to new physics. In the SM, b-quarks

[17] It is an interesting outcome of the QCD factorization calculations that the SM deviations from sin2β should be positive in all modes, except for $\rho^0 K^0$ [173, 174]. Taking the expected deviations into account would enhance the significance of the current discrepancy between the charmonium-based and the penguin-based results.

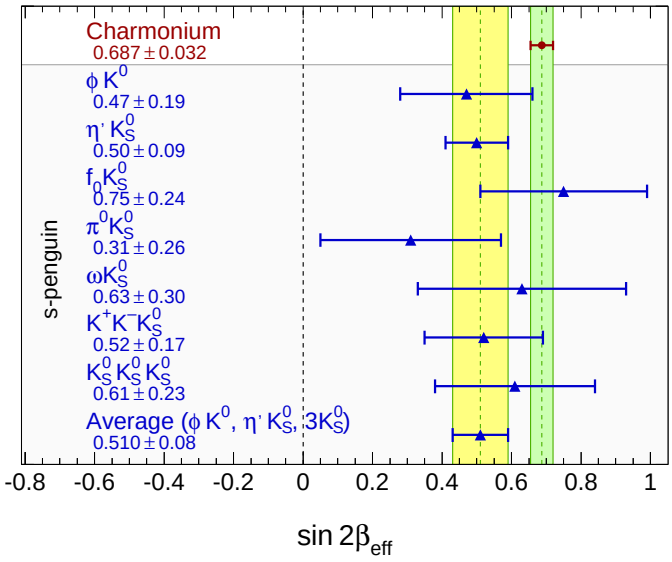

Figure 10: *Comparison of world average* $\sin 2\beta_{(\mathrm{eff})}$ *results from penguin-dominated decays, and the charmonium reference value [178, 121, 122, 66]. The light shaded band shows the average of the results from* $B^0 \to \phi K^0$, $\eta' K^0$, $K^0_S K^0_S K^0_S$, *considered to be theoretically cleaner than the other modes. The result for* $B^0 \to \pi^0\pi^0 K^0_S$ *is not shown, because it has a much larger error.*

mainly decay to $s\gamma_L$ and $\overline{b}$-quarks to $\overline{s}\gamma_R$, so their interference is suppressed, proportional to $r_{f_s} = A(\overline{B}^0 \to X_{f_s}\gamma_R)/A(\overline{B}^0 \to X_{f_s}\gamma_L)$. If only the electromagnetic penguin operator, $O_7 \sim \overline{s}\,\sigma^{\mu\nu}F_{\mu\nu}(m_b P_R + m_s P_L)b$ contributed to the rate, it would give $S_{K^*\gamma} = -2(m_s/m_b)\sin 2\beta$ [180]. This also holds in the nonresonant $B \to K^0_S\pi^0\gamma$ case [181]. Grinstein *et al.* [182] recently realized that four-quark operators contribute to r that are not suppressed by m_s/m_b. The numerically dominant term is due to the matrix element of $O_2 = (\overline{c}\,\gamma^\mu P_L b)(\overline{s}\,\gamma_\mu P_L c)$, and its contribution to the inclusive rate can be calculated reliably, $\Gamma(\overline{B}^0 \to X_s\gamma_R)/\Gamma(\overline{B}^0 \to X_s\gamma_L) \approx 0.01$ [182]. This suggests that for most final states, on average, $r \sim 0.1$ should be expected. A SCET analysis of the exclusive decay proved the power suppression of the amplitude ratio, $A(\overline{B}^0 \to \overline{K}^{0*}\gamma_R)/A(\overline{B}^0 \to \overline{K}^{0*}\gamma_L) = \mathcal{O}[(C_2/3C_7)\,(\Lambda_{\mathrm{QCD}}/m_b)] \sim 0.1$ [182], but the uncertainties are sizable.

7.3 The *D* System

The D meson system is complementary to K and B mesons, because it is the only neutral-meson system in which mixing and rare decays are generated by down-type quarks in the SM (or up-type squarks in SUSY). Therefore, flavor and CP violation are suppressed by both the GIM mechanism and by the Cabibbo angle. As a result, CP violation in D decays, rare D decays, and $D^0\overline{D}^0$ mixing are predicted to be small in the SM and have not yet been observed. There are well-motivated new physics scenarios, such as those based on quark-squark alignment [183], that predict $D^0\overline{D}^0$ mixing to be of order λ^2, so that if the current bounds improve by a factor of a few, these models become fine tuned.

The most interesting experimental hint for a possible $D^0\overline{D}^0$ mixing signal so far is the lifetime difference between the CP-even and CP-odd states [184]

$$y_{CP} = \frac{\Gamma(CP\text{-even}) - \Gamma(CP\text{-odd})}{\Gamma(CP\text{-even}) + \Gamma(CP\text{-odd})} = (0.9 \pm 0.4)\,\% \,. \tag{70}$$

Unfortunately, this central value alone cannot not be interpreted as a sign of new physics, because of possible long-distance hadronic effects [185]. At the present level of sensitivity, CP violation in mixing or decays, or enhanced rare decays, such as $D \to \pi\ell^+\ell^-$ would be the only clean signal of new physics in the D sector. Because the B-factories are also charm factories (however, without coherent production of $D^0\overline{D}^0$ pairs), it is possible to observe such unambiguous signals of new physics every time the analyzed data sample increases, independent of the tight constraints in the K and B sectors.

7.4 The B_s System

Although all present results show agreement with the SM, it is still possible that the new physics flavor structure is quite different from that in the SM, with $\mathcal{O}(1)$ effects in sectors of flavor physics that have not yet been probed with good precision. As mentioned above, many well-motivated models can lead to large new physics effects between the second and the third generations, while leaving the flavor-changing transitions between the other families unaffected. The B_s^0 sector, which is currently being investigated at the Tevatron (cf. Sec. 3.4) and will soon be studied by the LHC experiments, is suited to test such scenarios.[18]

Compared with the B^0 mesons, the properties of the B_s^0 are still less well known, although the measurement of Δm_s [95, 96] strongly indicates that $B_s^0\overline{B}_s^0$ mixing is SM-like. Although the uncertainty of Δm_s is already at the few percent level, we have no significant information yet on the $B_s^0\overline{B}_s^0$ mixing phase, β_s, and the width difference, $\Delta\Gamma_s$, is poorly known. Many extensions of the SM predicted large modifications of Δm_s owing to contributions from new particles to B_s^0 oscillations. Such models, or such parameter regions of models are now ruled out. The LHC experiments will determine $\sin 2\beta_s$ through the time-dependent measurement of mixing-induced CP violation in the decay $B_s^0 \to J/\psi\phi$ (and similar final states).[19] The expected precision of better than 0.02 for the combined LHC experiments will barely be enough for a significant measurement if $S_{B_s^0 \to J/\psi\phi}$ is as predicted by the SM. However, for the purpose of the search for new physics, which could still occur at the $\mathcal{O}(1)$ level, only the absolute error on $\sin 2\beta_s$ matters.

[18] During the Summer of 2005, the Belle experiment performed a three-day engineering run comprising a five-point energy scan between 10.825 GeV and 10.905 GeV, to locate the $\Upsilon(5S)$ peak, and data taking at the $\Upsilon(5S)$ (10.869 GeV). A data sample corresponding to an integrated luminosity of $1.9\,\mathrm{fb}^{-1}$ was collected during that period [186]. $\Upsilon(5S)$ resonant events decay into pairs of neutral and charged $B^{(*)}$ mesons as well as neutral $B_s^{(*)}$ mesons with opposite flavors. Belle found a fraction of events with $B_s^{(*)}$ pair production over the full $b\overline{b}$ production (including the continuum) at the $\Upsilon(5S)$ of $(16.4 \pm 1.4 \pm 4.1)\%$. Among these, $\Upsilon(5S) \to B_s^*\overline{B}_s^*$ events dominate. All inclusive and exclusive measurements performed are found in agreement with earlier results on the $\Upsilon(5S)$, with less statistics, obtained at the CLEO experiment [187].

[19] As all pseudoscalar decays to a pair of vector mesons, such as $B^0 \to J/\psi K^{*0}$ or $B^0 \to \rho^+\rho^-$, the final state in $B_s^0 \to J/\psi\phi$ is an admixture of CP-even and CP-odd components. To avoid a dilution of the CP-asymmetry measurement, they must be separated by an angular analysis, which complicates the measurement.

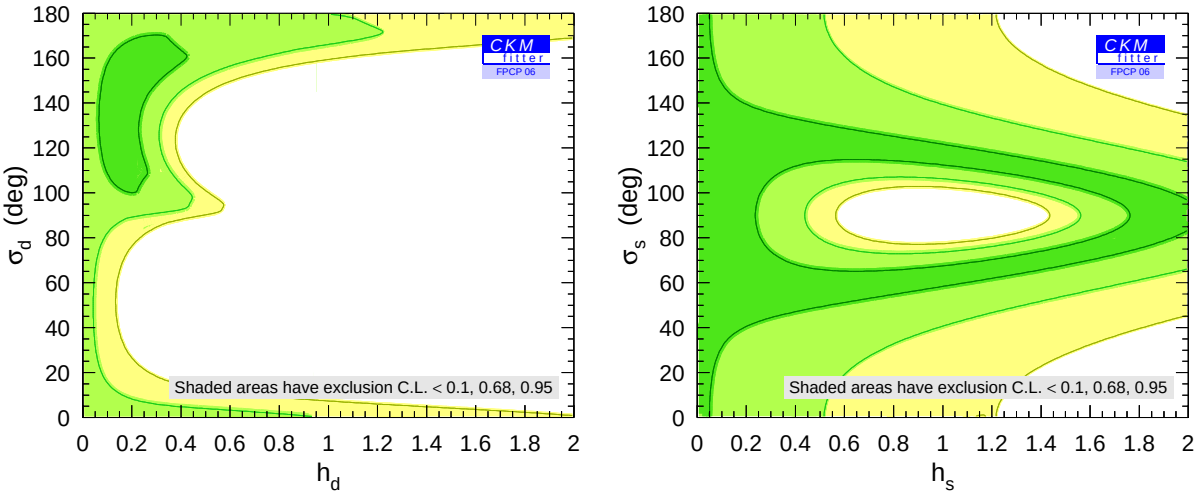

Figure 11: *Confidence levels of the h_d, σ_d (left) and h_s, σ_s (right) new physics parameters. The dark, medium, and light shaded areas indicate* 10%, 68% *and* 95% C.L. *allowed regions, respectively. The SM corresponds to $h_d = h_s = 0$.*

Because this phase is λ^2 suppressed, it can be predicted accurately (in terms of its absolute error) by the global CKM fit, giving $\sin 2\beta_s = 0.0365 \pm 0.0021$ [188, 51]. Hence this represents the first precision measurement, sensitive to a new physics phase, that can be confronted with a *precision prediction*. It could become the most sensitive test of the KM theory for *CP* violation.

The class of rare decays that proceed through penguin diagrams, such as $B \to K^* \gamma$ and $B \to K^* \ell^+ \ell^-$, will be augmented by the B_s^0 system through (among others) the measurement of the decay $B_s^0 \to \mu^+ \mu^-$ at the LHC. The best current limit on the branching fraction is 8×10^{-8} at 90% C.L. [189], which is well above the SM model expectation of 3.4×10^{-9} (whose dominant theoretical uncertainty is due to $f_{B_s}^2$) [190]. Expectations for the LHC experiments are hard to estimate owing to the difficulty in fully simulating sufficient background statistics, but all experiments expect to see a SM signal within one year. The decay $B^0 \to \mu^+ \mu^-$ will be a further challenge due to its even lower branching fraction in the SM. It should be observed by all experiments after several years of data taking. A precision measurement of $\mathcal{B}(B_s^0 \to \mu^+ \mu^-)/\mathcal{B}(B^0 \to \mu^+ \mu^-)$, which has a clean relation to $\Delta m_s / \Delta m_d$, will be beyond the scope of the LHC.

7.5 Model-Independent Constraints on New Physics in *B* Oscillation

In a large class of models the dominant new physics effects are new contributions to the $B^0 \overline{B}^0$ and $B_s^0 \overline{B}_s^0$ mixing amplitudes [191], which can be parameterized as

$$M_{12} = M_{12}^{\rm SM} \, (1 + h_{d,s} e^{2i\sigma_{d,s}}). \tag{71}$$

The allowed regions for σ_d vs. h_d and σ_s vs. h_s are shown in Fig. 11 (left and right plots, respectively). Numerically, one finds $h_d = 0.23^{+0.57}_{-0.23}$, corresponding to the 95% C.L. upper limit $h_d < 1.7$ [13]. The constraints on the new physics parameters are reasonably tight because $(\overline{\rho}, \overline{\eta})$ has been determined from (effectively) tree-level measurements independent of new physics in

$B^0\overline{B}^0$ mixing (before the α and γ measurements most of the plotted region was allowed) [13, 192, 193, 194]. In $B^0\overline{B}^0$ mixing, the $\mathrm{Im}\, e^{2i\sigma_d} > 0$ region is more strongly constrained than the $\mathrm{Im}\, e^{2i\sigma_d} < 0$ region due to the mild tension between $\sin 2\beta$ and $|V_{ub}|$. Although the constraints are significant, new physics with a generic weak phase may still contribute to the $B^0\overline{B}^0$ mixing amplitude of the order of 30% of the SM. Because Eq. (71) has two new parameters that need to be determined from the data, measurements irrelevant for the SM CKM fit, such as the *CP* asymmetries in semileptonic B^0_d and B^0_s decays become important for these constraints [188,195, 196]; the former is measured as[20] $A^d_{\rm SL} = -(0.5 \pm 5.5) \times 10^{-3}$ [118]. In $B^0_s\overline{B}^0_s$ mixing, even after the measurement of Δm_s, new physics and the SM may still give comparable contributions to the mixing amplitude, since we have no information on the mixing phase yet [166, 195]. This will change as soon as there is data on the *CP* asymmetry in $B^0_s \to J/\psi\phi$; even a measurement with an uncertainty as large as $\delta(S_{B_s\to\psi\phi}) \sim 0.1$ would bring the constraints on h_s, σ_s to a level comparable to those on h_d, σ_d [195]. At present, the lifetime difference between the *CP*-even and odd B^0_s states gives a useful additional constraint [197, 198, 195] (not included in Fig. 11), however, this is largely because the central value disfavors any deviation from the SM. After a nominal year of LHC data this constraint will probably be less important due to theoretical uncertainties. Similar results for the constraints in $K^0\overline{K}^0$ mixing can be found in Refs. [166,193].

8 Conclusions and Perspectives

The *B*-factories and the Tevatron experiments have provided a spectacular quantitative confirmation of the three-generation CKM picture. Even more interesting than the improved determination of the CKM elements is the emergence of redundant measurements that overconstrain the CKM matrix. The measurements of *CP* asymmetries, mixing, and semileptonic and rare decays allow us to severely constrict the magnitudes and phases of possible new physics contributions to flavor-changing interactions in a variety of neutral- and charged-current processes. We can meaningfully constrain flavor models with more parameters than the SM; in particular, within the last two years, the comparison between tree- and loop-dominated measurements significantly bounds new physics in $B\overline{B}$ mixing. This illustrates that it is the multitude of overconstraining measurements and their correlations (and not any single measurement) that carry the most compelling information. Nevertheless, as can be seen in Fig. 11, new physics in $B^0\overline{B}^0$ and in $B^0_s\overline{B}^0_s$ mixing may still be comparable to the SM contribution.

Having analyzed these results, one may ask where flavor physics should go from here. The sensitivity to short-distance physics will not be limited by hadronic physics in many interesting processes for a long time to come. The existing measurements could have shown deviations from the SM, and if there are new particles at the TeV scale, new flavor physics could show up any time as the measurements improve. If new physics is seen in flavor physics, we will want to study it in as many different processes as possible. If new physics is not seen in flavor physics, it is still interesting to achieve the experimentally and theoretically best possible limits. If new particles are observed at the LHC, the measurements from the flavor sector, as well as flavor-diagonal

[20] To avoid contamination from B^0_s mesons, only the measurements performed at the $\Upsilon(4S)$ are included in this average [197]. In the SM $A^s_{\rm SL} \ll A^d_{\rm SL}$, so one may average all data to bound $|q/p| - 1$, quoted on p. 30.

constraints from electric dipole moments, will strongly confine the degrees of freedom of the underlying new physics.

The large number of impressive new results speak for themselves, so that it is easy to summarize the main lessons we have learned so far:

- $\sin 2\beta = 0.687 \pm 0.032$ implies that the B and K constraints are consistent, and the KM phase is the dominant source of CP violation in flavor-changing processes at the electroweak scale.
- The difference between the measurements of $\sin 2\beta$ from B decays to charmonium plus K^0 and from the penguin-dominated $\eta' K^0$ mode (or the average of ϕK^0, $\eta' K^0$ and $K^0_S K^0_S K^0_S$) is approximately 2σ at present. More data are required to make this comparison conclusive.
- The measurements of $\alpha = (100^{+15}_{-8})^\circ$ and $\gamma = (62^{+35}_{-25})^\circ$ are in agreement with the SM expectations, and begin to improve the constraint on $\overline{\rho}$, $\overline{\eta}$. They also provide significant bounds on new physics in $B^0\overline{B}^0$ mixing.
- The CDF measurement of $\Delta m_s = 17.31\,^{+0.33}_{-0.18} \pm 0.07\,\mathrm{ps}^{-1}$ (in agreement with the SM expectation, $21.7\,^{+5.9}_{-4.2}$) together with the results of the other experiments lift the evidence for $B^0_s\overline{B}^0_s$ oscillation to the 4σ level.
- The determinations of $|V_{cb}| = (41.5\pm0.7)\times10^{-3}$, $\overline{m}_b(\overline{m}_b) = 4.18\pm0.04$ GeV, and $\overline{m}_c(\overline{m}_c) = 1.22\pm0.06$ GeV from inclusive semileptonic B decays reached unprecedented precision and robustness, as all hadronic inputs were simultaneously determined from data.
- Strong experimental evidence for the leptonic decay $B^+ \to \tau^+\nu_\tau$ has been found, with a world-average branching fraction of $(10.4\,^{+3.0}_{-2.7})\times10^{-5}$, in excellent agreement with the SM.
- $A_{K^+\pi^-} = -0.115 \pm 0.018$ implies large direct CP violation disproving "B-superweak" models. It also signifies that sizable strong phases occur in this decay. Many more decays exhibiting direct CP violation will emerge from the increasing data samples.
- The list is much longer, e.g., improvements in the determination of $|V_{ub}|$, observation of $B \to X_s\ell^+\ell^-$ and $B \to D^{0(*)}\pi^0$ decays, and a zoology of new D_s and $c\overline{c}$ states.

The next few years promise similarly interesting results (in arbitrary order):

- One of the most important outstanding questions is the comparison of $\sin 2\beta$ from tree and penguin decays. Three times more data than currently used in the analyses could be accumulated until data taking of the first generation B-factories ends.
- A measurement of $\sin 2\beta_s$ with mixing-induced CP-violation analysis of $B^0_s \to J/\psi\phi$ (and similar) decays. If $\sin 2\beta_s$ can be measured at the 0.02 level (absolute error) at the LHC, it will constitute the most sensitive probe so far for new CP-violating phases. Together with other SM-like observations in the K and B sectors, it would suggest that the flavor sector of any new physics at the TeV scale approximates minimal flavor violation.
- Improvements in the determination of α and γ can be expected. The angle γ will also be measured by LHCb. This will further constrain the right side of the UT, serving as the SM reference for the ratio $\Delta m_d/\Delta m_s$. Reduction of LQCD errors is also necessary for this comparison.

- The rigor of the determination of $|V_{ub}|$ may approach that of $|V_{cb}|$, and its error will also be reduced. It determines the side of the UT opposite to β, so any progress directly improves the accuracy of CKM tests (the error with continuum methods reach an asymptote at approximately 5%).
- The experimental precision approaching the limits from the theoretical uncertainties in $B \to X_s\gamma$ and $B \to X_s\ell^+\ell^-$ (for branching fractions, *CP*-violating asymmetries and forward-backward asymmetries) will impact model building. The (continuum) theory is most precise for inclusive decays, which, however, cannot be measured at the LHC.
- Improving the precision of the current $S_{K^*\gamma} = -0.13 \pm 0.32$ measurement will be important to constrain certain extensions of the SM.
- Improving the precision of the current $A_{\rm SL} = -2(|q/p| - 1) = -(0.5 \pm 5.5) \times 10^{-3}$ measurement is also important, in addition to a measurement of $A^s_{\rm SL}$ in $B^0_s\overline{B}^0_s$ oscillation.
- Future studies should firmly establish and precisely measure the $B \to \rho\gamma$ and $B \to \tau\nu$ rates, and try to measure $B \to X_d\gamma$ inclusively. They should also search for $B_{d,s} \to \ell^+\ell^-$ and other rare or forbidden decays.
- Similar to the "new" $c\overline{s}$ and $c\overline{c}$ states discovered by the B-factories, new physics could also be discovered in the charm sector. With increasing sensitivity, one may find clear signs of new physics in $D \to \pi\ell^+\ell^-$ or through *CP* violation in $D^0\overline{D}^0$ mixing.

Acknowledgments

We are indebted to Stephane T'Jampens and the CKMfitter Group for providing many of the plots and results given in this review. We thank Max Baak, Pat Burchat, Jérôme Charles, Roger Forty, Michael Luke, Stephane Monteil, Arnaud Robert and Frank Tackmann for helpful comments on the manuscript. The work of Z.L. was supported in part by the U.S. Department of Energy Contract number DE-AC02-05CH11231.

References

1. N. Cabibbo, Phys. Rev. Lett. **10**, 531 (1963).
2. M. Kobayashi and T. Maskawa, Prog. Theor. Phys. **49**, 652 (1973).
3. M. Dine, hep-ph/0011376 (2000).
4. A.D. Sakharov, Pisma Zh. Eksp. Teor. Fiz. **5**, 32 (1967) [JETP Lett. **5**, 24 (1967)].
5. G.R. Farrar and M.E. Shaposhnikov, Phys. Rev. D **50**, 774 (1994) [hep-ph/9305275]; S.M. Barr, G. Segre and H.A. Weldon, Phys. Rev. D **20**, 2494 (1979).
6. M. Fukugita and T. Yanagida, Phys. Lett. B **174** (1986) 45; for a review, see: W. Buchmuller and M. Plumacher, Int. J. Mod. Phys. A **15**, 5047 (2000) [hep-ph/0007176].
7. J.H. Christenson, J.W. Cronin, V.L. Fitch and R. Turlay, Phys. Rev. Lett. **13**, 138 (1964).
8. S.L. Glashow, J. Iliopoulos and L. Maiani, Phys. Rev. D **2**, 1285 (1970).
9. *BABAR* Collaboration (B. Aubert *et al.*), Phys. Rev. Lett. **87**, 091801 (2001) [hep-ex/0107013]; Belle Collaboration (K. Abe *et al.*), Phys. Rev. Lett. **87**, 091802 (2001) [hep-ex/0107061].

10. L.L. Chau and W.Y. Keung, Phys. Rev. Lett. **53**, 1802 (1984).
11. L. Wolfenstein, Phys. Rev. Lett. **51**, 1945 (1983).
12. A.J. Buras, M.E. Lautenbacher and G. Ostermaier, Phys. Rev. D **50**, 3433 (1994) [hep-ph/9403384].
13. CKMfitter Group (Charles *et al.*), Eur. Phys. J. C **41**, 1 (2005) [hep-ph/0406184].
14. C. Jarlskog, Phys. Rev. Lett. **55**, 1039 (1985).
15. G.C. Branco, L. Lavoura and J.P. Silva, *CP Violation*, International Series of Monographs on Physics, No. 103, Clarendon Press, Oxford, UK (1999).
16. K. Anikeev *et al.*, "B physics at the Tevatron: Run II and beyond," hep-ph/0201071 (2002).
17. A. Angelopoulos *et al.*, CPLEAR Collaboration, Phys. Lett. B **444**, 43 (1998).
18. D. Kirkby and Y. Nir, "*CP* violation in meson decays", Review for the Partice Data Group (2006).
19. H.E. Haber, Nucl. Phys. Proc. Suppl. **62**, 469 (1998) [hep-ph/9709450].
20. Y. Nir, hep-ph/0510413 (2005).
21. G. Buchalla, A.J. Buras and M.E. Lautenbacher, Rev. Mod. Phys. **68**, 1125 (1996) [hep-ph/9512380].
22. N. Isgur and M.B. Wise, Phys. Lett. B **237**, 527 (1990); Phys. Lett. B **232**, 113 (1989).
23. A.V. Manohar and M.B. Wise, Camb. Monogr. Part. Phys. Nucl. Phys. Cosmol. **10**, 1 (2000).
24. H. Georgi, Phys. Lett. B **240**, 447 (1990).
25. N. Isgur and M.B. Wise, Phys. Rev. D **42**, 2388 (1990).
26. J.D. Bjorken, Nucl. Phys. Proc. Suppl. **11**, 325 (1989).
27. M.J. Dugan and B. Grinstein, Phys. Lett. B **255**, 583 (1991).
28. C.W. Bauer, S. Fleming and M.E. Luke, Phys. Rev. D **63**, 014006 (2001) [hep-ph/0005275]; C.W. Bauer, S. Fleming, D. Pirjol and I.W. Stewart, Phys. Rev. D **63**, 114020 (2001) [hep-ph/0011336].
29. C.W. Bauer and I.W. Stewart, Phys. Lett. B **516**, 134 (2001) [hep-ph/0107001]; C.W. Bauer, D. Pirjol and I.W. Stewart, Phys. Rev. D **65**, 054022 (2002) [hep-ph/0109045].
30. C.W. Bauer, D. Pirjol and I.W. Stewart, Phys. Rev. Lett. **87**, 201806 (2001) [hep-ph/0107002].
31. M. Beneke, A.P. Chapovsky, M. Diehl and T. Feldmann, Nucl. Phys. B **643**, 431 (2002) [hep-ph/0206152].
32. S. Mantry, D. Pirjol and I.W. Stewart, Phys. Rev. D **68**, 114009 (2003) [hep-ph/0306254].
33. J. Charles, A. Le Yaouanc, L. Oliver, O. Pene and J.C. Raynal, Phys. Rev. D **60**, 014001 (1999) [hep-ph/9812358].
34. M. Beneke, G. Buchalla, M. Neubert and C.T. Sachrajda, Phys. Rev. Lett. **83**, 1914 (1999) [hep-ph/9905312]; Nucl. Phys. B **606**, 245 (2001) [hep-ph/0104110].
35. C.W. Bauer, D. Pirjol, I.Z. Rothstein and I.W. Stewart, Phys. Rev. D **70**, 054015 (2004) [hep-ph/0401188]; C.W. Bauer, I.Z. Rothstein and I.W. Stewart, hep-ph/0510241 (2005).
36. M. Beneke, G. Buchalla, M. Neubert and C.T. Sachrajda, Phys. Rev. D **72**, 098501 (2005) [hep-ph/0411171]; C.W. Bauer, D. Pirjol, I.Z. Rothstein and I.W. Stewart, Phys. Rev. D **72**, 098502 (2005) [hep-ph/0502094].
37. M. Ciuchini, E. Franco, G. Martinelli and L. Silvestrini, Nucl. Phys. B **501**, 271 (1997) [hep-ph/9703353]; M. Ciuchini, E. Franco, G. Martinelli, M. Pierini and L. Silvestrini, Phys. Lett. B

515, 33 (2001) [hep-ph/0104126].

38. J. Chay, H. Georgi and B. Grinstein, Phys. Lett. B **247**, 399 (1990); M.A. Shifman and M.B. Voloshin, Sov. J. Nucl. Phys. **41**, 120 (1985); I.I.Y. Bigi, N.G. Uraltsev and A.I. Vainshtein, Phys. Lett. B **293**, 430 (1992) [Erratum-ibid. B **297**, 477 (1993)] [hep-ph/9207214]; I.I.Y. Bigi, M.A. Shifman, N.G. Uraltsev and A.I. Vainshtein, Phys. Rev. Lett. **71**, 496 (1993) [hep-ph/9304225]; A.V. Manohar and M.B. Wise, Phys. Rev. D **49**, 1310 (1994) [hep-ph/9308246].
39. G. Savard *et al.*, Phys. Rev. Lett. **95**, 102501 (2005).
40. W.J. Marciano, A. Sirlin, Phys. Rev. Lett. **96**, 032002 (2006) [hep-ph/0510099].
41. E. Blucher *et al.*, hep-ph/0512039 (2005).
42. H. Abele *et al.*, Phys. Rev. Lett. **88**, 211801 (2002) [hep-ex/0206058].
43. D. Mund, Proceedings of *Ultracold and Cold Neutrons*, Physics and Sources, St. Petersburg, June 2003.
44. A. Serebrov *et al.*, Phys. Lett. B **605**, 72 (2005) [nucl-ex/0408009].
45. Particle Data Group (S. Eidelman *et al.*), Phys. Lett. B **592**, 1 (2004), and 2005 partial update for the 2006 edition available on `http://pdg.lbl.gov/`.
46. D. Pocanic for the PIBETA Collaboration, Talk given at 2nd Workshop on the CKM Unitarity Triangle, Durham, England, 5-9 Apr 2003, eConf **C0304052**, WG606.
47. MILC Collaboration (C. Bernard *et al.*), PoS **LAT2005**, 025 (2005) [hep-lat/0509137].
48. A. Ceccucci, Z. Ligeti, and Y. Sakai, "The CKM quark mixing matrix", Review for the Partice Data Group (2006).
49. B. Grinstein, Phys. Rev. Lett. **71**, 3067 (1993) [hep-ph/9308226];
    Z. Ligeti, eConf **C030603** (2003) JEU10 [hep-ph/0309219].
50. *BABAR* Collaboration (B. Aubert *et al.*), Phys. Rev. D **73** 057101 (2006) [hep-ex/0507069];
    Belle Collaboration (K. Ikado *et al.*), hep-ex/0604018 (2006)
51. CKMfitter Group (Charles *et al.*), numerical updates for the FPCP 2006 conferenec are taken from `http://ckmfitter.in2p3.fr`.
52. M. Ademollo and R. Gatto, Phys. Rev. Lett. **13**, 264 (1964).
53. H. Leutwyler and M. Roos, Z. Phys. C **25**, 91 (1984).
54. A. Sher *et al.*, Phys. Rev. Lett. **91**, 261802 (2003) [hep-ex/0305042].
55. Average by [51] using input for η_{+-} from: KTeV Collaboration (T. Alexopoulos *et al.*), Phys. Rev. Lett. **93**, 181802 (2004) [hep-ex/0406001]; Phys. Rev. D **70**, 092006 (2004) [hep-ex/0406002]; KLOE Collaboration (F. Ambrosino *et al.*), hep-ex/0603041 (2006).
56. O.P. Yushchenko *et al.*, Phys. Lett. B **589**, 111 (2004) [hep-ex/0404030];
    KTeV Collaboration (T. Alexopoulos *et al.*), Phys. Rev. D **70**, 092007 (2004) [hep-ex/0406003];
    NA48 Collaboration (A. Lai *et al.*), Phys. Lett. B **604**, 1 (2004) [hep-ex/0410065].
57. KLOE Collaboration (F. Ambrosino *et al.*), Phys. Lett. B **626**, 15 (2005) [hep-ex/0507088].
58. E. Gámiz *et al.*, JHEP **0301**, 060 (2003) [hep-ph/0212230].
59. M. Davier, A. Höcker and Z. Zhang, hep-ph/0507078 (2005).
60. LEP Electroweak Working Group, CERN-PH-EP/2005-051, hep-ex/0511027 (2005).
61. Fermilab Lattice, MILC, and HPQCD Collaborations (C. Aubin *et al.*), Phys. Rev. Lett. **94**, 011601

(2005) [hep-ph/0408306].

62. M. Artuso, hep-ex/0510052 (2005).
63. M.E. Luke, Phys. Lett. B **252**, 447 (1990).
64. A. Czarnecki, Phys. Rev. Lett. **76** (1996) 4124 [hep-ph/9603261]; A. Czarnecki and K. Melnikov, Nucl. Phys. B **505** (1997) 65 [hep-ph/9703277].
65. S. Hashimoto *et al.*, Phys. Rev. D **61**, 014502 (2000) [hep-ph/9906376]; Phys. Rev. D **66**, 014503 (2002) [hep-ph/0110253].
66. The Heavy Flavor Averaging Group (HFAG) (E. Barberio *et al.*), hep-ex/0603003 (2006), and updates at `http://www.slac.stanford.edu/xorg/hfag/`.
67. A.H. Hoang, Z. Ligeti and A.V. Manohar, Phys. Rev. D **59**, 074017 (1999) [hep-ph/9811239]; Phys. Rev. Lett. **82**, 277 (1999) [hep-ph/9809423].
68. I.I.Y. Bigi, M.A. Shifman and N. Uraltsev, Ann. Rev. Nucl. Part. Sci. **47**, 591 (1997) [hep-ph/9703290].
69. A.H. Hoang and T. Teubner, Phys. Rev. D **60**, 114027 (1999) [hep-ph/9904468].
70. S. J. Brodsky, G. P. Lepage and P. B. Mackenzie, Phys. Rev. D **28**, 228 (1983).
71. C.W. Bauer, Z. Ligeti, M. Luke, A.V. Manohar and M. Trott, Phys. Rev. D **70** (2004) 094017 [hep-ph/0408002]; C.W. Bauer, Z. Ligeti, M. Luke and A.V. Manohar, Phys. Rev. D **67**, 054012 (2003) [hep-ph/0210027].
72. O.L. Buchmüller and H.U. Flächer, Phys. Rev. D **73**, 073008 (2006) [hep-ph/0507253].
73. A.H. Hoang and A.V. Manohar, Phys. Lett. B **633**, 526 (2006) [hep-ph/0509195].
74. M. Okamoto *et al.*, Nucl. Phys. Proc. Suppl. **140**, 461 (2005) [hep-lat/0409116].
75. J. Shigemitsu *et al.*, Nucl. Phys. Proc. Suppl. **140**, 464 (2005) [hep-lat/0408019].
76. M. Okamoto, PoS LAT2005, 013 (2005) [hep-lat/0510113].
77. P. Ball and R. Zwicky, Phys. Lett. B **625**, 225 (2005) [hep-ph/0507076];
    E. Bagan, P. Ball and V.M. Braun, Phys. Lett. B **417**, 154 (1998) [hep-ph/9709243].
78. C.G. Boyd, B. Grinstein and R.F. Lebed, Phys. Rev. Lett. **74**, 4603 (1995) [hep-ph/9412324].
79. M.C. Arnesen, B. Grinstein, I.Z. Rothstein and I.W. Stewart, Phys. Rev. Lett. **95**, 071802 (2005) [hep-ph/0504209]; I. Stewart, Talk at Lepton-Photon 2005, June 30–July 5 2005, Uppsala, Sweden, `http://lp2005.tsl.uu.se/%7Elp2005/LP2005/programme/index.htm`.
80. M. Fukunaga and T. Onogi, Phys. Rev. D **71**, 034506 (2005) [hep-lat/0408037];
    T. Becher and R.J. Hill, Phys. Lett. B **633**, 61 (2006) [hep-ph/0509090].
81. M. Neubert, Phys. Rev. D **49**, 3392 (1994) [hep-ph/9311325]; *ibid.* 4623 [hep-ph/9312311].
82. I.I.Y. Bigi, M.A. Shifman, N.G. Uraltsev and A.I. Vainshtein, Int. J. Mod. Phys. A **9**, 2467 (1994) [hep-ph/9312359].
83. C.W. Bauer, M.E. Luke and T. Mannel, Phys. Rev. D **68**, 094001 (2003) [hep-ph/0102089]; Phys. Lett. B **543**, 261 (2002) [hep-ph/0205150]; A.K. Leibovich, Z. Ligeti and M.B. Wise, Phys. Lett. B **539**, 242 (2002) [hep-ph/0205148]; C.N. Burrell, M.E. Luke and A.R. Williamson, Phys. Rev. D **69**, 074015 (2004) [hep-ph/0312366]; K.S.M. Lee and I.W. Stewart, Nucl. Phys. B **721**, 325 (2005) [hep-ph/0409045]; S.W. Bosch, M. Neubert and G. Paz, JHEP **0411**, 073 (2004) [hep-ph/0409115]; T. Mannel and F. J. Tackmann, Phys. Rev. D **71**, 034017 (2005) [hep-ph/0408273].

84. C.W. Bauer and A. V. Manohar, Phys. Rev. D **70**, 034024 (2004) [hep-ph/0312109].
85. S.W. Bosch, B.O. Lange, M. Neubert and G. Paz, Nucl. Phys. B **699**, 335 (2004) [hep-ph/0402094].
86. A.K. Leibovich, I. Low and I.Z. Rothstein, Phys. Rev. D **61**, 053006 (2000) [hep-ph/9909404]; Phys. Lett. B **486**, 86 (2000) [hep-ph/0005124];
A.H. Hoang, Z. Ligeti and M. Luke, Phys. Rev. D **71**, 093007 (2005) [hep-ph/0502134];
B.O. Lange, JHEP **0601**, 104 (2006) [hep-ph/0511098].
87. C.W. Bauer, Z. Ligeti and M.E. Luke, Phys. Lett. B **479**, 395 (2000) [hep-ph/0002161]; Phys. Rev. D **64**, 113004 (2001) [hep-ph/0107074].
88. CLEO Collaboration (A. Bornheim *et al.*), Phys. Rev. Lett. **88**, 231803 (2002) [hep-ex/0202019];
BABAR Collaboration (B. Aubert *et al.*), hep-ex/0408075 (2004);
Belle Collaboration (A. Limosani *et al.*), Phys. Lett. B **621**, 28 (2005) [hep-ex/0504046].
89. B. Aubert *et al.* [BABAR Collaboration], hep-ex/0601046 (2006).
90. *BABAR* Collaboration (B. Aubert *et al.*), Phys. Rev. Lett. **94**, 011801 (2005); Phys. Rev. D **70**, 112006 (2004);
Belle Collaboration (K. Abe *et al.*), hep-ex/0506079 (2005); Phys. Rev. D **69**, 112001 (2004);
CLEO Collaboration (T.E. Coan *et al.*), Phys. Rev. Lett. **84**, 5283 (2000).
91. B. Grinstein and D. Pirjol, Phys. Rev. D **62**, 093002 (2000) [hep-ph/0002216]; P. Ball and R. Zwicky, hep-ph/0603232 (2006); A. Ali, E. Lunghi and A.Y. Parkhomenko, Phys. Lett. B **595**, 323 (2004) [hep-ph/0405075]; M. Beneke, T. Feldmann and D. Seidel, Nucl. Phys. B **612**, 25 (2001) [hep-ph/0106067]. S.W. Bosch and G. Buchalla, Nucl. Phys. B **621**, 459 (2002) [hep-ph/0106081]. Z. Ligeti and M.B. Wise, Phys. Rev. D **60**, 117506 (1999) [hep-ph/9905277]; D. Becirevic, V. Lubicz, F. Mescia and C. Tarantino, JHEP **0305**, 007 (2003) [hep-lat/0301020].
92. T. Inami and C.S. Lim, Prog. Theor. Phys. **65**, 297 (1981); Erratum-ibid. **65**, 1772 (1981).
93. H.G. Moser and A. Roussarie, Nucl. Inst. Meth. **A384**, 491 (1997).
94. D. Abbaneo and G. Boix, JHEP **9908**, 004 (1999) [hep-ex/9909033].
95. DØ Collaboration (V. Abazov *et al.*), FERMILAB-PUB-06-055-E, hep-ex/0603029 (2006).
96. CDF Collaboration (A. Abulencia *et al.*), hep-ex/0606027 (2006).
97. C. Dawson, PoS **LAT2005**, 007 (2005).
98. Results presented at the CKM workshop, San Diego, USA, 2005, `http://ckm2005.ucsd.edu`.
99. J. Bijnens and J. Prades, Nucl. Phys. B **444**, 523 (1995) [hep-ph/9502363]; JHEP **0001**, 002 (2000) [hep-ph/9911392]; S. Peris and E. de Rafael, Phys. Lett. B **490**, 213 (2000) [hep-ph/0006146].
100. S. Herrlich and U. Nierste, Nucl. Phys. B **419**, 292 (1994) [hep-ph/9310311].
101. NA31 Collaboration (G.D. Barr *et al.*), Phys. Lett. B **317**, 233 (1993).
102. NA48 Collaboration (J.R. Batley *et al.*), Phys. Lett. B **544**, 97 (2002) [hep-ex/0208009].
103. KTeV Collaboration (A. Alavi-Harati *et al.*), Phys. Rev. D **67**, 012005 (2003) [hep-ex/0208007].
104. J.M. Flynn and L. Randall, Phys. Lett. B **224**, 221 (1989).
105. A.J. Buras, M. Jamin and M.E. Lautenbacher, Nucl. Phys. B **408**, 209 (1993) [hep-ph/9303284].
106. M. Ciuchini, E. Franco, G. Martinelli and L. Reina, Phys. Lett. B **301**, 263 (1993) [hep-ph/9212203].
107. E787 Collaboration (S. Adler *et al.*), Phys. Rev. Lett. **88** (2002) 041803 [hep-ex/0111091].
108. E949 Collaboration (V.V. Anisimovsky *et al.*), Phys. Rev. Lett. **93**, 031801 (2004) [hep-ex/0403036].

109. G. Buchalla and A.J. Buras, Nucl. Phys. B **548**, 309 (1999) [hep-ph/9901288].

110. W.J. Marciano and Z. Parsa, Phys. Rev. D **53**, 1 (1996).

111. A.J. Buras, M. Gorbahn, U. Haisch and U. Nierste, Phys. Rev. Lett. **95**, 261805 (2005) [hep-ph/0508165]; hep-ph/0603079 (2006).

112. G. Isidori, F. Mescia and C. Smith, Nucl. Phys. B **718**, 319 (2005) [hep-ph/0503107];
A.F. Falk, A. Lewandowski and A.A. Petrov, Phys. Lett. B **505**, 107 (2001) [hep-ph/0012099];
M. Lu and M.B. Wise, Phys. Lett. B **324**, 461 (1994) [hep-ph/9401204].

113. L.S. Littenberg, Phys. Rev. D **39**, 3322 (1989).

114. Y. Grossman and Y. Nir, Phys. Lett. B **398**, 163 (1997) [hep-ph/9701313].

115. G. Buchalla and G. Isidori, Phys. Lett. B **440**, 170 (1998) [hep-ph/9806501].

116. A.J. Buras, F. Schwab and S. Uhlig, hep-ph/0405132 (2004)

117. G. Buchalla, G. D'Ambrosio and G. Isidori, Nucl. Phys. B **672**, 387 (2003) [hep-ph/0308008]; and references therein.

118. BABAR Collaboration (B. Aubert *et al.*), hep-ex/0603053;
Belle Collaboration (K. Abe *et al.*), hep-ex/0409012;
CLEO Collaboration (D.E. Jaffe *et al.*), Phys. Rev. Lett. **86**, 5000 (2001) [hep-ex/0101006].

119. DØ Collaboration, `http://www-d0.fnal.gov/Run2Physics/WWW/results/prelim/B/B29/B29.pdf`;
ALEPH Collaboration (R. Barate *et al.*), Eur. Phys. J. C **20**, 431 (2001);
OPAL Collaboration (G. Abbiendi *et al.*), Eur. Phys. J. C **12**, 609 (2000) [hep-ex/9901017].

120. M. Beneke, G. Buchalla, A. Lenz and U. Nierste, Phys. Lett. B **576**, 173 (2003) [hep-ph/0307344];
M. Ciuchini, E. Franco, V. Lubicz, F. Mescia and C. Tarantino, JHEP **0308**, 031 (2003) [hep-ph/0308029].

121. *BABAR* Collaboration (B. Aubert *et al.*), Phys. Rev. Lett. **94**, 161803 (2005) [hep-ex/0408127].

122. Belle Collaboration (K. Abe *et al.*), BELLE-CONF-0569, hep-ex/0507037 (2005).

123. Y. Grossman and H. R. Quinn, Phys. Rev. D **56**, 7259 (1997) [hep-ph/9705356].

124. I. Dunietz, H. Quinn, A. Snyder, W. Toki and H.J. Lipkin, Phys. Rev. D **43**, 2193 (1991);
J. Charles *et al.*, Phys. Rev. D **58**, 114021 (1998) [hep-ph/9806347];
A.S. Dighe, I. Dunietz and R. Fleischer, Eur. Phys. J. C **6**, 647 (1999) [hep-ph/9804253];
C.W. Chiang, Phys. Rev. D **62**, 014017 (2000) [hep-ph/0002243].

125. LASS Collaboration (D. Aston *et al.*), Nucl. Phys. B **296**, 493 (1988).

126. M. Suzuki, Phys. Rev. D **64**, 117503 (2001) [hep-ph/0106354].

127. *BABAR* Collaboration (B. Aubert, *et al.*), Phys. Rev. D **71**, 032005 (2005) [hep-ex/0411016].

128. Belle Collaboration (R. Itoh, Y. Onuki, *et al.*), Phys. Rev. Lett. **95**, 091601 (2005) [hep-ex/0504030].

129. A. Bondar, T. Gershon and P. Krokovny, Phys. Lett. B **624**, 1 (2005) [hep-ph/0503174].

130. Belle Collaboration (K. Abe *et al.*), BELLE-CONF-0546, hep-ex/0507065 (2005).

131. M. Gronau and D. London, Phys. Rev. Lett. **65**, 3381 (1990).

132. H.R. Quinn and A.E. Snyder, Phys. Rev. D **48**, 2139 (1993).

133. R. Aleksan, F. Buccella, A. Le Yaouanc, L. Oliver, O. Pène and J.-C. Raynal Phys. Lett. B **356**, 95 (1995) [hep-ph/9506260].

134. M. Beneke and M. Neubert, Nucl. Phys. B **675**, 333 (2003) [hep-ph/0308039].

135. M. Neubert and J.L. Rosner, Phys. Lett. B **441**, 403 (1998) [hep-ph/9808493]; Phys. Rev. Lett. **81**, 5076 (1998) [hep-ph/9809311].

136. M. Gronau, D. Pirjol and T.M. Yan, Phys. Rev. D **60**, 034021 (1999); [Erratum-ibid. D **69**, 119901 (2004)] [hep-ph/9810482].

137. A.J. Buras and R. Fleischer, Eur. Phys. J. C **11**, 93 (1999) [hep-ph/9810260].

138. M. Gronau and J. Zupan, Phys. Rev. D **71**, 074017 (2005) [hep-ph/0502139];
S. Gardner, Phys. Rev. D **72**, 034015 (2005) [hep-ph/0505071].

139. Y. Grossman and H.R. Quinn, Phys. Rev. D **58**, 017504 (1998) [hep-ph/9712306].

140. M. Gronau, D. London, N. Sinha and R. Sinha, Phys. Lett. B **514**, 315 (2001) [hep-ph/0105308].

141. J. Charles, Phys. Rev. D **59**, 054007 (1999) [hep-ph/9806468].

142. *BABAR* Collaboration (B. Aubert *et al.*), Phys. Rev. Lett. **95**, 151803 (2005) [hep-ex/0501071]; BABAR-CONF-05/13 [hep-ex/0508046] (2005); Phys. Rev. Lett. **94**, 181802 (2005) [hep-ex/0412037]; Phys. Rev. Lett. **94**, 181802 (2005) [hep-ex/0412037];
Belle Collaboration (K. Abe *et al.*), Phys. Rev. Lett. **95**, 101801 (2005) [hep-ex/0502035]; Phys. Rev. D **69**, 111102 (2004) [hep-ex/0311061]; Phys. Rev. Lett. **94**, 181803 (2005) [hep-ex/0408101]; Phys. Rev. D **69**, 111102 (2004) [hep-ex/0311061];
CLEO Collaboration (A. Bornheim *et al.*), Phys. Rev. D **68**, 052002 (2003) [hep-ex/0302026].

143. *BABAR* Collaboration (B. Aubert *et al.*), B. Lau at Rencontres de Moriond - QCD and Hadronic Interactions at High Energy, La Thuile, Italy (2006); Phys. Rev. Lett. **95**, 041805 (2005) [hep-ex/0503049]; Phys. Rev. Lett. **94**, 131801 (2005) [hep-ex/0412067]; Phys. Rev. Lett. **93**, 231801 (2004) [hep-ex/0404029]; Phys. Rev. Lett. **91**, 171802 (2003) [hep-ex/0307026];
Belle Collaboration (A. Somov and A. J. Schwartz *et al.*), Phys. Rev. Lett. **96**, 171801 (2006) [hep-ex/0601024]; Belle Collaboration (J. Zhang *et al.*), Phys. Rev. Lett. **91**, 221801 (2003) [hep-ex/0306007].

144. J.G. Körner and G.R. Goldstein, Phys. Lett. B **89**, 105 (1979).

145. A. Falk, Z. Ligeti, Y. Nir and H.R. Quinn, Phys. Rev. D **69**, 011502 (2004) [hep-ph/0310242].

146. H.J. Lipkin, Y. Nir, H.R. Quinn and A. Snyder, Phys. Rev. D **44**, 1454 (1991).

147. *BABAR* Collaboration (B. Aubert *et al.*), SLAC-PUB-10658, BABAR-CONF-04-38, hep-ex/0408099 (2004).

148. M. Gronau and D. London, Phys. Lett. B **253**, 483 (1991);
M. Gronau and D. Wyler, Phys. Lett. B **265**, 172 (1991).

149. D. Atwood, I. Dunietz, and A. Soni, Phys. Rev. Lett. **78**, 3257 (1997) [hep-ph/9612433]; Phys. Rev. D **63**, 036005 (2001) [hep-ph/0008090].

150. A. Giri, Y. Grossman, A. Soffer and J. Zupan, Phys. Rev. D **68**, 054018 (2003) [hep-ph/0303187]; Belle Collaboration (A. Poluektov *et al.*), Phys. Rev. D **70**, 072003 (2004) [hep-ex/0406067].

151. *BABAR* Collaboration (B. Aubert *et al.*), BABAR-PUB-05/051 [hep-ex/0512067] (2005); Phys. Rev. D **71**, 031102 (2005) [hep-ex/0411091]; Phys. Rev. D **72**, 071103 (2005) [hep-ex/0507002];
Belle Collaboration (K. Abe *et al.*), Belle preprint 2006-1 [hep-ex/0601032] (2006).

152. *BABAR* Collaboration (B. Aubert *et al.*), Phys. Rev. D **72**, 032004 (2005) [hep-ex/0504047]; Phys. Rev. D **72**, 071104 (2005);
Belle Collaboration (K. Abe *et al.*), BELLE-CONF-0552 [hep-ex/0508048] (2005);

153. A. Bondar and T. Gershon, Phys. Rev. D **70**, 091503 (2004) [hep-ph/0409281].

154. *BABAR* Collaboration (B. Aubert *et al.*), Phys. Rev. Lett. **95**, 121802 (2005); BABAR-CONF-05/018, hep-ex/0507101 (2005).

155. A. Poluektov for the Belle Collaboration, Les Rencontres de Physique de la Vallée d'Aoste (2006).

156. *BABAR* Collaboration (B. Aubert *et al.*), Phys. Rev. Lett. **92**, 251801 (2004) [hep-ex/0308018].

157. *BABAR* Collaboration (B. Aubert *et al.*), Phys. Rev. D **71**, 112003 (2005) [hep-ex/0504035]; BABAR-PUB-06/01 [hep-ex/0602049] (2006);
Belle Collaboration (K. Abe *et al.*), Phys. Lett. B **624**, 11 (2005) [hep-ex/0408106]; Phys. Rev. Lett. **93**, 031802 (2004); Erratum-ibid.**93**, 059901 (2004) [hep-ex/0308048];

158. *BABAR* Collaboration (B. Aubert *et al.*), Phys. Rev. Lett. **93**, 131801 (2004) [hep-ex/0407057]; Belle Collaboration (K. Abe *et al.*), BELLE-CONF-0523, hep-ex/0507045 (2005).

159. *BABAR* Collaboration (B. Aubert *et al.*), Phys. Rev. D **72**, 072003 (2005) [hep-ex/0507004]; Belle Collaboration, (K. Abe etal), BELLE-CONF-0528, hep-ex/0509001 (2005).

160. A. Höcker, H. Lacker, S. Laplace and F. Le Diberder, Eur. Phys. J. C **21**, 225 (2001) [hep-ph/0104062].

161. The CKM Matrix and the Unitarity Triangle (M. Battaglia *et al.*), CERN Yellow Report, CERN-2003-002, hep-ph/0304132 (2003).

162. UTfit Collaboration (M. Bona *et al.*), JHEP **0507**, 028 (2005) [hep-ph/0501199].

163. B. Aubert *et al.*, BABAR-CONF-04/038, hep-ex/0408099 (2004).

164. CDF and DØ Collaborations, and the Tevatron Electroweak Working Group, hep-ex/0603039 (2006)

165. A.G. Cohen, D.B. Kaplan and A.E. Nelson, Phys. Lett. B **388**, 588 (1996) [hep-ph/9607394]; A.G. Cohen, D.B. Kaplan, F. Lepeintre and A.E. Nelson, Phys. Rev. Lett. **78**, 2300 (1997) [hep-ph/9610252].

166. K. Agashe, M. Papucci, G. Perez and D. Pirjol, hep-ph/0509117 (2005).

167. D. Chang, A. Masiero and H. Murayama, Phys. Rev. D **67**, 075013 (2003) [hep-ph/0205111]; R. Harnik, D.T. Larson, H. Murayama and A. Pierce, Phys. Rev. D **69**, 094024 (2004) [hep-ph/0212180].

168. K.S. Babu and C.F. Kolda, Phys. Rev. Lett. **84**, 228 (2000) [hep-ph/9909476];
C. Hamzaoui, M. Pospelov and M. Toharia, Phys. Rev. D **59**, 095005 (1999) [hep-ph/9807350].

169. A.J. Buras, P.H. Chankowski, J. Rosiek and L. Slawianowska, Nucl. Phys. B **619**, 434 (2001) [hep-ph/0107048].

170. J.R. Ellis, K.A. Olive, Y. Santoso and V.C. Spanos, Phys. Rev. D **71**, 095007 (2005) [hep-ph/0502001];
J.L. Feng, K.T. Matchev and F. Wilczek, Phys. Rev. D **63**, 045024 (2001) [astro-ph/0008115].

171. M. Ciuchini, G. Degrassi, P. Gambino and G.F. Giudice, Nucl. Phys. B **534**, 3 (1998) [hep-ph/9806308]; A. Ali and D. London, Eur. Phys. J. C **9**, 687 (1999) [hep-ph/9903535]; A.J. Buras, P. Gambino, M. Gorbahn, S. Jager and L. Silvestrini, Phys. Lett. B **500**, 161 (2001) [hep-ph/0007085]; G.D'Ambrosio, G.F. Giudice, G. Isidori and A. Strumia, Nucl. Phys. B **645**, 155 (2002) [hep-ph/0207036].

172. G. Buchalla and A.J. Buras, Phys. Lett. B **333**, 221 (1994) [hep-ph/9405259].

173. G. Buchalla, G. Hiller, Y. Nir and G. Raz, JHEP **0509**, 074 (2005) [hep-ph/0503151].

174. M. Beneke, Phys. Lett. B **620**, 143 (2005) [hep-ph/0505075].

175. A.R. Williamson and J. Zupan, hep-ph/0601214 (2006).

176. Y. Grossman, Z. Ligeti, Y. Nir and H. Quinn, Phys. Rev. D **68**, 015004 (2003) [hep-ph/0303171].

177. M. Gronau, Y. Grossman and J.L. Rosner, Phys. Lett. B **579**, 331 (2004) [hep-ph/0310020].

178. *BABAR* Collaboration (B. Aubert *et al.*), Phys. Rev. D**71**, 091102 (2005) [hep-ex/0502019]; BABAR-CONF-05/14 [hep-ex/0507087] (2005); BABAR-CONF-04/19 [hep-ex/0408095] (2004); Phys. Rev. D **71**, 111102 (2005) [hep-ex/0503011]; BABAR-CONF-05/020 [hep-ex/0508017] (2005); BABAR-PUB-05/01 [hep-ex/0503018] (2005); hep-ex/0507016 (2005); BABAR-CONF-04/12 [hep-ex/0507052] (2004).

179. *BABAR* Collaboration (B. Aubert *et al.*), Phys. Rev. D **72**, 051103 (2005) [hep-ex/0507038]; Belle Collaboration (K. Abe *et al.*), BELLE-CONF-0570 [hep-ex/0507059] (2005).

180. D. Atwood, M. Gronau and A. Soni, Phys. Rev. Lett. **79**, 185 (1997) [hep-ph/9704272].

181. D. Atwood, T. Gershon, M. Hazumi and A. Soni, Phys. Rev. D **71**, 076003 (2005) [hep-ph/0410036].

182. B. Grinstein, Y. Grossman, Z. Ligeti and D. Pirjol, Phys. Rev. D **71**, 011504 (2005) [hep-ph/0412019].

183. Y. Nir and N. Seiberg, Phys. Lett. B **309**, 337 (1993) [hep-ph/9304307].

184. B.D. Yabsley, Int. J. Mod. Phys. A **19**, 949 (2004) [hep-ex/0311057].

185. A.F. Falk, Y. Grossman, Z. Ligeti and A.A. Petrov, Phys. Rev. D **65**, 949 (2002) [hep-ph/0110317]; A.F. Falk *et al.*, Phys. Rev. D **69**,114021 (2004) [hep-ph/0402204].

186. A. Drutskoy for the Belle Collaboration, SLAC Experimental Seminar, Jan 17, 2006, SLAC, Stanford, `https://www.slac.stanford.edu/exp/seminar/talks/2006/Drutskoy_Bs_Belle.ppt`.

187. R. Sia for the CLEO Collaboration, Int. J. Mod. Phys. A **20**, 3669 (2005) [hep-ex/0410087]; CLEO Collaboration (D. Besson *et al.*), Phys. Rev. Lett. **54**, 381 (1985); D.M.J. Lovelock *et al.*, Phys. Rev. Lett., **54**, 377 (1985).

188. S. Laplace, Z. Ligeti, Y. Nir and G. Perez, Phys. Rev. D **65**, 094040 (2002) [hep-ph/0202010].

189. CDF Collaboration, `http://www-cdf.fnal.gov/physics/new/bottom/060316.blessed-bsmumu3`

190. A.J. Buras, Phys. Lett. B **566**, 115 (2003) [hep-ph/0303060].

191. J.M. Soares and L. Wolfenstein, Phys. Rev. D **47**, 1021 (1993); T. Goto, N. Kitazawa, Y. Okada and M. Tanaka, Phys. Rev. D **53**, 6662 (1996) [hep-ph/9506311]; J.P. Silva and L. Wolfenstein, Phys. Rev. D **55**, 5331 (1997) [hep-ph/9610208]; Y. Grossman, Y. Nir and M. P. Worah, Phys. Lett. B **407**, 307 (1997) [hep-ph/9704287].

192. Z. Ligeti, Int. J. Mod. Phys. A **20**, 5105 (2005) [hep-ph/0408267].

193. UTfit Collaboration (M. Bona *et al.*), JHEP **0603**, 080 (2006) [hep-ph/0509219]; hep-ph/0408079 (2004).

194. F. J. Botella, G. C. Branco, M. Nebot and M. N. Rebelo, Nucl. Phys. B **725**, 155 (2005) [hep-ph/0502133].

195. Z. Ligeti, M. Papucci and G. Perez, hep-ph/0604112 (2006).

196. M. Blanke, A. J. Buras, D. Guadagnoli and C. Tarantino, hep-ph/0604057 (2006).

197. Y. Grossman, Y. Nir and G. Raz, hep-ph/0605028 (2006).

198. M. Bona *et al.* [UTfit Collaboration], hep-ph/0605213 (2006).